

TR 95-63

**THE MINERALOGY AND GEOCHEMISTRY
OF THE VOËLWATER BANDED IRON-FORMATION,
NORTHERN CAPE PROVINCE**

RHODES UNIVERSITY
LIBRARY

Cl. No. TR 95-63

SRN 168881

THESIS

**Submitted in partial fulfilment of the
requirements for the Degree of
MASTER OF SCIENCE (ECONOMIC GEOLOGY)
of Rhodes University**

by

HARILAOS TSIKOS

February 1994

**NOT TO BE TAKEN AWAY
FROM THE LIBRARY**



a 1 1 7 5 8 7 3 1 b

To my beloved parents, whose
contribution made everything
possible...

ABSTRACT

Banded iron-formations (BIFs) are chemically precipitated sedimentary rocks in which Fe-rich bands or laminae alternate with Fe-poor ones. They formed within a specific time-span of the geological record. Their occurrence is restricted between 2.3 and 1.9 Ga, and characterises virtually all the major-Precambrian-aged sedimentary basins of the world.

The Precambrian Transvaal Basin in Griqualand West, South Africa, is noted for its well-developed BIF units. The Kuruman and Griquatown BIFs comprising the Asbesheuwels Subgroup (up to 1000m thick) are the best known and thickest of these. As far as metallogenesis is concerned, the Kuruman BIF is of major importance, for it carries the world's largest crocidolite (blue asbestos) deposits.

The uppermost, youngest member of iron-formation deposition in the Griqualand West Sequence is represented by the Voëlwater BIF. The direct association between the latter and the giant Mn-deposits of the Kalahari Field, renders the Voëlwater association unusual, if not unique, in the geological record. The Voëlwater BIF represents a typical example of the so-called "Superior-type", and in the area of study it has undergone late-diagenetic to low-grade metamorphic processes. This is evident from the mineralogical composition and textural signature of the various BIF lithologies. Specifically, the minerals that make up the Voëlwater BIF are mainly chert(quartz), Fe-oxides (magnetite and hematite), Fe-silicates (greenalite, stilpnomelane, minnesotaite, riebeckite, Fe-mica), Fe-carbonates (members of the dolomite-ankerite series and siderite), calcite and pyrite. Soft-sediment deformation structures and shear-stress indicators are abundant in carbonate-rich and granular, silicate-rich BIF lithologies respectively.

The bulk chemical composition of the study rocks is relatively simple and is characterised by the abundance of essentially three elements, namely Si, Fe, and Ca, which make up more than 90% of the total chemical composition of the Voëlwater BIFs. The detrital component of the study rocks is negligible. Mn-

enrichments characterise all the transitional lithologies towards the interbedded Mn-orebodies, as well as the well-developed, hematitic BIF-unit between the Ongeluk lavas and the lower Mn-horizon. In terms of trace element composition, no significant enrichments or depletions were encountered, except for some unusually high values of Sr and Ba and Co in carbonate-rich and Mn-rich lithologies respectively. Geochemical comparisons on the basis of major, trace and light rare-earth element composition verified the similarity between the Voëlwater BIF and other major Superior-type BIFs of the world (e.g. Kuruman, Griquatown, Sokoman, Biwabik, Gunflint, Mara-Mamba, Brockman, etc.).

The processes that led to the formation of the Voëlwater BIFs may have been very similar to the ones described in various genetic models proposed in recent years. They would have involved a combination of: i. hydrothermal processes related to mid-ocean ridge (MOR) or hot-spot activity that acted as major iron-suppliers; ii. storm-mixing in stratified oceans (bottom, anoxic, Fe^{+2} reservoir-thermo-pycnocline zone-upper, mixed, SiO_2 -saturated layer), largely dictated by seasonal changes and contemporaneous volcanism; iii. periodic, convection-driven upwelling mechanisms acting as major Fe-precipitators; and, iv. organic carbon productivity that was responsible for the anoxic diagenesis of the initial sediment. However, the origin of Fe and Mn for the genesis of the Voëlwater sediments was difficult to explain with typical convection-cell models in active mid-ocean ridges, in contrast to previous hypotheses. Instead, large-scale endogenous processes in the form of magma convection, underplating, differentiation and associated degassing, may have played a critical role in the supply of metals for the formation of large amounts of BIFs in the Precambrian.

The present study of the Voëlwater BIF also bears strong implications regarding the metallogenesis of Mn in the Precambrian. The common association of Mn with carbonate-bearing sediments, the transitional character of the Voëlwater BIF towards carbonate lithologies (Mooirdraai dolomites) and the critical timing of the deposition of the former in terms of the Precambrian atmospheric-lithospheric-hydrospheric evolution, may be important indicators for the exploration of large Mn-deposits in Precambrian sedimentary basins of the world.

CONTENTS

	Page
1. INTRODUCTION	1
1.1 General	1
1.2 BIFs and Mn	5
1.3 Bibliographic review	8
2. REGIONAL GEOLOGICAL SETTING	11
2.1 The Transvaal Sequence	11
2.2 The Transvaal Sequence in Griqualand West	14
2.2.1 The Ghaap Group	16
2.2.1.1 The Schmidtsdrif Subgroup	16
2.2.1.2 The Campbellrand Subgroup	17
2.2.1.3 The Asbesheuwels Subgroup	18
a The Kuruman BIF	18
b The Griquatown BIF	20
2.2.1.4 The Koegas Subgroup	22
2.2.2 The Postmasburg Group	24
2.2.2.1 The Makganyene Diamictite	24
2.2.2.2 The Ongeluk lavas	26
2.2.2.3 The Voëlwater Subgroup	27
2.3 Economic Geology of Griqualand West	29
3. PETROGRAPHY OF THE VOËLWATER BANDED IRON-FORMATION ..	30
3.1 Introduction	30
3.2 Methods of study	31
3.3 Mineralogy	32
3.3.1 Silicates	33
3.3.1.1 Greenalite	33

3.3.1.2	Stilpnomelane	35
3.3.1.3	Minnesotaite	37
3.3.1.4	Riebeckite	39
3.3.1.5	Other silicates	40
3.3.1.6	Chert (quartz)	42
3.3.2	Carbonates	43
3.3.2.1	Members of the dolomite-ankerite series	43
3.3.2.2	Siderite	45
3.3.2.3	Calcite	46
3.3.3	Oxides and sulphides	46
3.3.3.1	Magnetite	46
3.3.3.2	Hematite	48
3.3.3.3	Pyrite	48
3.4	Textural relations	50
3.4.1	Primary textures	51
3.4.2	Diagenetic textures and soft-sediment deformation structures	52
3.4.3	Textural evidence for post-depositional tectonic effects	54
3.5	Regional implications	55
4.	GEOCHEMISTRY OF THE VOËLWATER BANDED IRON-FORMATION	57
4.1	Introduction	57
4.2	Sample collection, preparation and analytical procedure	58
4.3	Bulk geochemical composition	59
4.3.1	Major elements	59
4.3.1.1	Si-Fe-Ca	60
4.3.1.2	Mn	63
4.3.1.3	Chemical comparison with other iron-formations	63
4.3.2	Trace elements	66
4.4	Chemical distinction between Fe-bearing sedimentary rocks	67
4.4.1	Si-(Fe + Mn)-Al	67
4.4.2	Fe/Al-Ca/Mg	69
4.4.3	Si-Al	70

4.5 Comparison with recent metalliferous sediments	71
4.5.1 Mn, Fe, Si and minor metals	71
4.5.2 Cr and P	73
4.5.3 LREE	75
4.5.3.1 La vs Ce	75
4.5.3.2 Ce anomalies	75
4.6 Suggestions for further study	78
5. DISCUSSION: THE GENESIS OF THE VOËLWATER Fe-Mn SEDIMENTS . .	80
5.1 Genesis of BIFs	80
5.1.1 Palaeodepositional environment	81
5.1.2 Sources and transportation of iron and silica	82
5.1.3 Conditions of precipitation	84
5.1.3.1 The atmosphere and oceans in the Precambrian	84
5.1.3.2 The role of organisms	87
5.1.3.3 Genetic modelling of BIFs	88
5.2 Genesis of the Voëlwater BIF-Mn sediments	94
5.2.1 The depositional model	96
5.2.2 Applications of Eh-pH systematics	98
5.2.3 Considerations of local significance	101
5.2.4 Broad-scale geotectonic implications	104
5.2.5 Suggestions for exploration	107
5.3 The origin of the Kalahari Mn-deposits	109
5.3.1 Previous hypotheses	109
5.3.2 The currently accepted model	110
5.3.3 A possible alternative	115
6. SUMMARY AND CONCLUSIONS	119
7. ACKNOWLEDGEMENTS	125
8. REFERENCES	127

LIST OF FIGURES

- Fig. 1.1.** Estimated abundance of iron-formation deposited through geologic time. Horizontal scale is non-linear, approximately logarithmic; range 0-10¹⁵ tonnes (after James, 1983). **Page 3**
- Fig. 1.2.** Location of major manganese deposits and BIF occurrences in the world. Note the absence of Mn-deposits in the Lake Superior Region, the Labrador Trough and the Hamersley Basin, whereas the Mn-deposits in Nikopol, Tchiatura and Bolshoi Tokmak are Oligocene in age and have no relation with the BIFs of the Krivoy Rog Basin (modified after Laznicka, 1992) **Page 6**
- Fig. 2.1.** Simplified geology of the Transvaal and Griqualand West Sequences (after Beukes, 1987) **Page 11**
- Fig. 2.2.** Simplified Geological map of the Transvaal Sequence in Griqualand West. Ts = Tsineng; Ku = Kurumankop; Wh = White Bank; Sp = Spitsberg; Ga = Garakosa; De = Derby; Gl = Gladstone; Da = Danielskuil; Ou = Ouplaas; Wa = Warrendale; Fi = Finch Mine; Ho = Hopefield; Sp-1 = Spioenskop; Kn = Klein Naute; W = Westerberg; Ro = Rooinekke; Po = Postmasburg; Ka = Katu; Si = Sishen; H = Hotazel (after Hälbich et al., 1993) **Page 13**
- Fig. 2.3.** East-west stratigraphic section through the Maremane Dome in Griqualand West, illustrating thrust faulting and the relationship of the ore deposits to the unconformity at the base of the Gamagara Formation (after Beukes, 1986b). **Page 14**
- Fig. 2.4.** South-north section illustrating stratigraphic and sedimentological facies relationships in the Transvaal Sequence in Griqualand West (after Beukes, 1986a) **Page 19**
- Fig. 2.5.** South-north section illustrating stratigraphic relationships and inferred palaeodepositional environments of the Asbesheuwels Subgroup in Griqualand West (after Beukes, 1983). **Page 21**
- Fig. 2.6.** Regional stratigraphic relationships in the Koegas Subgroup along a southwest-northeast section (after Beukes, 1983) **Page 23**
- Fig. 2.7.** Lithostratigraphic succession in the Makganyene diamictite between Sishen and Postmasburg (modified after De Villiers & Visser; in Beukes, 1983) **Page 25**
- Fig. 2.8.** Simplified stratigraphic column of the Hotazel BIF and Mn-beds from the study area (not to scale; modified after Schutte, 1992) **Page 28**

Fig. 3.1. Compositional ranges of stilpnomelane, members of the talc-minnesotaite series and greenalite in late diagenetic to very low-grade metamorphic BIFs (modified after Lesher, 1978; in Klein, 1983) **Page 39**

Fig. 3.2. Compositions of representative rhombohedral carbonates from carbonate-rich horizons of the Voëlwater iron-formation (analytical data are summarised in Table A4) **Page 44**

Fig. 3.3. Mineral occurrences in the Voëlwater BIF. a. Dark, deformed siderite-bearing granules in a very fine-grained, chert-greenalite-calcite-±carbon(?) assemblage. b. Dark brown, pleochroic stilpnomelane sprays inside a calcite-ankerite matrix. Note the characteristic fascicular habit of stilpnomelane. c. Felted masses of minnesotaite which have obliterated all original texture of, what used to be, a chert-greenalite assemblage. d. Coexistence of minnesotaite sprays with coarse, rhombohedral ankerite in a quartz-±magnetite-±pyrite matrix. e. Riebeckite needles in a matrix of microcrystalline quartz-±magnetite. f. Carbonate-stilpnomelane-magnetite assemblage. Note the greenish-brown flaky grains in the centre and bottom centre of what is believed to be ferri-annite. g. Ankerite-quartz assemblage. The ankerite is coarse-grained, with an apparent rhombohedral habit. Quartz forms the fine-grained matrix with lesser magnetite and occasional pyrite. h. Same as g, but under cross polars. Note the cloudy interiors and clearer edges of ankerite crystals. All photomicrographs were taken under 100x magnification. **Page 49**

Fig. 3.4. Representative textures of rocks from the study area. a. Sinuous quartz vein transecting the hematitic BIF. Similar features have been reported by Simonson (1987), from North American BIFs that have undergone silica cementation and related diagenetic processes. b. Fascicular stilpnomelane needles arranged along the contact between a twinned calcite and a chert-magnetite-carbonate band. c. Grain of unknown mineralogical character now completely replaced by microcrystalline quartz and riebeckite needles. Note preferential riebeckite growth along cleavage(?) planes of the original crystal. d. Quartz-ankerite veinlets in a quartz-carbonate assemblage. The core of the veins consists of microcrystalline quartz and the outer parts of coarse rhombohedral ankerite. Stilpnomelane needles are found in the apophyses of the veins, at the contact with a chert-carbonate-magnetite-stilpnomelane band. e. Granular feature replaced by coarse-grained quartz in a quartz-magnetite-carbonate matrix. These coarser quartz crystals have irregular grain boundaries, indicating high total surface energy due to recrystallisation under very low-grade conditions. f. Granule "ghosts", now totally replaced by microcrystalline quartz. Note the later overprint by rhombohedral ankerite and coarse, subhedral magnetite. g. The same as f, but under cross polars. The granules are now very hard to distinguish due to the intense recrystallisation. h. Stylolite, separating a very fine-grained chert-carbonate-magnetite-stilpnomelane band from a chert-riebeckite-magnetite one. All photomicrographs were taken under 100x magnification, except for photo 3.4h (30x) **Page 53**

Fig. 3.5. a. Soft sediment deformation structure in carbonate-rich BIF from the study area. This "microdiapir" has probably formed under late-diagenetic conditions but certainly before complete consolidation of the sediment took place. The mechanism for the formation of such features would include: i. burial of fluidised carbonate sediment under thick overload; ii. compaction, "squeezing" and upward escape of the relatively lighter carbonate-rich fluids through diagenetic cracks; iii. subsequent trapping by the denser overburden; and, iv. growth of coarse ankerite on the edges of the structure, followed by crystallisation of microcrystalline quartz. Fig. 3.5a represents a compilation of photomicrographs taken under 30x magnification. **b. Shear-sense indicators in granular, BIF lithologies from the study area,** in the form of σ structures (i, iv), possible rolling (δ) structures (iii), and "domino" (bookshelf) sliding (ii, iii, iv). All photomicrographs are taken under 100x magnification; shear sense along the shear plane is shown. **Page 55**

Fig. 3.6. Relative stabilities of minerals in metamorphosed banded iron-formations as a function of metamorphic grade (compiled after James, 1954; French, 1968; Klein, 1978; Floran & Papike, 1978; in Klein, 1983) **Page 56**

Fig. 4.1. Ternary diagram Ca-Si-Fe illustrating the compositional range of BIF lithologies from this study (filled squares) **Page 61**

Fig. 4.2. Bivariate diagrams of: (a) CaO vs FeO; (b) CaO vs SiO₂; SiO₂ vs FeO; (d) (SiO₂ + CaO) vs FeO; (e) CaO vs LOI; and, (f) CaO vs Sr, for rocks of this study (filled squares) **Page 62**

Fig. 4.3. Bivariate plots of MnO vs: (a) CaO; (b) FeO; and, (c) SiO₂ for samples of the study area (filled squares) **Page 64**

Fig. 4.4. Plot of averaged bulk chemical analyses of banded iron-formations given in Table A2, as compared to analytical data from this study. The analyses are recalculated to 100% on an H₂O and CO₂-free basis. Total Fe is represented as Fe₂O₃. Data are from Gole and Klein (1981), Klein and Beukes (1989) and Beukes and Klein (1990a) **Page 65**

Fig. 4.5. A comparison of average transition metal contents of the Voëlwater BIF (filled squares), and those characterise the Kuruman and Griquatown BIFs, S. Africa (Klein & Beukes, 1989; Beukes & Klein, 1990a; Hälbich et al., 1993), the Brockman BIF of Australia (Trendall & Pepper, 1977; in Davy, 1983), as well as several Algoma- and Superior-type BIFs of Canada (Gross & McLeod, 1980). Analytical data are normalised using averaged crustal abundances of transition metals, as reported by Shaw (1980) **Page 67**

Fig. 4.6. Ternary diagram of Si-(Fe + Mn)-Al showing the fields defined for: (1) ironstones; and, (2) BIFs, by James (1969). Data from the present study are shown as filled squares **Page 68**

- Fig. 4.7.** Plot of Ca/Mg and Fe/Al ratios (on log scale) for rocks from this study. Also plotted are the fields of: (a) British Jurassic ironstones (Taylor, 1974); and, (b) Precambrian banded iron-formations (James, 1966) **Page 69**
- Fig. 4.8.** Plot of Si vs Al for BIF lithologies from the study area (filled squares), compared to hydrothermal and hydrogenous-detrital Fe-Mn deposits, and detrital-diagenetic ironstones (after Crerar et al., 1982) **Page 70**
- Fig. 4.9.** Ternary diagrams of: (a) Fe-(Ni+Cu+Co)x10-Mn; and, (b) Fe-Si(x2)-Mn, showing the positions of rocks from the study area (filled squares) relative to the fields of various marine sediments (after Bonatti et al., 1972; in Toth, 1980) **Page 72**
- Fig. 4.10.** Bivariate plots of: (a) Zr vs Cr; (b) TiO₂ vs Cr; (c) Y vs P₂O₅; and, (d) Y/P₂O₅ vs Zr/Cr for iron-formations from the study area (filled squares) (after Marchig et al., 1982) **Page 74**
- Fig. 4.11.** Bivariate plot of La vs Ce for banded iron-formations from the study area (after Toth, 1980) **Page 76**
- Fig. 4.12.** Chondrite-normalised LREE patterns for the study rocks and several other Superior-type BIFs of the world. Data are plotted in two diagrams (4.12a and b) where the average LREE pattern of the study rocks is compared with respective averages of BIFs from S. Africa (Beukes & Klein, 1990a) and Australia (1: Fryer, 1977a; 2: Danielson et al., 1992), as well as with average LREE data of BIFs from Canada and the U.S.A (1: Fryer, 1977a; 2: Danielson et al., 1992). Data were normalised using average chondrite values obtained from Evenson et al. (1978) **Page 77**
- Fig. 5.1.** Schematic diagram showing the three expected stages in the evolution of atmospheric oxygen. "O" indicates oxidising conditions; "R" indicates reducing conditions (after Kasting, 1987). **Page 86**
- Fig. 5.2.** Effects of suboxic diagenesis of increasing amounts of organic carbon on the mineralogy of banded iron-formations, as a result of progressive reduction of Fe⁺³ to Fe⁺² (after Walker, 1984) **Page 88**
- Fig. 5.3.** Idealised depositional environment of a banded iron-formation. The term "hematite" includes all ferric oxides and hydroxides (after Drever, 1974) **Page 90**
- Fig. 5.4.** Vertical structure of the ocean in the model for the deposition of BIFs (after Francois, 1986); w is the advective velocity **Page 91**

Fig. 5.5. Schematic depositional environment for iron-formation deposition and that of associated lithofacies in a marine system with a stratified water column in (a) a regressive stage, and (b) a transgressive stage. In (a) the photic zone reaches the floor of the deep shelf, allowing for cryptalgalaminated limestone deposition. In (b) the photic zone is considerably above the floor of the deep shelf, causing the deposition of various iron-formation facies and chert. The thick arrows labeled C (carbon) in (a) represent high carbon productivity and supply, and the narrow arrows in (b) represent much less carbon productivity and supply. The vertical depth scale is based upon the basinal reconstruction of Klein et al. (1987) (after Klein & Beukes, 1989) **Page 93**

Fig. 5.6. A summary of the main features of the genetic model for BIF and associated sedimentary rocks in the Hamersley Group (after Morris, 1993). Atmospheric conditions are modified by volcanic emissions. Supply of materials is (1) from surface ocean currents, giving rise to hematite varves, interrupted periodically by (2) high iron supply from upwelling currents and MOR hydrothermal output, both modified by (3) fine ash from distal sources. Photic depths are controlled by seasonal changes, and turbidity in the water and atmosphere. Precipitation of iron is primarily by oxidation in the photic zone, and the precipitate consolidates as ferric oxide; or is modified by partial reduction to form magnetite (2 ferric/1 ferrous); or is substantially reduced, dependant on the organic supply, augmenting iron in the sub-photic zone and leading to the precipitation of ferrous-rich compounds. Increasing volcanisms improves the nutrient content of sea-water for organic growth, but also adds limits to growth by curtailing the amount of available light, leading to S macroband (chert-carbonate-silicate BIF with shaly bands) deposition. Maximum organic supply with minimum oxidation results in black shales. The mineralogical distributions are qualitative **Page 95**

Fig. 5.7. a. Eh-pH diagram for part of the system Fe-C-Si-O-H. Assumed activities for dissolved species are: $Fe = 10^{-6}$, $Si = 10^{-3}$, $C = 10^{-3}$. Goethite and magnetite assumed as Fe^{+3} solid phases. **b.** Eh-pH diagram for part of the system Mn-C-S-O-H. Assumed activities for dissolved species are: $Mn = 10^{-6}$, $C = 10^{-3}$, $S = 10^{-3}$ (after Brookins, 1988) **Page 100**

Fig. 5.8. Model for deposition of Mn and BIFs from upwelling anoxic waters (after Button et al., 1982; modified after Cannon & Force, 1983, in Schissel & Aro, 1992) **Page 101**

Fig. 5.9. NNW-SSE section between the Mamatwan (operating) and Smartt (non-operating) Mn-mines of the Kalahari Manganese Field (see also Fig. A1) **Page 103**

Fig. 5.10. Estimates of abundances of sedimentary rock-types (log-scale) throughout Earth history (modified after Ronov, 1964; in Frakes, 1979) **Page 107**

Fig. 5.11. Schematic section through the Molopo Farms Complex area, illustrating the relationship between the complex and the surrounding country rocks. The relation of the Bushveld Complex to the country rocks is shown for comparison (after von Gruenewaldt et al., 1987) . . . **Page 112**

Fig. 5.12. According to Jacobsen and Pimentel-Klose (1987), the required Fe^{+2} for the genesis of BIFs would have derived from hydrothermal convection in active mid-ocean ridges . . **Page 114**

LIST OF TABLES

Table 1.1. Abundance of the 4 most common elements in the Earth's crust (after Mason, 1966; in Vokes, 1976, modified) **Page 1**

Table 1.2. Abundance of iron in common rock types (after Wedepohl, 1969, 1971; in Maynard, 1983, modified) **Page 2**

Table 1.3. Comparison of typical ironstones with iron-formations (after James, 1966; in Holland, 1984, modified) **Page 4**

Table 2.1. Simplified stratigraphy of the Transvaal Sequence in Griqualand West (modified after Beukes & Smit, 1987) **Page 15**

Table 3.1. Selected bibliography on the mineralogy and petrography of BIFs from three major Precambrian areas of the world **Page 30**

Table 3.2. The six most characteristic reflections of greenalite from this study, as compared to respective reflections of greenalites from the Mesabi Range (Youell & Steadman, 1961, in Zajac, 1974; Blake, 1965) and the Sokoman BIF (Zajac, 1974) **Page 35**

1. INTRODUCTION

1.1 General

Iron (Fe) is the fourth most common element of the earth's crust and the second most common metal after aluminium (Table 1.1). It is the backbone of modern civilisation and it accounts for more than 95% of all the metals consumed by man. A significant proportion of the remainder-Ni, Cr, W, V, Co and Mn-are mined principally to be added to iron to give it more desirable properties of strength and resistance to corrosion (Riley, 1959; Skinner, 1969).

Table 1.1. Abundance of the 4 most common elements in the Earth's crust (after Mason, 1966; in Vokes, 1976, modified).

Element	Weight %	Atom %	Radius (Å)	Volume %
O	46.60	62.55	1.40	93.77
Si	27.72	21.22	0.42	0.86
Al	8.13	6.47	0.51	0.47
Fe	5.00	1.92	0.74	0.43

Iron is present in practically all igneous and sedimentary rocks to the extent of a few percent (Table 1.2), with a little over 5% of the rocks of the outer "shell" of the earth consisting of iron. It has been mined from a variety of kinds of deposits (including the mafic magmatic Fe-Ti and P-Fe-Ti associations), but production is now almost entirely from ores which have resulted from secondary enrichment of two major rock-types, where the primary iron content exceeds 15%: **banded iron-formations (BIFs)** and **Phanerozoic ironstones** (Table 1.3). The former are typically thick sequences of various iron minerals interbedded with chert and deposited in large intracratonic basins of Precambrian age; the latter are usually thin sequences, often oolitic in character, which were deposited in

localised areas (Maynard, 1983; Guilbert & Park, 1986).

Table 1.2. Abundance of iron in common rock types (after Wedepohl, 1969, 1971; in Maynard, 1983, modified).

Various lithotypes	FeO (%)	Fe ₂ O ₃	Fe ₂ O ₃ /FeO + Fe ₂ O ₃
Alkali-olivine Basalts	7.9	4.2	0.35
Tholeiitic Basalts	9.5	3.2	0.25
Granodiorites	2.6	1.3	0.33
Granites	1.5	0.8	0.35
Quartz Arenites	0.2	0.4	0.67
Lithic Arenites	1.4	3.8	0.73
Graywackes	3.5	1.6	0.31
Arkoses	0.7	1.5	0.68
Red Shales/Slates	1.26	5.36	0.81
Green Shales/Slates	1.42	3.48	0.71
Black Shales/Slates	4.88	0.52	0.10
Seawater (as Fe)	0.007 ppm		

According to Gross (1965, 1973, 1980), two principal types of Precambrian banded iron-formations can be recognised, based on the characteristics of their depositional basins and the kinds of associated rock:

1. the **Lake Superior**-type, which was deposited with quartzite, dolomite and black shale in continental-shelf environments of Early Proterozoic age; and,
2. the **Algoma**-type, which is found in all ages of rock (confined to the Archaean according to some authors, e.g. Eichler, 1976; Blatt, 1982; James, 1983; Pirajno, 1992; Evans 1993; see also Fig. 1.1), is associated with greywacke sedimentary units and volcanic rock assemblages, and is closely related to volcanic arcs, rift zones and deep-seated fault and fracture systems.

For the sake of convenience and in order to avoid any misinterpretations or misconceptions of semantic nature, the writer will adopt the above terminology,

sometimes modified as **BIF s.s.** (*sensu stricto*) and **BIF s.l.** (*sensu lato*) respectively, on the basis of the age restriction that characterises the former. The main reason for the above modification is the uncertainty whether or not the genesis of the large volumes of Superior-type BIFs in Precambrian Shields of the world may have been (directly or indirectly) related to mid-ocean ridge (MOR) geotectonic environments, hot spot activity (e.g. Morris, 1993), or even simple rifting processes (e.g. Kimberley, 1989b). This has resulted in several

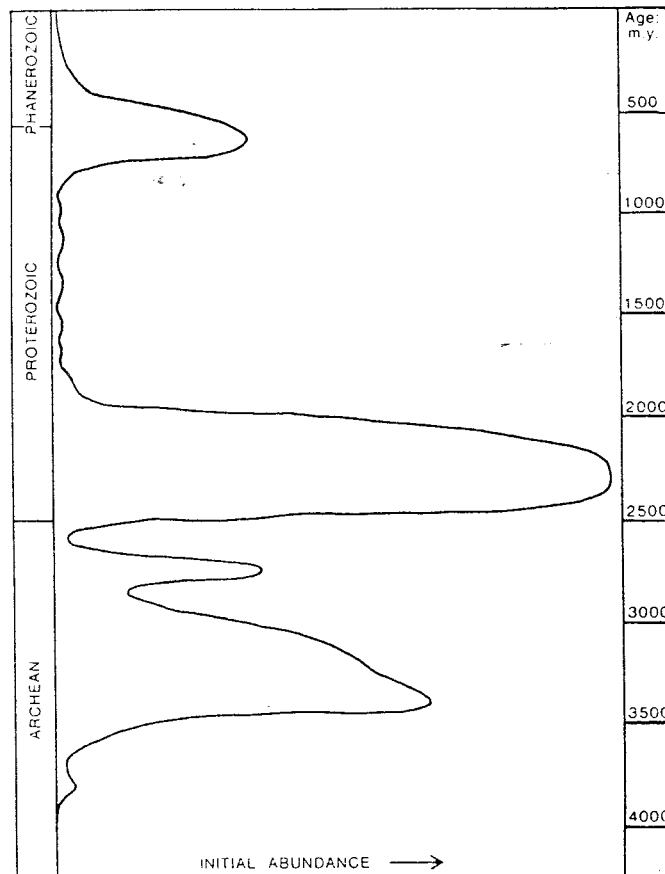


Fig 1.1. Estimated abundance of iron-formation deposited through geologic time. Horizontal scale is non-linear, approximately logarithmic; range 0-10¹⁵ tonnes (after James, 1983).

confusions and misinterpretations in the past, such as the characterisation of the, presumably Superior-type, BIFs of the Hamersley Group in Western Australia and of the Transvaal Basin in South Africa, as Algoma-type without further justification (Dimroth, 1975).

It should be also added that it is beyond the scope of this study to establish new terminologies or even discuss the problems of nomenclature for iron-rich sedimentary rocks. Excellent reviews can be found in the papers by Beukes (1980c), Trendall (1983a) and Kimberley (1978, 1989a). Other terms commonly used in the literature to describe certain types of these rocks, such as Clinton- and Minette-type ironstones, taconites, itabirites, jaspilites, etc., will be used in this study along with brief rock descriptions, whenever this is regarded necessary.

Table 1.3. Comparison of typical ironstones with iron-formations (after James 1966; in Holland, 1984, modified).

	Ironstones	Iron Formations
<i>Age</i> Minimum age Major development Maximum age	Pliocene L. Paleozoic & Jurassic M. Precambrian (ca. 2.0 b.y.)	Cambrian or L. Precambrian M. Precambrian (2.0-2.5 b.y.b.p.) E. Precambrian
<i>Thickness of Major Units</i>	a few meters to a few tens of meters	50-600 meters
<i>Original Areal Extent</i>	individual basins rarely more than 100 miles in maximum dimension	some basins several hundred miles long
<i>Physical Character</i>	massive to poorly banded; silicate and oxide-facies oolitic	thinly bedded; layers of Fe-oxide, Fe-carbonate, or Fe-silicate alternating with chert; chert ca. 50%
<i>Mineralogy of unmetamorphosed units</i> goethite hematite magnetite chamosite-berthierine glauconite siderite calcite dolomite-ankerite pelletal collophane greenalite stilpnomelane riebeckite minnesotaite quartz (chert) pyrite	dominant fairly common relatively rare dominant primary silicates minor common common common relatively abundant in some none none none none rare common	none common common absent absent common relatively rare common absent common common common common major constituent common
<i>Chemistry</i>	no distinctive aspect except high iron content	remarkably low in Al, Na, K, and minor elements; phosphorous content generally much lower than in ironstones
<i>Associated rocks</i> No distinctive differences. Both ironstones and iron formations are typically interbedded with shale, sandstone, or graywacke, or their metamorphosed equivalents. Carbonate rocks are common in iron formation sequences; limestone and/or dolomite in ironstone sequences not rare but subordinate to clastic rocks in immediately associated areas.		
<i>Relative abundance of types</i>	1. oxide 2. silicate (chamosite) 3. carbonate (siderite) 4. sulfide	1. oxide 2. silicate 3. carbonate 4. sulfide

1.2 BIFs and Mn

Another metallic element with geochemical characteristics similar to iron is **manganese** (Mn), which is twelfth in abundance among the elements in the earth's crust (0.1%). This fact, in accordance with the value given for iron in the previous paragraph, indicates that the latter is fifty times as common as manganese. The concentration factor necessary to produce an ore of iron ranges from about 4 to 14; for manganese it is more than 350. Hence, it is not surprising that ore-bodies of iron greatly outnumber those of manganese (Taylor, 1974; Sidder, 1991; Gross, 1991).

It is extensively reported in the literature, that areas with major Proterozoic BIF occurrences worldwide, such as the Lake Superior Region in the U.S.A, the Krivoy Rog Basin in the former U.S.S.R, the Hamersley Basin in Australia and the Labrador Trough in Canada, have been the leading centers of Fe-ore exploration and mining activities (Gross, 1965; Anderson, 1970; Marsden, 1970; Marsden et al., 1970; Dutton & Zimmer, 1970; Belevtsev, 1973; MacLeod, 1973; Trendall, 1975, 1979, 1983b; Sokolov & Grigorev, 1977; Blockley et al., 1989; Blockley & Myers, 1990; Harmsworth et al., 1990), whereas Mn-ore was very seldom found in those areas in economically viable quantities (Fig. 1.2). There are only a few exceptions on a global scale, where economic manganese ores are either hosted or are intimately associated with banded iron-formations (Roy, 1981) and these include:

- the banded iron-formations and associated Mn-deposits in Minas Gerais, Brazil (Van N. Dorr, 1973a,b);

- the iron-manganese associations of the Singhbhum Region, Eastern India (Banerji, 1977; Rai et al., 1980); and,

- the Fe-Mn sediments of the well-known "Kalahari Manganese Field" in South Africa (De Villiers, J., 1960; De Villiers, P.R., 1970; Kleyenstuber, 1979, 1984, 1985, 1991; Beukes et al., 1982; Nel, 1984; Dixon, 1985, 1986, 1989; Beukes & Kleyenstuber, 1986; Nel et al., 1986; Miyano & Beukes, 1987;

Grobelaar, 1988; Gutzmer & Beukes, 1993; see also Fig. A1).

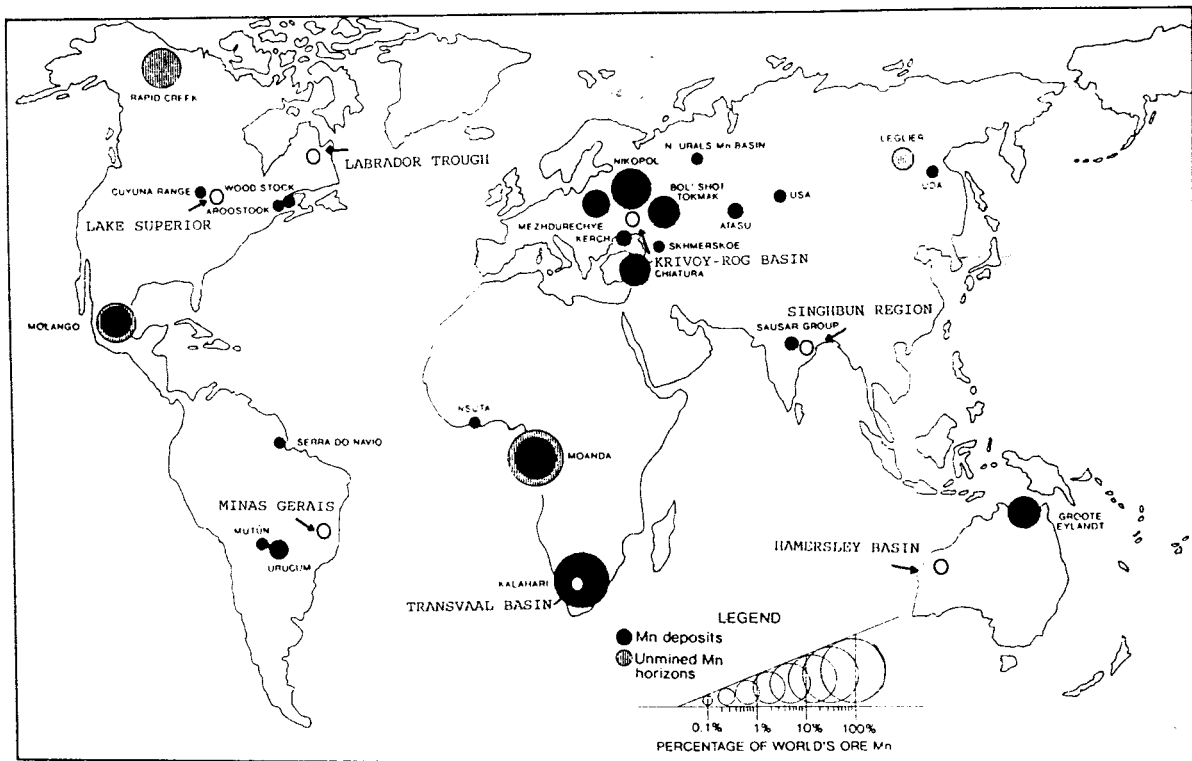


Fig. 1.2. Location of major manganese deposits and BIF occurrences in the world. Note the absence of Mn-deposits in the Lake Superior Region, the Labrador Trough and the Hamersley Basin, whereas the Mn-deposits in Nikopol, Tchiatura and Bolshoi Tokmak are Oligocene in age and have no relation with the BIFs of the Krivoy Rog Basin (modified after Laznicka, 1992).

Any correlation between the above major Fe-Mn provinces in terms of regional geological signature appears to be very difficult due to the limited literature available, and will not be attempted in this chapter. However, the writer believes that the banded iron-formations and the interbedded manganese deposits of the Kalahari Field represent a rather unusual lithological association, which becomes even more exceptional if certain facts are taken into account, such as:

- The actual size as well as the relative volume of the manganese deposits compared to the host BIF. The Kalahari Mn-bodies attain considerable thicknesses (up to 45m), they carry some 50% of the metal accumulated in Mn-ores of the world (Laznicka, 1992), and they are intercalated with essentially thin banded iron-formation units;

-The distinct mineralogical and petrographic character of BIFs that were encountered in the stratigraphic sequence of the Voëlwater Subgroup during the present study, as compared to the Superior-type "banded hematite jaspers (BHJ)" of the Indian ores and the "itabirites" of Brazil (Van N. Dorr, 1973a,b; Banerji, 1977; Rai et al., 1980; Acharya et al., 1982; see also §6);

-The virtual absence of any Mn-ores of economic grade in North America, Western Australia and former U.S.S.R in direct association with Proterozoic BIFs, with the only exception perhaps being the very-low grade ores of the Cuyuna range, Minnesota, where Mn has been mined as a by-product of Fe-ores (Sidder, 1991).

It must be stressed that the writer does not intend to propose **"the"** genetic model which will satisfactorily answer all the existing questions or resolve all the arguments regarding the Kalahari Mn-deposits. The main objective of this research is to supply further information about the rocks that host these very important ores, as well as to put forward some of the writer's views concerning their depositional environment, the physicochemical conditions of their precipitation and diagenesis and to determine to what extent any post-depositional processes (deformation and/or metamorphism, hydrothermal alterations etc.) have affected these rocks. This attempt will be made in two main stages:

-A detailed description and interpretation of this unusual occurrence of BIF and Mn-rich sediments in the same stratigraphic sequence, focusing mainly on the mineralogical, petrographic and geochemical characteristics of the host rock; any correlation between all the different lithotypes present, on both a vertical and a lateral sense (changes in mineralogical and geochemical composition, thickness variations, etc.); evidence for tectonic and/or metamorphic effects; and similarities with, and differences from other BIF occurrences in the world, whenever the literature allows for systematic comparisons.

-A compilation of all the results of this study, combined with critical evaluation of all the theories that have been suggested in the past for the

deposition of both BIFs and the Kalahari Mn-rich sediments, **irrespective of their current validity**, since none of them alone has managed to explain adequately the genesis of these enigmatic rock-types so far. The expected outcome of such an attempt should be an integrated model for the essentially contemporaneous BIF-Mn depositional event, which took place at Early Proterozoic times and led to the formation of probably the largest land-based Mn-accumulation on earth.

1.3 Bibliographic review

The origin of the sedimentary rocks commonly known in the literature as "Precambrian banded iron-formations (BIFs)", started receiving considerable attention in the early 1920's, with the publication of two papers by Van Hise and Leith (1911), and Grout (1919), on the geology of the Lake Superior Region and on the nature and origin of the Biwabik banded iron-formation of the Mesabi Range, Minnesota, respectively. In 1922, John Gruner, a pioneer in Precambrian geology and mineralogy, published his first paper on the origin of sedimentary iron-formations, as an outcome of his personal research on the Biwabik iron-formation. Several other papers by the same author followed, concentrated mainly on pure mineralogical studies of sheet-structure minerals, which resulted in the determination of the crystal structure of greenalite (1936) and stilpnomelane (1937, 1944a), and the discovery of minnesotaite (1944b), although the amphibole grunerite was neither named after him, nor discovered by him (Doe, 1972).

In 1954, Harold James published a paper in the Bulletin "Economic Geology" titled: "Sedimentary Facies of Iron-Formation", which marked the beginning of a new era in the research of this peculiar rock-type in the geological record. Numerous papers on the mineralogy, geochemistry, sedimentology and origin of these rocks were subsequently published in various geological journals and special publications. A considerable number of these papers has been included and will be found in the reference list of this study. Several geologists dedicated

their scientific potential to the study of banded iron-formations for more than 20 years, paving the path to our current knowledge of virtually all the aspects of iron-formation deposition. The peak was reached in 1973 with the UNESCO-published volume on the "**Genesis of Precambrian Iron and Manganese Deposits**" resulting from the 1970 Kiev Symposium, and the Economic Geology Special Issue on "**Precambrian Iron-Formations of the World**". Research activities and further publications on BIFs continued in the following years and culminated in the publication of two milestone volumes of the series: "Developments in Precambrian Geology", dealing with Precambrian iron-formations: The first was published in 1982 under the title: "**Precambrian Banded Iron-Formations: Physicochemical Conditions of Formation**" and it was followed by a volume entitled: "**Iron-Formation: Facts and Problems**" one year later. The latter was a compilation of several papers on banded iron-formations from all the major Precambrian-aged depositional basins of the world, including overviews of their geochemistry, diagenesis and metamorphism, palaeontology and palaeoecology, distribution in space and time and supergene alteration. The last two textbooks are essentially the most updated reviews of banded iron-formations that can still be found in any scientific library of the world, since the interest in BIF research has remarkably diminished over the past 10 years.

As far as the BIFs of the Transvaal Sequence are concerned, significant amounts of work have been done by LaBerge (1966), Button (1976a,b), Beukes (1973, 1978, 1980a,c, 1983, 1984, 1986a,b), Perry and Ahmad (1980), Lamprecht and Hälbich (1988), Klein and Beukes (1989), Beukes and Klein (1990a,b), Beukes et al. (1990a,b), Dirr and Beukes (1990), Altermann and Hälbich (1990), Hälbich and Altermann (1992), Hälbich et al. (1992, 1993), Bau and Dülski (1992, 1993), Bau (1993) and Frick (1986), the latter being the only paper among them with some published bulk geochemical data on the Voëlwater BIF. Very little work has actually been done on the latter rocks, which represent the youngest member of iron-formation deposition in the Transvaal Sequence and host the major Mn-ores in the Northern Cape Province. This is due to the fact that samples of the Voëlwater BIFs have only recently become available from

drilling in the Kalahari basin, with the latter being almost completely covered by thick Tertiary sands and calcretes. On the other hand, the manganese deposits of the Kalahari Field have been extensively studied by Boardman (1941, 1964), Frankel (1958), J. De Villiers (1960), P.R. De Villiers (1970), Söhnge (1977), Kleyenstuber (1979, 1984, 1985), J.E. De Villiers (1983, 1990), Nel (1984), Beukes and Kleyenstuber (1986), Nel et al. (1986), Dixon (1985, 1986, 1989), Jennings (1986), Grobelaar (1988), Beukes (1993) and Gutzmer and Beukes (1993), and any further information regarding the Voëlwater BIF will be found in those papers in relatively limited extents, with indeed only a few exceptions (J. De Villiers, 1960; Kleyenstuber, 1984, 1985).

2. REGIONAL GEOLOGICAL SETTING

2.1 The Transvaal Sequence

The Transvaal Sequence occupies some 250,000 km² of the Republic of South Africa and Botswana and is preserved in two structural basins, namely **Transvaal** and **Griqualand West** (Fig. 2.1). The former is developed in the Transvaal Province, in parts of the Orange Free State and in Eastern Botswana and is also known as the north-eastern sub-basin; the latter is located in the Northern Cape Province and adjoining parts of Botswana, and is also referred to as the south-western sub-basin (Button, 1986).

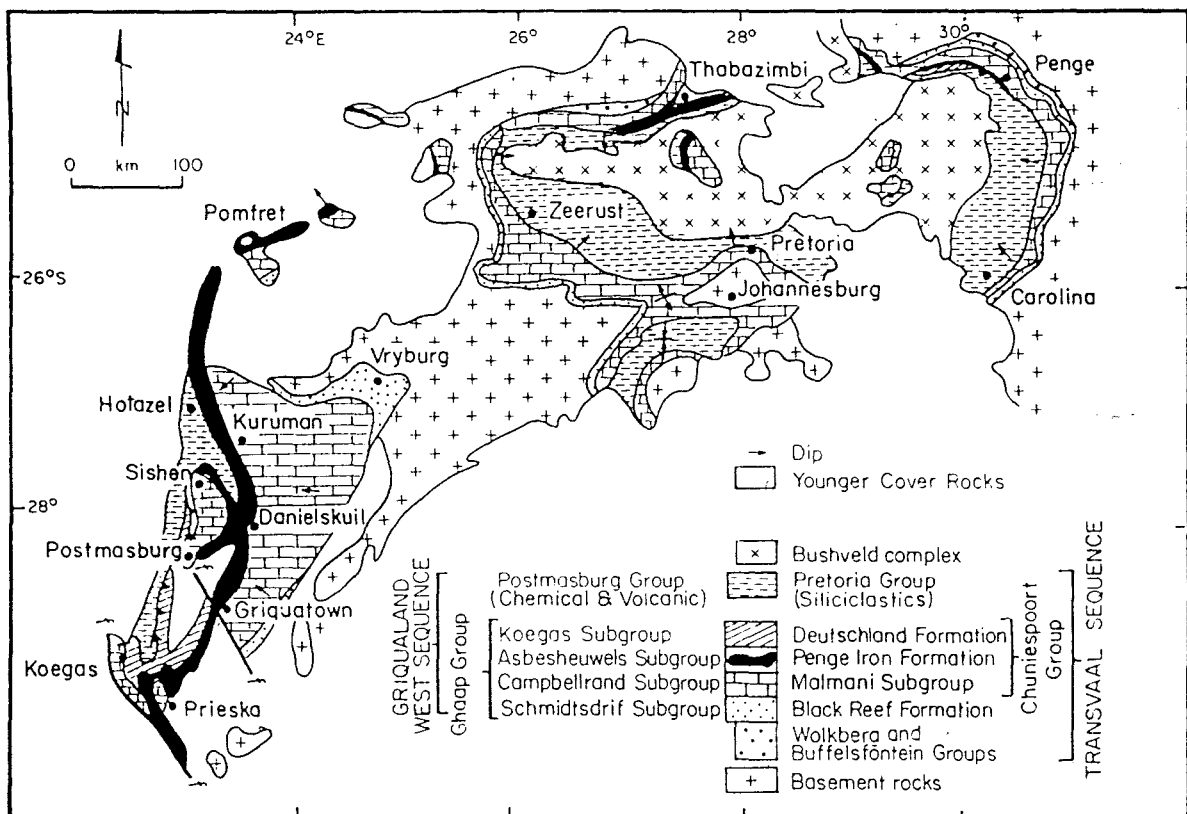


Fig. 2.1. Simplified geology of the Transvaal and Griqualand West Sequences (after Beukes, 1987).

Rocks of the Transvaal Sequence may rest on either Archaean gneisses, granites

and greenstone belts, or on Ventersdorp volcanics and younger sediments of the Witwatersrand Supergroup. The gross stratigraphic subdivision of the Transvaal rocks is very similar in both the sub-basins mentioned above: it consists of a basal, mixed siliciclastic and volcanic unit, followed conformably by a chemical sedimentary unit which is in turn unconformably overlain by a mixed chemical-volcanic-siliciclastic rock unit. Facies changes are most pronounced in the latter unit and are represented by the siliciclastics of the Pretoria Group in the Transvaal basin and the mixed volcanogenic-chemical sedimentary succession which characterizes the Postmasburg Group in Griqualand West (Beukes, 1983).

The age of the Transvaal rocks is Proterophytic (Beukes, 1983, 1986a), which according to Cloud (1972) marks the time span between 2.6 and 1.9 Ma. This corresponds to the Lower Proterozoic eon, and substitutes at the same time the term "Upper Proterozoic" with the "true (or "proper", according to the same author) Proterozoic" one. In terms of absolute ages, the age of the Transvaal Sequence can only be bracketed between 2700 and 2061 Ma, on the basis of the lowest of the most reliable datings of the underlying Ventersdorp volcanics, and the approximate age of the, post-Transvaal, Bushveld igneous intrusion respectively (Beukes, 1983; Truswell, 1990b).

The Griqualand West area (Fig. 2.2) is noted for its well-developed iron-formation units, although rocks of this type are not absent from the Transvaal sub-basin (e.g. Penge iron-formation). Several BIF units are encountered throughout the stratigraphic sequence of the Griqualand West Supergroup, with the best examples being the well-studied Kuruman and Griquatown iron-formations, which comprise the Asbesheuwels Subgroup and attain a thickness of up to 1000m (Beukes, 1983). It is therefore essential to make a brief description of the geology of Griqualand West focusing primarily on the various stages of iron-formation deposition, whereas no further reference will be made on the portion of the Transvaal Sequence in the Transvaal Province. For the terminology used in this chapter the reader is referred to the paper: "Suggestions towards a Classification of, and Nomenclature for iron-formations" (Beukes, 1980c).

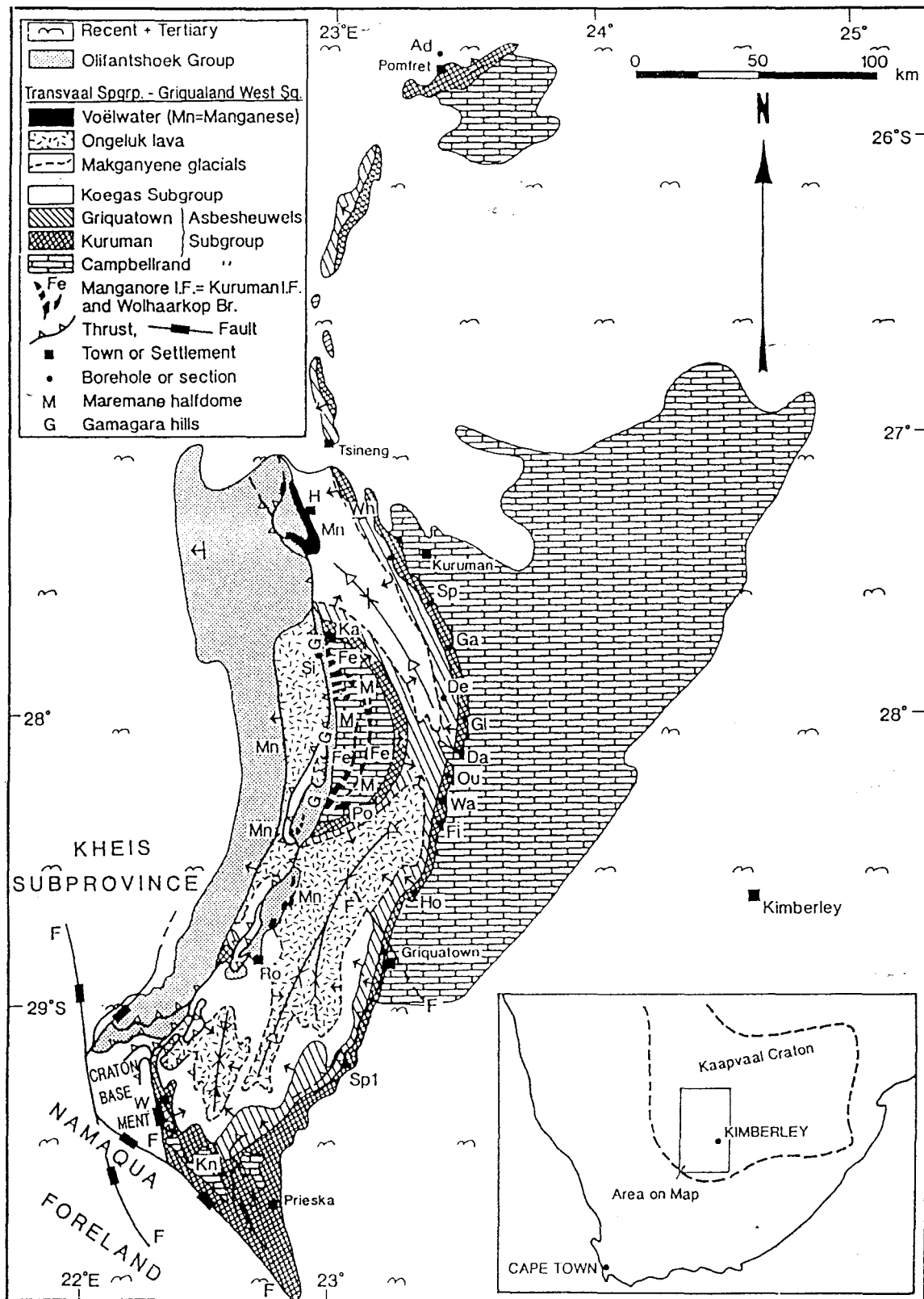


Fig. 2.2. Simplified Geological map of the Transvaal Sequence in Griqualand West. Ts = Tsineng; Ku = Kurumankop; Wh = White Bank; Sp = Spitsberg; Ga = Gakarosa; De = Derby; Gl = Gladstone; Da = Danielskuil; Ou = Ouplaas; Wa = Warrendale; Fi = Finsch Mine; Ho = Hopfield; Sp-1 = Spienskop; Kn = Klein Naute; W = Westerberg; Ro = Rooinette; Po = Postmasburg; Ka = Katu; Si = Sishen; H = Hotazel (after Hälbig et al., 1993).

2.2 The Transvaal Sequence in Griqualand West

The Early Proterozoic Griqualand West Sequence consists of essentially unmetamorphosed volcanic, clastic and chemical sedimentary rocks which can be divided in two major groups: The **Ghaap Group**, a relatively pure chemical sedimentary succession, which is overlain by a mixed volcanic-chemical rock unit termed the **Postmasburg Group** (Beukes, 1986a). A simplified stratigraphic column with all the further subdivisions of the above-mentioned groups in Griqualand West is shown in Table 2.1.

It should be stressed that the Griqualand West strata were only mildly deformed prior to the deposition of the Olifantshoek Supergroup, mainly in the form of open folding (e.g. Maremane Dome; Beukes, 1983). However, major tectonic disturbances in the form of intense folding and thrusting which characterize the post-Olifantshoek period have obliterated the lithostratigraphic succession in Griqualand West (Fig. 2.3). Beukes and Smit (1987) report that rocks of the Gamagara Formation in Griqualand West can be correlated with the Mapedi shales of the Olifantshoek Sequence, and that there is strong evidence from several localities that Transvaal strata have been thrust over rocks of Olifantshoek age. It is thus believed, that lithologies such as the Gamagara red-beds do not form part of the Griqualand West Sequence and for that reason they have been excluded from the stratigraphic column.

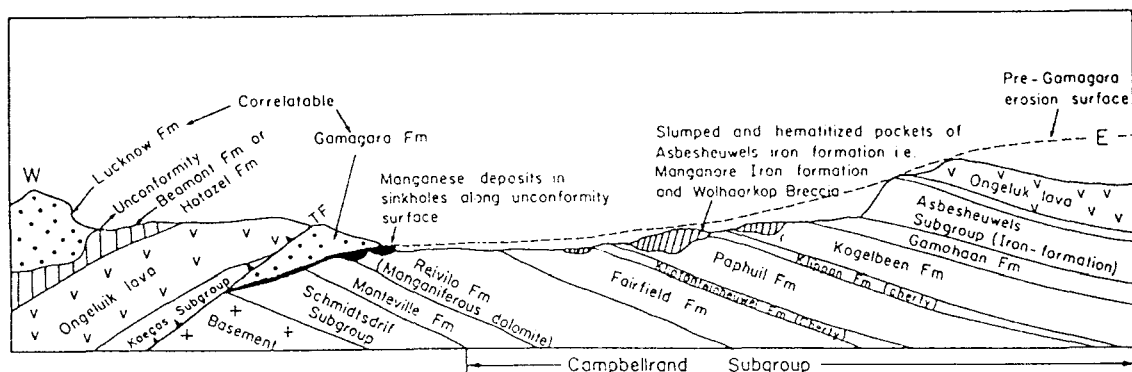


Fig. 2.3. East-west stratigraphic section through the Maremane Dome in Griqualand West, illustrating thrust faulting and the relationship of the ore deposits to the unconformity at the base of the Gamagara Formation (after Beukes, 1986b).

Table 2.1. Simplified stratigraphy of the Transvaal Sequence in Griqualand West (modified after Beukes & Smit, 1987).

SUPER GROUP	GROUP	SUB GROUP	FORMATION	MAJOR LITHOLOGY	APPROXIMATE THICKNESS IN M
G R I Q U A L A N D W E S T	POSTMASBURG	VOEL- WATER	Mooidraai	Dolomite, chert	250
			Hotazel	Fe-formation, Mn, lava	
			Ongeluk	Andesitic lava	900
			Makganyene	Diamictite	50-150
	GHAAP	KOEKAS	Nelani	Shale	400
			Rooinukke	Fe-formation	
			Naragas	Quartz-wacke, shale	240-600
			Kwakwas	Riebeckitic slate	
			Doradale	Fe-formation	
			Pannetjie	Quartz-wacke, shale	
			Griquatown	Cl. text. Fe-formation	200-300
			Kuruman	Microbanded Fe-formation	150-750
		CAMBELLRAND	Gamohaam	Sparry limestone, shale	1500-1700
			Kogelbeen	Dolomite, limestone	
			Klippan	Cherty dolomite	
			Papkuil	Dolomite	
			Klipfonteinheuwel	Cherty dolomite	
			Fairfield	Sparry dolomite	
	Reivilo		Micritic dolomite		
	Monteville		Dolomite, limestone, shale		
	SCHMID- TSTDRIF	Lokammona	Shale	10-250	
Boomplaas		Dolomite, limestone, shale			
Vryburg		Quartzite, shale, lava			

(*). Note that in the above table are not included: i. the Naute and Naragas Formations of the Prieska facies, which are lateral equivalents of the Campbellrand Subgroup, as well as: ii. the Beaumont Formation which is considered to be equivalent of the Voëlwater Subgroup.

2.2.1 The Ghaap Group

The Ghaap Group starts with the interbedded siliciclastic and carbonate rocks of the Schmidtsdrif Subgroup which is followed by several carbonate facies of the Campbellrand Sequence. The first major stage of banded iron-formation deposition is represented by the deep-water facies microbanded ferhythmites of the Kuruman iron-formation. These rocks are in turn overlain by the shallower-water, clastic-textured Griquatown iron-formation lithotypes. The latter sediments grade up to the Koegas quartz-chlorite mudstones and wackes which were probably deposited in a fresh-water lake (Beukes, 1984, 1986a). According to Beukes (1983) and Beukes and Klein (1990a,b), the increase in the grain size of the iron-formations observed in the Ghaap Group probably reflects filling of the depositional basin, with resultant upward shallowing and an increase in energy conditions (storm-dominated deposits). The sequence attains a maximum thickness of approximately 4000m and is terminated by a regional unconformity which separates rocks of the Ghaap Group from diamictite beds of the Makganyene Formation.

2.2.1.1 *The Schmidtsdrif Subgroup*

The base of the Ghaap Group is formed by the Schmidtsdrif Subgroup (Fig. 2.4) which comprises: i. feldspathic arenites, quartz arenites, quartz wackes, argillites, carbonate rocks and lavas of the **Vryburg** Formation; ii. carbonate rocks and argillites of the **Boomplaas** Formation; and, iii. tuffaceous lagoonal siltstones and shales, carbonate oolite shoal and stromatolite reef deposits, banded siderite lutites and pyritic carbonaceous shales of the **Lokammona** Formation (Beukes, 1979). The banded lutites of the Lokammona Formation represent devitrified, chertified and sideritized volcanic ash beds, and their lagoonal setting is rendered coincidental, since the presence of devitrified volcanic ash and lapilli in the form of chert bands and nodules has also been observed in other units of the Schmidtsdrif Subgroup (Beukes, 1983).

2.2.1.2 *The Campbellrand Subgroup*

The Campbellrand Carbonate Sequence (Fig. 2.4) consists of two major lithofacies:

1. The shallow water, stromatolitic carbonate platform facies of the **Ghaap Plateau**, which comprises:

- intertidal to supratidal light-grey cherty dolsparites;
- platform lagoonal cryptalgal laminated dolmicrites; and,
- subtidal stromatolitic dolmicrite mounds (Beukes, 1978, 1980b), and:

2. The **Prieska** clastic-algal laminated ferruginous carbonates with carbonaceous shale, banded ferruginous chert and basic tuffs, which represent deeper water carbonate turbidite facies (Beukes, 1980b, 1983). The platform edge facies is represented by oolite shoal deposits and elongated stromatolitic columns, i.e. stromatolite reefs (Beukes, 1983).

The Prieska turbidites represent debris which derived from the Ghaap Plateau carbonate platform and washed down onto a deep shelf below a storm-wave base (Beukes, 1978). The distal facies of these turbidites have been ankeritized and partially silicified, giving rise to banded ferruginous cherts. The latter interfinger with carbonaceous shales which were deposited in an euxinic basin in front of the carbonate platform. Mafic tuffaceous beds are interbedded with the Prieska facies carbonate turbidites, indicating contemporaneous volcanic activity. However, according to Beukes (1983), no relation between the ankerite banded-cherts and these tuffs exists, in terms of source of iron and silica.

A thin iron-formation unit is known to occur in rocks of the Campbellrand Subgroup, extending from the basinal Prieska facies into the shallow-water Ghaap Plateau facies. It is known as the **Kamden** Member (Beukes, 1983) and it is considered to be a result of deposition during a transgressive event. The significance of this iron-formation lies in the presence of jasper bands which indicate precipitation under conditions of high oxygen fugacity, necessary for the oxidation of iron from the ferrous to the ferric state.

2.2.1.3 *The Asbeshuewels Subgroup*

a. **The Kuruman BIF**

The base of the Kuruman iron-formation (Fig. 2.4) is formed by ankerite-banded cherts of the **Kliphuis** Member (Fig. 2.5), which are similar to the ankeritized carbonate turbidites of the Campbellrand Sequence (Beukes, 1983). These rocks are followed by stacked stilpnomelane lutite → ferhythmite macrocycles of the **Groenwater** Member (Fig. 2.5), which were deposited in an open shelf environment (Beukes, 1984). These macrocycles in their most complete form consist of (Beukes, 1980a, 1983; from bottom to top):

- stilpnomelane lutite;
- siderite-microbanded chert;
- siderite\siderite-silicate bandrhythmite;
- siderite\siderite-silicate (+ magnetite) bandrhythmite;
- magnetite-hematite\magnetite-siderite ribbonrhythmite.

It should be noted that the chert content and thickness of chert mesobands decrease upwards away from stilpnomelane lutite beds and sharply increase again immediately below such beds (Beukes, 1983, 1984).

The stilpnomelane lutite beds represent altered acidic volcanic ash beds which were deposited during periods of explosive vulcanicity, probably under acidic conditions. Evidence for volcanic input in these stilpnomelane-bearing iron-formations has been considered the presence of tricusate shards (La Berge, 1966). On the other hand, the macrocyclicality described above is believed to be of a mixed volcanic-biological origin (Beukes, 1983). The combination of both these processes is invoked, in order to account for the presence of ferhythmite microbands in the macrocycles which require neutral-alkaline conditions to precipitate. During periods of volcanic quiescence, the flourishing of photosynthesizing organisms would promote the precipitation of siderite and hematite bands in the form of seasonal geochemical varves. Mesobanding in the ferhythmites is attributed to diagenetic processes, which also led to the

development of magnetite, stilpnomelane and riebeckite (Beukes, 1983, 1984).

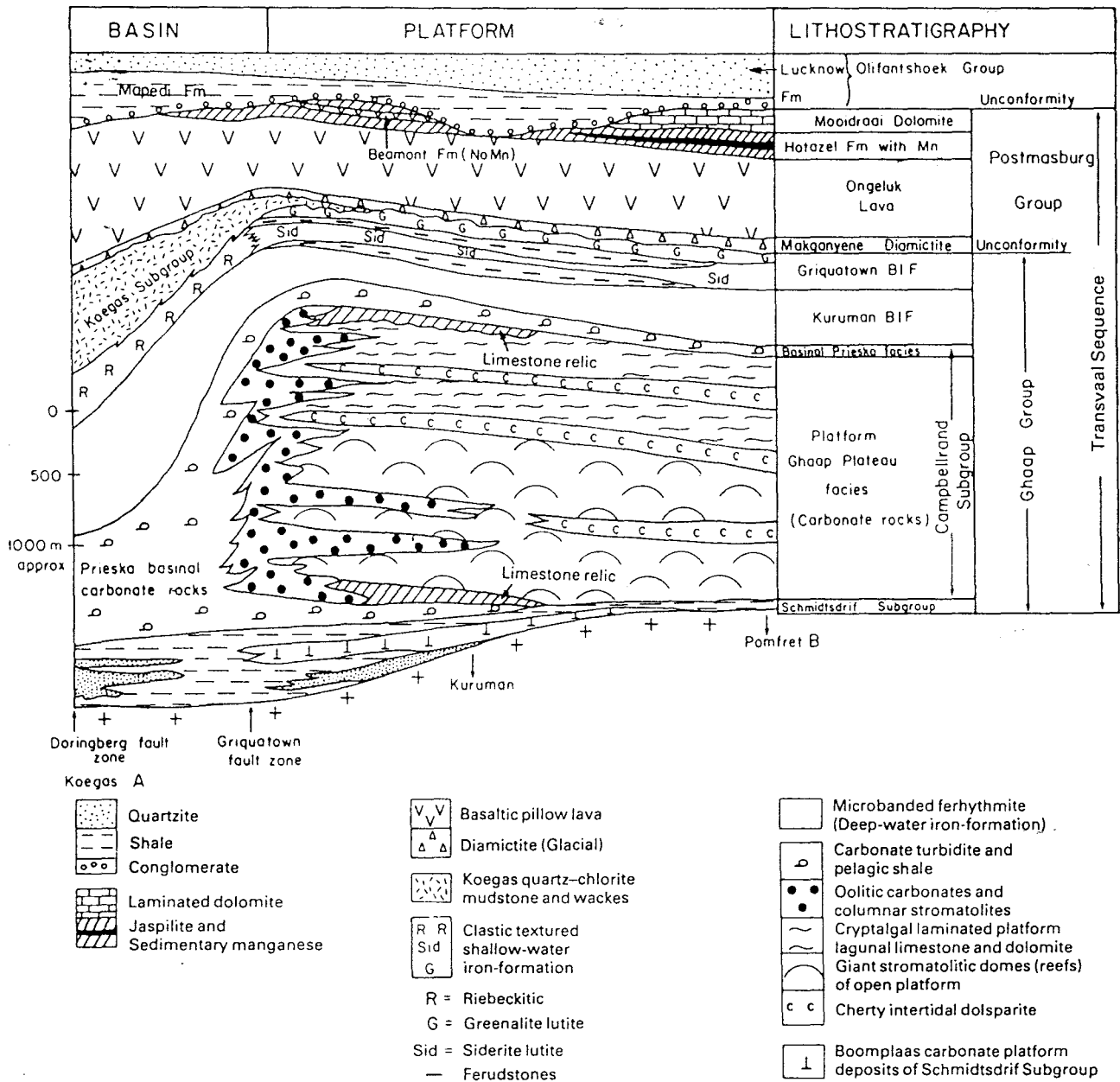


Fig. 2.4. South-north section illustrating stratigraphic and sedimentological facies relationships in the Transvaal Sequence in Griqualand West (after Beukes, 1986a).

Towards the top of the stratigraphic sequence, the chert content decreases and

greenalite-siderite rhythmites almost devoid of chert mesobands which belong to the **Riries Member**, are found immediately above the Groenwater Member (Fig. 2.5). A shift towards well-established, neutral-weakly alkaline conditions of precipitation is now more apparent due to the abundance of greenalite (Beukes, 1983). The greenalite-siderite ferhythmites were probably deposited at the toe of a slope, below wave-base. Notwithstanding, the presence of grainflow mesobands in the rhythmites indicates that part of these sediments were deposited along a platform slope.

A rapid transition from greenalite rhythmites to orthochemical and allochemical iron-formations of the **Ouplaas Member** (Fig. 2.5), marks an abrupt change in the depositional environment towards the top of the Kuruman sequence. Siderite lutites and sideritic grainstones and discstones were deposited on a shallow-water platform above wave-base under alkaline conditions (Beukes, 1978, 1983, 1984), thus completing the upward-shallowing progradational sedimentary cycle which characterizes the Kuruman iron-formation (Beukes, 1983).

b. The Griquatown BIF

Asymmetrical, upward-coarsening orthochemical → allochemical iron-formation megacycles characterize the **Danielskuil** and **Skietfontein Members** (Fig. 2.5) of the Griquatown iron-formation (Fig. 2.4), as well as the Ouplaas Member of the Kuruman iron-formation which was described in the previous paragraph. The megacycles most typically consist of a zone rich in banded siderite lutite, followed by sideritic grainstones and disclutites which become finer upwards into greenalite lutite (Beukes, 1980a, 1983, 1984).

The siderite lutites which belong to the Danielskuil Member, are considered to be of abiogenic origin in a weakly alkaline and reducing epeiric sea. The greenalite lutites represent lagoonal precipitates that were brought about by the inflow of acidic freshwater from a nearby low-lying land area (Beukes, 1978, 1983). Chert mesobands and magnetite are again, as in the case of the Kuruman

iron-formation, of (early) diagenetic origin. The Skietfontein Member greenalitic disclutites, on the other hand, probably represent storm wave deposits on supratidal flats, with the poorly sorted and angular chert disks originating from cherty hardgrounds which were broken up either by slumping or by wave action (Beukes, 1978).

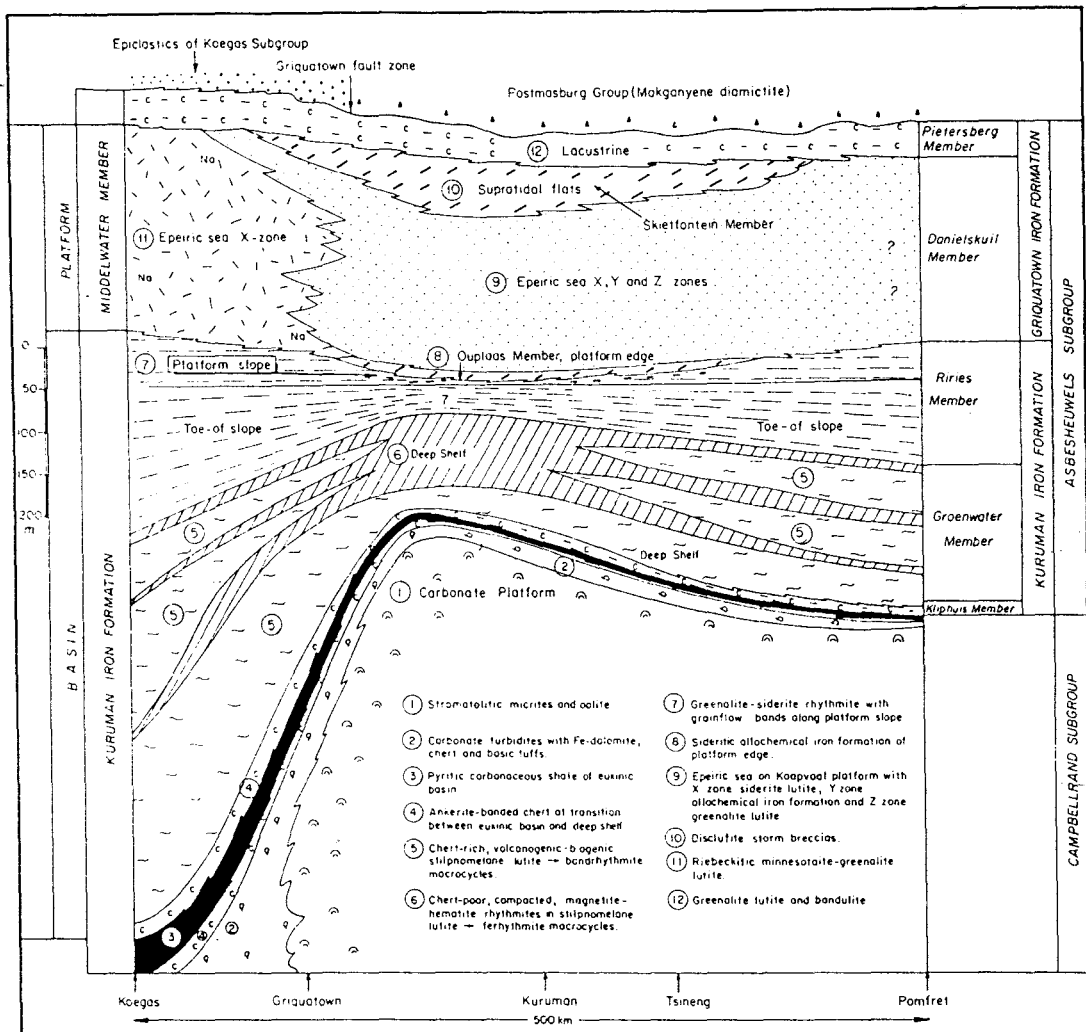


Fig. 2.5. South-north section illustrating stratigraphic relationships and inferred palaeodepositional environments of the Asbesheuwels Subgroup in Griqualand West (after Beukes, 1983).

The iron-formations of the Daniëlskuil Member interfinger basinwards with minnesotaite-greenalite lutites of the Middelwater Member (Fig. 2.5). The minnesotaite was formed under very low metamorphic reactions at the expense

of greenalite which was deposited in a shallow water environment below wave base. The abundance of riebeckite in these rocks indicates that the depositional basin was partly or totally enclosed (Beukes, 1978, 1983).

Finally, the banded greenalite lutites of the **Pietersberg** Member (Fig. 2.5), represent the basal part of an upward-coarsening sedimentary cycle which marks the transition between the Griquatown iron-formation and the Koegas Subgroup. They formed as lake bottom deposits and are capped by prodelta (chloritic mudstones and siltstones) and delta front or nearshore lake deposits (quartz wackes) of the **Pannetjie** Formation, which forms the lowermost part of the Koegas Subgroup (§2.2.1.4). In simple terms, the depositional environment of the Pietersberg-Pannetjie sedimentary cycle was probably a fresh water lake (due to the presence of greenalite in the Pietersberg member), that was infilled by deltaic sediments (Beukes, 1983).

2.2.1.4 *The Koegas Subgroup*

The **Doradale**, **Kwakwas** and **Naragas** Formations overly the Pannetjie Formation and constitute the lowermost of three upward-coarsening iron-formation → siliciclastic sedimentary cycles encountered in the Koegas Subgroup (Fig. 2.6). This cycle is similar in composition and palaeo-environmental setting to the major Kuruman → Griquatown → Pannetjie cycle that underlies it. The main difference between the two cycles is the much lower rate of iron-formation deposition and higher rate of siliciclastic influx that characterizes the former. The thin Doradale iron-formation is similar in character to the Kuruman iron-formation (magnetite-siderite ribbon-rhythmite and siderite bandlutite interbedded with disclutite) and it grades up to the Kwakwas iron-formation (riebeckite minnesotaite greenalite-lutite) which in turn is similar in composition and character to the Middelwater Member of the Griquatown iron-formation. The Kwakwas iron-formation is overlain by an upward-coarsening siliciclastic cycle of the Naragas Formation, which probably represents a progradational deltaic sequence, or the infill of the

basin by offshore chloritic mudstones and nearshore quartz-wackes (Beukes, 1983). The top of the Naragas Formation is characterised by manganese-bearing siderite lutites which form the base of manganese-bearing siderite lutite → ferruginous chloritic mudstone cycles, indicating a period of transgression below the Rooinekke iron-formation.

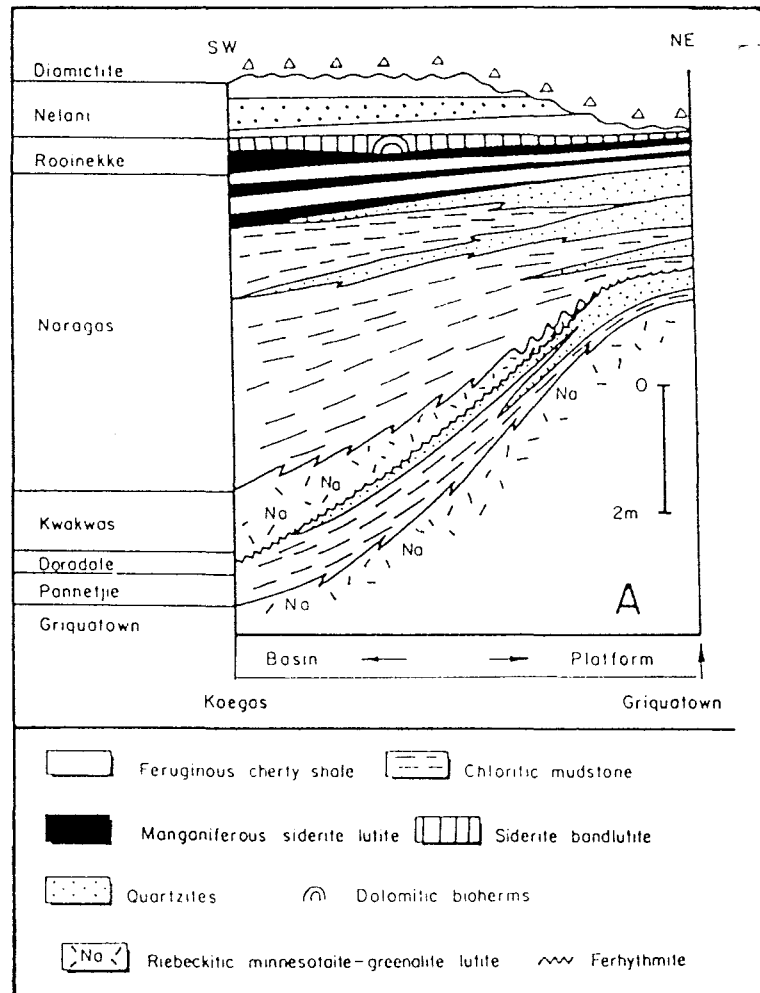


Fig. 2.6. Regional stratigraphic relationships in the Koegas Subgroup along a southwest-northeast section (after Beukes, 1983).

Manganiferous siderite lutites are also present at the base of the **Rooinekke** iron-formation and are overlain by siderite bandlutite and pillowlutite. Stromatolitic ferruginous dolomite bioherms are developed along the contact between the Mn-bearing siderite lutites and the siderite bandlutites, representing a transitional stage from a deep-water basin to a platform lagoonal environment (Beukes,

1983). A second upward coarsening iron-formation → siliciclastic sedimentary cycle is then completed by the **Klipputs Member** of the **Nelani Formation** (Fig. 2.6), which rests unconformably on the Rooinekke iron-formation. The Klipputs Member comprises interbedded ferruginous chloritic mudstone and chert which are thought to represent nearshore lagoonal deposits of the Rooinekke sedimentary increment (Beukes, 1983).

Stromatolitic dolomite bioherms re-appear at the top of the Klipputs Member, marking another transgressive event. They are overlain by the Nelani iron-formation, which consists of riebeckitic felutites and cherty-sideritic grainstones and is followed by interbedded ferruginous mudstone, chert, gritstone and conglomerate, a succession similar to the Klipputs Member. The Nelani Formation represents another upward-coarsening sedimentary cycle which is the last encountered in the Koegas sequence, before subsequent uplift and erosion took place.

2.2.2 The Postmasburg Group

The Postmasburg Group consists of three major lithological units: At the bottom, glacial sediments of the Makganyene Formation lie below a thick volcanic succession (Ongeluk andesites), which in turn is overlain by sediments of the Voëlwater Subgroup. The latter comprises: i. the Hotazel BIF and Mn-deposits, which are laterally interfingered with rocks of the Beaumont Formation; and, ii. the Mooidraai dolomites. The sequence attains a thickness of approximately 1500m and is unconformably overlain by younger rocks of the Olifantshoek Sequence.

2.2.2.1 *The Makganyene diamictite*

The Makganyene Diamictite Formation forms the base of the Postmasburg

Group, and its position in the stratigraphic column is defined by: i. a disconformable contact which brings the Makganyene sequence either on top of rocks of the Koegas Subgroup or on Griquatown BIF (Truswell, 1990b); and, ii. a vertical transition to the overlying Ongeluk volcanics through beds rich in pyroclastic material (Beukes, 1983).

The Makganyene Formation (Fig. 2.7) was described by Visser (1971) as a piedmont glacial and fluvio-glacial assemblage of massive and poorly bedded diamictite, interbedded with a wide range of clastic sediments (shales to conglomerates). However, this is one of the two facies encountered in the Postmasburg group (Beukes, 1983). The second facies consists of stacked cycles of graded bedded diamictite-greywacke-sideritic banded iron-formation. It is believed (De Villiers & Visser, 1977), that this second facies represents periodic subaqueous debris-flow deposits, whereby the debris was derived from the piedmont glaciers of

Visser (1971) and moved into a marine environment of chemical deposition of iron-rich sediments. The glacial derivation of the components of the diamictite beds is based mainly on striated clasts observed by Visser (1971) and De Villiers and Visser (1977), but this possibility has been questioned by Beukes (1983) mainly due to the absence of: i.

glacial pavements in the Makganyene assemblage; and, ii. sediments of

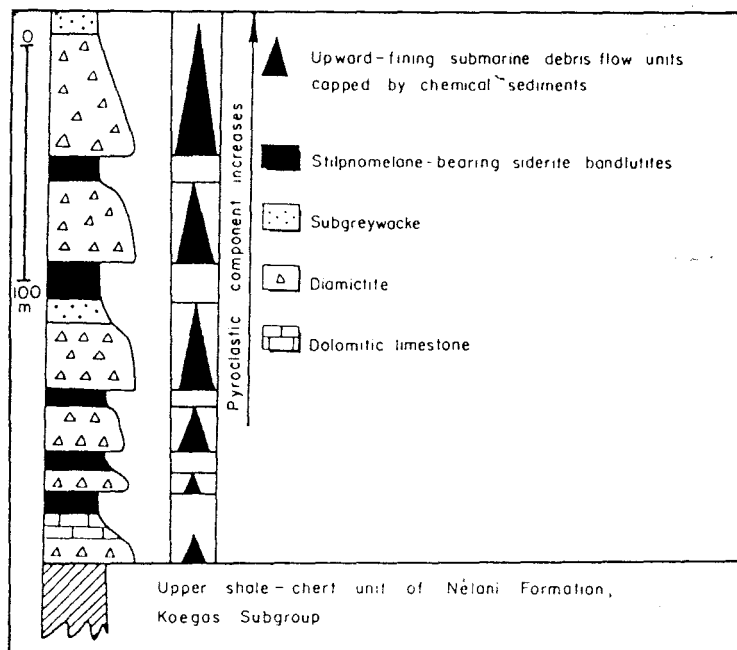


Fig. 2.7. Lithostratigraphic succession in the Makganyene Diamictite between Sishen and Postmasburg (modified after De Villiers & Visser, 1977; in Beukes, 1983).

glacial character in the fluviatile Boshhoek Formation (Schreiber et al., 1990), which is regarded as correlative of the Makganyene Sequence in Eastern Transvaal (Button, 1973a; in Beukes, 1983).

2.2.2.2 *The Ongeluk lavas*

The **Ongeluk** lavas represent sub-continental andesitic flows of tholeiitic character (Sharpe et al., 1983; Marsh, 1985) and attain an average thickness of approximately 400 m. They display spectacular pillow structures with fine-grained to aphanitic margins and crystalline interior (Schutte, 1992) which indicate extrusion of volcanic material under submarine conditions. In some cases, red jasper fills the tricusate inter-pillow spaces. Also, jasper beds which cap the lava flows and associated hyaloclastites at the contact with the overlying Hotazel Formation, suggest an interfingering relationship between the lavas and the latter (Grobler & Botha, 1976). It is believed that the Ongeluk andesites and their equivalents in the Transvaal basin **Hekpoort** basalts, are products of a stepwise procedure of partial melting → assimilation → fractionation → (subaqueous) extrusion, that involves a compositionally homogeneous mantle and lower crust, with uniform temperatures and pressures at the base of the crust (Sharpe et al., 1983). This model has been proposed in order to account for the unusually widespread, and at the same time, homogeneous andesitic volcanic event that the Ongeluk and Hekpoort lavas represent in the Transvaal Sequence.

Schutte (1992), distinguished two types of Ongeluk lavas which are similar in textural and mineralogical character but exhibit different alteration signatures. She describes the alteration of the lavas around the Hotazel area as a result of exhalative processes in an Early Proterozoic sea, which provided the depositional basin with the necessary amounts of iron and manganese for the formation of the Mn-BIF sediments. The validity of an exhalative model for the genesis of such vast amounts of Mn and Fe will be further discussed later in this study

(see ¶5.3).

2.2.2.3 *The Voëlwater Subgroup*

Directly above the Ongeluk lavas rests the **Hotazel** Formation (Fig. 2.8), which comprises Fe- and Mn-rich sedimentary rocks and is located in the southernmost portion of the Kalahari area (widely known in the literature as the "Kalahari Manganese Field"; see Fig. A1). Jasper and jaspilitic units constitute the base of the sequence. The jaspers are also known as cherty hematite lutites and cherty hematite rhythmites, whereas the jaspilites occur in two types, namely hematite-magnetite ribbon-rhythmite and hematite-magnetite ribbon-lutite (Beukes, 1983).

The chert content of the jaspers decreases upwards and the character of the rocks changes to kutnahorite-bearing pisolitic hematite lutites, which gradually turn to kutnahoritic pisolitic braunite lutite. The kutnahorite is concentrated in diagenetic oolites and pisolites of a concretionary origin, in a hematite-braunite lutite matrix. The braunite-kutnahorite lutite unit is the main ore-bed with a thickness which varies between 5 and 45 m, covering an area of about 425 km² (Beukes & Kleyenstuber, 1986).

The main manganese body is then followed by a minnesotaite ribbon- and bandlutite BIF bed, through a transitional thin horizon of hematite lutite. The same rock type (hematite lutite) marks the transition between the BIF unit and the second Mn-bed which is very thin and has no economic significance. A similar sequence of BIF → hematite lutite → kutnahorite braunite lutite is repeated once again towards the top of the stratigraphic column, encompassing the third Mn-body (up to 10m thick) which is also uneconomic, unless it has undergone enrichment due to hypogene and/or supergene processes. The rocks that overly the upper Mn-body are essentially sideritic ribbon- and bandlutites that display soft-sediment deformation structures (Beukes et al., 1982; Beukes, 1983).

The cyclicity described above in the Fe-rich and Mn-rich beds is the main characteristic of the Hotazel Formation, and has been interpreted as the result of transgressions and regressions in the depositional basin during Early Proterozoic times. Duplication of strata due to thrusting has also been documented in the western part of the basin. The associations of jaspers and Mn-ores are considered similar to the greenstone-jasperoid, volcanogenic-sedimentary Mn-deposits described by Shatskiy (1954), and they imply a direct connection between the Hotazel sediments and the underlying Ongeluk lavas in terms of source of iron and manganese (Beukes et al., 1982; Beukes, 1983; Beukes & Kleyenstuber, 1986).

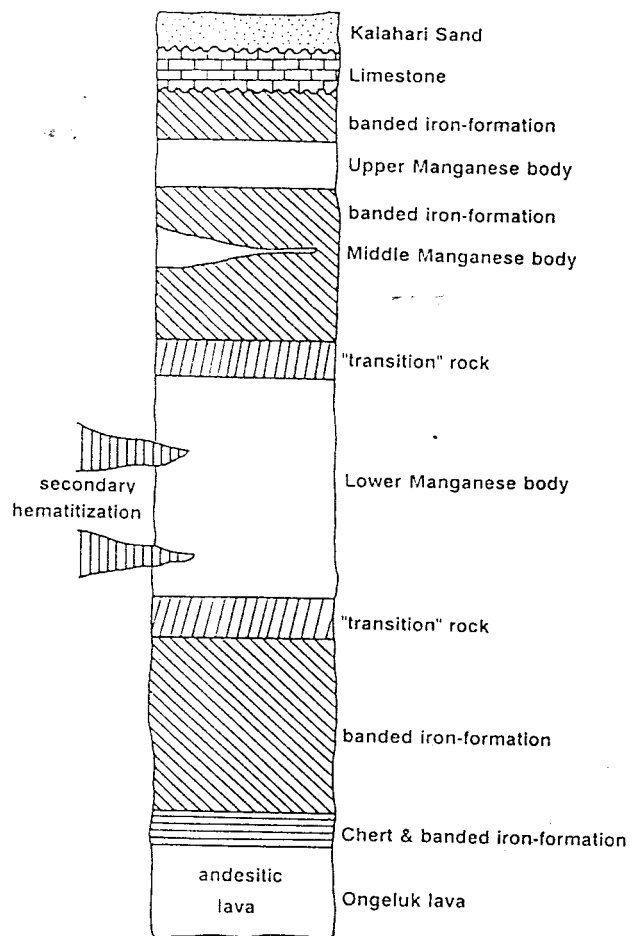


Fig. 2.8. Simplified stratigraphic column of the Hotazel BIF and Mn-beds from the study area (not to scale; modified after Schutte, 1992).

The sideritic BIFs of the Hotazel Formation grade up to brecciated and laminated, clastic-textured, pinkish-grey cherty dolomites of the **Moidraai** Formation. The clastic textured dolomites display slump folds and are interfingered with the chert-dolomite breccias, indicating deposition under gravity flow processes in front of a shallow water carbonate platform. Higher up in the sequence, fine-grained dolarenite units are interbedded with the laminated dolomites and are overlain by thinly bedded dolarenites with cryptalgal laminations. The depositional environment thus became even shallower, with the true shallow platform facies presumably being eroded in pre-Olifantshoek times (Beukes, 1983).

2.3 Economic Geology of Griqualand West

Mineral deposits of major economic importance not only for the South African but also for the global economy, are either hosted by or are intimately associated with rocks of the Griqualand West Supergroup. The best example is probably the BIF-hosted manganese deposits of the Kalahari Field, which account for about 50% of the world's total reserves (Laznicka, 1992). The iron-formations of the Asbesheuwels and Koegas Subgroups contain the bulk of the world's crocidolite reserves (Button, 1976b; Beukes & Dreyer, 1986), with only two other areas in the world having similar deposits of economic grade: the Hamersley Basin in Australia (Trendall & Blockley, 1970; Blockley & Myers, 1990) and the Chapare Group of eastern Andes, Bolivia (Redwood, 1993). Dolomitic rocks of the Campbellrand Carbonate Sequence carry large fluorite deposits (e.g. Zeerust), economic MVT-type Pb-Zn mineralisations (e.g. Pering), and metamorphosed karst fill-type manganese ores which have subsequently formed detrital deposits in recent solution hollows (e.g. Lohathla, Beeshoek and Glosam) (J. De Villiers, 1960; Button, 1976b; Beukes, 1986a,b; Grobelaar & Beukes, 1986; Kleyenstuber, 1991; Beukes, 1993). Finally, a very large hematitic iron-ore deposit of the replacement type occurs at Sishen (van Schalkwyk & Beukes, 1985), and is related to the period of weathering and erosion that preceded the deposition of the Gamagara and Mapedi formations of the Olifantshoek Group (Beukes, 1986a,b).

3. PETROGRAPHY OF THE VOËLWATER BANDED IRON-FORMATION

3.1 Introduction

Detailed studies on the mineralogy and petrography of Proterozoic BIFs have been conducted over the past 50 years by several authors (e.g. Gruner, Gole, Klein, Miyano; see also reference list), with particular reference on the major Precambrian sedimentary basins of the world (Table 3.1). These studies have provided us with sufficient data on the properties of literally all the minerals

Table 3.1. Selected bibliography on the mineralogy and petrography of BIFs from three major Precambrian areas of the world.

	1961-1976	1976-1991
Hamersley Basin	Trendall & Blockley (1970), Grubb (1971), Ayres (1972)	Ewers & Morris (1981), Klein & Gole (1981), Miyano (1982), Miyano & Miyano (1982), Miyano & Klein (1983)
Labrador Trough	Kranck (1961), Klein (1966, 1974), Butler (1969), Dimroth & Chauvel (1973), Chauvel & Dimroth (1974), Zajac (1974)	Klein (1978), Klein & Fink (1976), Leshner (1978)
Lake Superior Region	French (1968), Morey et al. (1972), Bonnischen (1975), Floran & Papike (1975)	Floran & Papike (1978), Haase (1982)

that occur in BIFs, including possible genetic mechanisms for the deposition of primary iron-rich precipitates, mineral facies forming under diagenetic and/or metamorphic processes of various grades, mineral chemistry, natural mineral

reactions, phase equilibria, mineral compatibilities, etc. The above wealth of literature made a significant contribution to the mineralogical studies of the Voëlwater BIF, particularly with regard to the identification and characterisation of certain mineral facies. This was due to the fact that the present study was being tackled over a relatively short period of time, and therefore, advanced analytical techniques such as electron probe microanalyses, received only limited use. Particular focus in this chapter is drawn on certain textural features which are indicative of both syn- and post-depositional processes (diagenesis, tectonism, metamorphism etc.), as well as on correlations between the various lithologies which are of major significance in the interpretation of the physicochemical conditions which prevailed during the deposition of the Voëlwater sediments (see also ¶5.2).

3.2 Methods of study

The main characteristic of virtually all the Proterozoic iron-formations, as far as mineralogical studies are concerned, is their extremely fine grained nature, and the Voëlwater BIF does certainly not make an exception. The very fine mineral intergrowths frequently encountered in BIFs require a combination of detailed petrographic studies and various analytical methods (sometimes with the aid of mineral separation), in order to allow for identification and textural characterisation of all the coexisting phases. For the Voëlwater BIF, the X-Ray diffraction technique was essentially the only one employed, and along with detailed microscopic studies and, in certain cases (see **carbonates**, ¶3.3.2), microprobe analyses, led to the determination of the bulk mineralogical composition of these rocks. On the contrary, detailed mineral chemistry studies are absent, since they were beyond the scope of this research project.

Identification of minerals by X-Ray diffraction was done on powder patterns which were obtained using a Phillips Standard water-cooled diffractometer. The powdered samples (for details on collection and preparation see ¶4.2), were

packed onto aluminium slide holders. CoK α_1 radiation was used with variable instrumental settings (30-40 kV, 20-30 mA) and a scan rate of 1°/30 sec. Minerals were identified by comparison with the values of d-spacings given in the Powder Diffraction Data File, published by the International Centre for Diffraction Data (JCPDS, 1974, 1980). For each of the collected samples, a representative piece (approximately 5 cm long) was kept prior to crushing. Polished and thin sections were then prepared for petrographic studies in both reflected and transmitted light respectively.

Electron probe microanalyses were performed on polished thin sections using a JEOL JXA-733 electron probe microanalyser at Rhodes University. Three different analysing crystals were used to ensure best detection with minimum error for each element included in the analyses. Corrections for background noise and interferences by other elements were made in all determinations.

3.3 Mineralogy

The presence of the three manganese intercalations in the Voëlwater sedimentary "package" offers a unique opportunity for a systematic mineralogical study of the several BIF lithologies. Pure stratigraphic observations on the four selected boreholes (Fig. A1) enabled the writer to distinguish four stratigraphically-defined banded iron-formation units (see also Fig. 2.8): i. the hematite-rich unit (HBIF) which occurs below the lower Mn-horizon; ii. the lower unit (LBIF), between the lower and middle Mn horizons; iii. the middle unit (MBIF), between the middle and upper Mn horizons, and iv. the upper unit (UBIF) which occurs above the upper Mn-horizon and below the Mooidraai Formation. The above distinction was adopted with the purpose of facilitating the mineralogical descriptions of the several BIF lithofacies by means of direct reference to the four individual BIF units, and it should not be considered that it has any implications for the mineralogical character of the various lithologies or that it affects any attempts for petrographic correlations, particularly those on

a vertical sence.

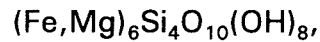
The minerals which make up the rocks of this study have been subdivided into three major categories, in a similar manner to the facies classification formulated by James (1954): i. the **silicate group**, which comprises (in random order) the minerals chert (quartz), greenalite, minnesotaite, stilpnomelane and riebeckite, with subordinate amounts of other Fe-bearing phyllosilicates; ii. the **carbonate group**, with members of the dolomite-ankerite series, siderite and calcite; and: iii. the **oxide-sulphide group**, comprising the oxides magnetite and hematite and the sulphide pyrite.

3.3.1 Silicates

3.3.1.1 *Greenalite*

Greenalite is a relatively common mineral in diagenetic to low-grade metamorphic Proterozoic iron-formations (James, 1954; French, 1973; Klein & Bricker, 1977; Klein, 1983). It occurs in the Sokoman iron-formation of the Labrador Trough, Canada (Zajac, 1974; Klein, 1974, 1978; Klein & Fink, 1976), although it is not reported in the papers by Dimroth and Chauvel (1973), Chauvel and Dimroth (1974) and Lesher (1978). It is present in the Biwabik iron-formation (French, 1968) and the Gunflint iron-formation (Floran & Papike, 1975, 1978) of Minnesota, and it also represents one of the major mineralogical facies in several BIF units of the Transvaal Sequence in South Africa (Beukes, 1973, 1978, 1980a, 1983, 1984; Miyano & Beukes, 1984; Beukes & Klein 1990a). Greenalite is less common in rocks of the Hamersley Group, W. Australia (Trendall & Blockley, 1970). Specifically, it is scarce in the Mara Mamba iron-formation (Klein & Gole, 1981) and virtually absent from the Brockman iron-formation (Grubb, 1971; Ayres, 1972; Ewers & Morris, 1981). It occurs, however, in slightly metamorphosed Archaean iron-formations of the Yilgarn Block (Gole, 1980, 1981).

According to Gruner (1936), greenalite is the Fe-rich analogue of antigorite, although its structure is quite different from that of the serpentine minerals (Klein, 1983). In chemical terms it may be characterised as:



with fairly restricted compositional range (Fig. 3.1). With the exception of MgO (Klein, 1974) and to a lesser extent Al_2O_3 which can reach contents of sometimes up to 3 wt. % (Floran & Papike, 1975; Gole, 1980; Miyano & Beukes, 1984), all the other oxide components are generally present in amounts less than 1 wt. %. Greenalite is most commonly microcrystalline, with a grain size always many orders finer than that of any of its coexisting minerals. It occurs mainly in granules, oolites and irregular masses (Klein, 1974; Klein & Fink, 1976), and coarse varieties are indeed very rare. Recrystallized varieties of greenalite have been reported from the Gunflint and Sokoman BIFs (Zajac, 1974; Floran & Papike, 1978), although in the latter case it could be argued that the greenalite "porphyroblasts" might also resemble sprays of minnesotaite (Zajac, 1974, Fig. 73). Because of its common poor-crystalline texture, greenalite is considered as one of the most possible primary minerals in BIFs (Klein, 1983), and its positive identification almost always requires a combination of petrographic, XRD and microprobe studies.

The presence of greenalite in the rocks of this study was confirmed by means of XRD methods (Table 3.2). X-Ray powder diagrams of several samples exhibit reflections of greenalite remarkably similar to greenalites from the Mesabi Range, Minnesota and from the Sokoman BIF, Canada. Greenalite is abundant in chert-rich microbands and laminations from the lower parts of the LBIF. It occurs as very fine-grained flakes disseminated in a matrix of chert with minor amounts of magnetite, hematite, calcite, \pm siderite, \pm pyrite, (\pm carbon?), forming distinct mineral assemblages which give the rock a characteristic greenish colour (Figs. 3.3a, 3.5b_{i,ii,iii,iv}). Greenalite is present in lesser amounts in the HBIF as occasional, thin chert-minnesotaite-greenalite-carbonate bands, and it may be

also found in association with quartz-ankerite microbands immediately above the lower Mn-horizon. Alternate microbands of chert-greenalite assemblages with siderite-calcite-± magnetite granular microbands are mostly common, and carbonate-stilpnomelane microbands only rarely intervene. Greenalite is very often replaced by laths and sprays of minnesotaite, a process which is clearly evident by their characteristic crosscutting textural relations. The greenalite content in the rocks of this study decreases dramatically towards higher stratigraphic horizons and it becomes negligible in very carbonate-rich lithologies.

Table 3.2. The six most characteristic reflections of greenalite from this study, as compared to respective reflections of greenalites from the Mesabi Range (Youell & Steadman, 1961, in Zajac, 1974; Blake, 1965) and the Sokoman BIF (Zajac, 1974).

Mesabi Range, (Lake Superior)				Labrador Trough		Transvaal Basin	
Greenalite (Blake, 1965).		Greenalite (Youell & Steadman, 1961).		Greenalite, Sokoman IF (Zajac, 1974).		Greenalite, Voëlwater IF (this study).	
dÅ	I/I ₁	dÅ	I/I ₁	dÅ	I/I ₁	dÅ	I/I ₁
7.20	100	7.21	70	7.18	100	7.18	100
3.60	50	3.60	40	3.60	60	3.59	60
2.58	70	2.59	100	2.60	90	2.59	60
2.20	30	2.20	90	2.21	70	2.20	25
1.60	30	1.60	60	1.61	60	1.61	15
1.56	20	1.56	60	1.57	40	1.56	15

3.3.1.2 *Stilpnomelane*

One of the most abundant silicate minerals in late diagenetic to low-grade metamorphic banded iron-formations is stilpnomelane. It occurs in virtually all the major iron-formations of the world (Klein, 1983), in the form of thin but quite

continuous laminations, as fine-grained mattes of sheaves and needles and often in coarse-grained sprays, flakes and irregularly shaped patches. In some occurrences, stilpnomelane exhibits textural habits which may very well resemble minnesotaite laths (Miyano, 1982, Fig. 2A). It is mostly common in chert (quartz)-carbonate-magnetite-stilpnomelane assemblages (Klein, 1974; Zajac, 1974; Klein & Fink, 1976; Klein, 1978; Lesher, 1978; Gole, 1980; Klein & Gole, 1981; Ewers & Morris, 1981; Miyano, 1982; Haase, 1982; Miyano & Beukes, 1984; Miyano & Klein, 1989) but it may also occur in crosscutting relationships with greenalite (Klein, 1974), giving a good indication that stilpnomelane is probably a later phase. However, in most cases stilpnomelane occurs as a single mineral and its relation to possible precursor minerals is debatable (Klein, 1983). Beukes (1983) considers stilpnomelane as a product of fumarolic activity and subsequent ash flow, which took place contemporaneously with the deposition of the Kuruman iron-formation in S. Africa. This stilpnomelane is often K-rich and is commonly found in close association with riebeckite (Miyano & Beukes, 1984). Similar riebeckite-stilpnomelane associations are also known from the Brockman iron-formation of the Hamersley Group in W. Australia (Miyano & Miyano, 1982).

The chemistry of stilpnomelane is much more complex than that of greenalite, due to the presence of small and variable amounts of alkali cations (K^+ and Na^+) and large and variable amounts of Al_2O_3 (Fig. 3.1). An oversimplified, though incorrect, chemical formula of stilpnomelane (because it ignores the alkali content), has been suggested by Klein (1974, 1983):



to facilitate comparisons with other Fe-silicates, mainly greenalite and minnesotaite. The identification of stilpnomelane under the microscope is sometimes difficult because of its fine-grained nature, and it may be overlooked even in thin section. In relatively coarser varieties, however, the high birefringence and strong pleochroism (pale yellow to dark brown) are sufficient

for positive identification, which can be confirmed by the characteristic reflection at approximately 12\AA (about 9.2 degrees 2θ) in X-Ray powder patterns.

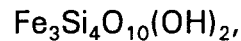
Stilpnomelane-rich bands in rocks of the study area make their first appearance in the LBIF unit immediately below the middle Mn-body. Characteristic chert-stilpnomelane-carbonate- \pm magnetite bands followed by chert-riebeckite assemblages are encountered within a few metres in this part of the Voëlwater Sequence, and strongly suggest a similarity to the riebeckite-stilpnomelane associations of the Kuruman iron-formation (Beukes & Dreyer, 1986). Stilpnomelane almost always coexists with calcite, ankerite, magnetite, hematite, \pm Fe-mica and chert throughout the upper part of the LBIF and the entire MBIF and UBIF units, forming characteristic mineral assemblages with the calcite-stilpnomelane association most common (Figs. 3.3b, 3.4b). Flaky grains of, presumably, stilpnomelane that strongly resemble biotite were also distinguished in the study rocks, but it was not possible to determine their exact mineralogical character by XRD studies, due to their limited abundance.

3.3.1.3 *Minnesotaite*

Minnesotaite is one of the most common minerals in diagenetic to low-grade metamorphic banded iron-formations, such as the Sokoman iron-formation, Canada (Dimroth & Chauvel, 1973; Zajac, 1974; Klein, 1974; Klein & Fink, 1976; Leshner, 1978; Klein, 1978), the Biwabik, Gunflint and Negaunee iron-formations, U.S.A (French, 1968; Floran & Papike, 1975, 1978; Haase, 1982), the Mara Mamba and Brockman iron-formations, W. Australia (Trendall & Blockley, 1970; Grubb, 1971; Ayres, 1972; Klein & Gole 1981; Ewers & Morris, 1981) and the Griquatown iron-formation, S. Africa (Beukes, 1978, 1983; Beukes et al., 1982). It commonly occurs as fine- to medium-grained needles that are arranged in sprays, "bow-ties" and irregular patches (Klein, 1983). Its crosscutting relationship with chert (or quartz), carbonates, greenalite and stilpnomelane has been reported by many authors (French, 1968, 1973; Klein

1974, Floran & Papike, 1975, 1978; Klein & Fink, 1976; Gole, 1980; Klein & Gole, 1981; Haase, 1982), and suggests that minnesotaite is a likely reaction product of these minerals.

The ideal chemical formula of minnesotaite as given by Klein (1983), is:



but the mineral shows a considerable range of Fe-Mg substitutions (Fig. 3.1). Hence, ferroan-talc mineral facies may also be present in essentially unmetamorphosed iron-formations, and several examples where Fe-rich talc is even more common than minnesotaite can be found in the literature: The Sokoman (Leshner, 1978) and Gunflint (Floran & Papike, 1975, 1978) iron-formations, as well as the Mara Mamba and Brockman iron-formations of the Hamersley Group (Klein & Gole, 1981; Ewers & Morris, 1981) are probably the best examples. As far as mineralogical studies are concerned, minnesotaite can easily be identified by its distinct textural signature under transmitted light, as well as by its characteristic reflection at 9.6Å (10.7 degrees 2θ) in X-Ray powder diagrams.

Minnesotaite is a common mineral in the Voëlwater BIF. It may occur in any part of the stratigraphy, in the form of sprays, laths and bow-tie textures that replace greenalite, or Fe-carbonates (Figs. 3.3c,d). Its replacement origin is undoubted, since all the minnesotaite occurrences exhibit crosscutting relations with the minerals with which it coexists. The presence of minnesotaite in the rocks of this study may have either regional or local significance because it is uncertain whether this particular mineral has formed under pure diagenetic processes or, perhaps, as a result of metasomatic effects in the vicinity of basic intrusives. The reason for that uncertainty is the fact that minnesotaite may be found throughout the stratigraphic column in certain boreholes (e.g. R-65, R-59) and it may be virtually absent in others (e.g. R-63), indicating a vertical consistence as well as some lateral impersistence in its occurrence.

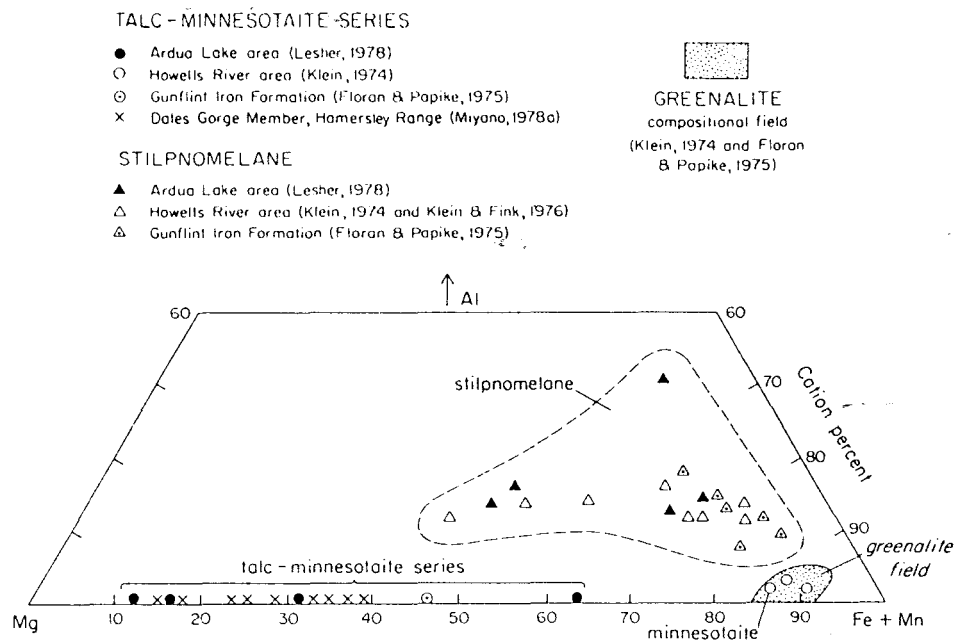


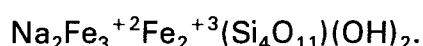
Fig. 3.1. Compositional ranges of stilpnomelane, members of the talc-minnesotaite series and greenalite in late diagenetic to very low-grade metamorphic BIFs (modified after Leshler, 1978; in Klein, 1983).

3.3.1.4 Riebeckite

Riebeckite is a major constituent in banded iron-formations of the Griqualand West Supergroup, South Africa (Beukes, 1973, 1978, 1980a, 1986a; Miyano and Beukes, 1984; Beukes & Dreyer, 1986) as well as of some parts of the Brockman iron-formation of the Hamersley Group, W. Australia (Trendall & Blockley, 1970; Ayres, 1972; Grubb, 1972; Ewers & Morris, 1981; Klein & Gole, 1981; Miyano, 1982; Miyano & Miyano, 1982; Miyano & Klein, 1983; Miyano & Beukes, 1984). In these two areas, the asbestiform variety of riebeckite, namely *crocidolite*, occurs in probably the largest mineable quantities on earth, although Redwood (1993) has recently reported a third economically viable crocidolite occurrence in banded iron-formations of the Chapare Group, Bolivia. Nevertheless, in most other banded iron-formations that have undergone late-diagenetic to very low-grade metamorphic processes such as the Sokoman iron-formation (Dimroth & Chauvel, 1973; Zajac, 1974; Klein, 1974; Leshler, 1978), riebeckite is a very sporadic constituent. Exceptions constitute the BIFs

of the Krivoy Rog Basin in U.S.S.R, where soda-amphiboles have formed under metasomatic processes in the vicinity of acidic intrusions (Semenenko et al., 1956; in Zajac, 1974).

The ideal chemical formula of riebeckite as the end member of Glaucophane-Crossite-Riebeckite series with no significant substitution of Fe^{+2} by Mg^{+2} can be written as (Philips & Griffen, 1981):

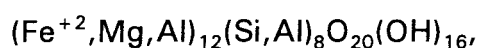


Riebeckite commonly occurs as acicular needle-like crystals, felted masses of interlocking fibres, or asbestiform varieties (crocidolite proper: Trendall & Blockley, 1970; Zajac, 1974). When relatively coarse, it can be easily identified by its characteristic textural appearance in thin section, as well as by its typical blue pleochroic colours.

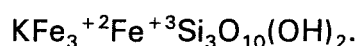
Riebeckite is a rather uncommon constituent in the Voëlwater rocks. It has a restricted occurrence at the top of the LBIF and it is closely associated with underlying stilpnomelane rich-bands and certain diagenetic features such as stylolites (Fig. 3.4h). It is found in recrystallised quartz microbands in the form of sheaves and needle-like crystals (Figs. 3.3e, 3.4c) and it gives good textural indication for a diagenetic origin.

3.3.1.5 Other silicates

Some of the most common varieties of iron-rich phyllosilicates that may be present in late diagenetic to low-grade metamorphic iron-formations are the minerals *ripidolite* and *feri-annite*. Ripidolite is a member of the Chlorite Group although it is uncertain whether it is a normal 14Å chlorite or a 7Å septachlorite (Klein, 1983). Its chemical formula as it has been proposed by Klein and Bricker (1977) is (next page):



and it occurs in fine-grained irregular patches and stringers or in somewhat coarser textures with a bladed habit, occasionally forming fans and sheaves (Klein & Fink, 1976; Haase, 1982; Klein 1983). Ferri-annite, on the other hand, is an Fe-rich mica reported mainly from BIFs of South Africa (Kuruman) and Australia (Dales Gorge and Jofree Members of the Brockman iron-formation), with an ideal chemical formula as proposed by Miyano and Beukes (1984):



It occurs as flaky to tabular grains, or as massive aggregates of fine acicular grains near riebeckite-rich zones of iron-formations, often in crosscutting relationship with stilpnomelane (Miyano & Miyano, 1982; Miyano & Beukes, 1984). Ferri-annite commonly coexists with hematite, magnetite, quartz, ankerite, stilpnomelane and riebeckite and it is distinguished from stilpnomelane and other micas by its pleochroic colours (reddish brown to pale yellow greenish brown; Klein, 1983).

Nonetheless, the situation regarding Fe-bearing chlorites and micas in BIFs appears rather complex in the literature: Grubb (1971) refers to the presence of Fe-chlorites from the Brockman iron-formation, while Fe-chlorite occurrences are also known from the Gunflint iron-formation (Floran & Papike, 1978). True ripidolite is known to occur in the Sokoman iron-formation (Klein & Fink, 1976; Klein 1978) and in the Negaunee iron-formation (Haase, 1982) whereas both ripidolite and Fe-chlorite have been reported again from the Sokoman iron-formation (Leshner, 1978) as well as from the Mara Mamba iron-formation (Klein & Gole, 1981). Fe-mica is present in the Brockman iron-formation (Miyano 1982), commonly with chlorite (Ewers & Morris, 1981) and ferri-annite (+ Fe-chlorite) is a conspicuous facies in both the Kuruman and the Brockman iron-formations, where it occurs in two distinct varieties (Miyano & Miyano, 1982; Miyano & Beukes, 1984).

Because minerals such as ripidolite and ferri-annite normally occur in BIFs in minor to trace amounts, their presence in the rocks of this study was very difficult to establish by pure petrographic studies and XRD data. However, mineral grains with a micaceous habit and distinct optical properties as compared to other Fe-silicates were occasionally found in the Voëlwater rocks and are believed to be some variety of Fe-rich mica (Fig. 3.3f). The common association of this mineral with carbonate-stilpnomelane-magnetite assemblages could be a good indication that this Fe-mica is true ferri-annite.

3.3.1.6 Chert (quartz)

Chert is a major constituent of the bulk of iron-formation lithotypes. In most of the iron-formations that have undergone only late diagenesis, the SiO_2 tends to be very fine-grained and is referred to as chert when the grain size is less than 0.05mm. Well-crystallized varieties would normally be referred to as quartz, although clear-cut distinction between the terms chert and quartz does not appear to exist in the literature (Klein, 1983). The variability in the grain size of quartz might also be an indicator of change in the conditions during metamorphism, on the assumption that any increase in the metamorphic grade should normally be accompanied by recrystallization of SiO_2 , to form gradually coarser varieties. This concept was proposed by James (1955), but its validity is questionable, since the presence or absence of H_2O in unconsolidated silica-rich sediments would lead to variable grain sizes of quartz under diagenetic conditions (Klein & Fink, 1976; Klein, 1983).

Chert is the most abundant mineral facies in the Voëlwater rocks and it frequently makes up more than 50% of the individual rock unit. It is an integral part of almost all the mineral assemblages and it occurs in various grain sizes depending each time on the degree of diagenetic recrystallization. In carbonate-poor samples it is most commonly very fine-grained, whereas coarser varieties are ubiquitous in the carbonate-rich lithologies (Figs. 3.3h, 3.4d, 3.5a).

Replacement of "primary" minerals and textures by quartz is also common and will be discussed in detail later in this chapter (see ¶3.4.2).

3.3.2 Carbonates

3.3.2.1 *Members of the dolomite-ankerite series*

Carbonates belonging to the dolomite-ankerite series are probably the most common mineral facies in essentially unmetamorphosed carbonate-rich BIFs. They are universally known to occur as well-crystallised, medium- to coarse-grained rhombs and are almost always coarser than siderite and quartz with which they commonly coexist (Klein, 1983). Euhedral ankerites are most abundant in the upper parts of the Mara Mamba BIF, W. Australia where they coexist with calcite (Klein & Gole, 1981), and in the BIFs of the Asbesheuwels Subgroup in S. Africa, associated with lesser amounts of siderite (Klein & Beukes, 1989; Beukes & Klein, 1990a). Typical ankerite-siderite coexistence with subordinate amounts of calcite is common in the Sokoman iron-formation (Klein, 1974; Zajac, 1974; Klein & Fink, 1976; Lesher, 1978), the Biwabik and Gunflint iron-formations (French, 1968; Floran & Papike, 1975, 1978), the Negaunee iron-formation (Haase, 1982) and the Brockman iron-formation (Ewers & Morris, 1981). Because carbonates of the dolomite-ankerite series frequently show a medium grain size with a rhombohedral habit, the edges of their grains tend to cut across the grains of coexisting minerals (French, 1973; Carrigan & Cameron, 1990). Such textural relations have been described either as a result of reactions of precursor materials and subsequent recrystallisation during diagenesis, or as replacements of coexisting minerals (Klein, 1983). They also imply a similar origin to the medium-grained euhedral habit of magnetite (see also ¶3.3.3.1).

Ankerite is the most abundant carbonate mineral in all the carbonate-rich assemblages of this study. It occurs immediately above the lower Mn-body, in

the upper parts of the LBIF and throughout the MBIF and UBIF units. It is almost always coarse-grained and well-crystallised with a rhombohedral habit (Figs. 3.3d,g,h, 3.4d,f,g, 3.5a). The rhombic crystals are similar to ankeritic granules from the Sokoman iron-formation (Klein, 1974), in the sense that they commonly exhibit clear edges with a somewhat cloudy interior (Fig. 3.3h). Ankerite forms characteristic mosaic textures in assemblages with microcrystalline quartz, magnetite and pyrite (Figs. 3.3g,h), although other textures (e.g quartz-ankerite veins; see Fig. 3.4.d) are not uncommon. Calcite-ankerite pairs are also present.

The electron microprobe analytical technique was employed for the precise determination of the chemical composition of representative rhombohedral carbonates of this study, and in combination with XRD studies it confirmed that ankerite is the predominant mineral facies (Fig. 3.2). The average Mn-content of

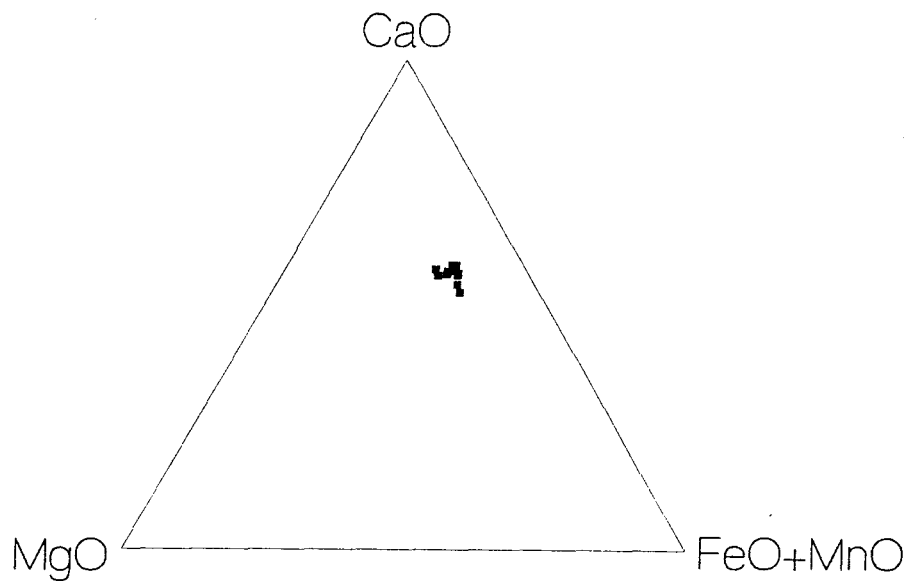


Fig. 3.2. Compositions of representative rhombohedral carbonates from carbonate-rich horizons of the Voëlwater iron-formation (analytical data are summarised in Table A4).

the analysed ankerites in combination with the abundance of the latter in carbonate-rich lithologies may explain the relatively elevated overall Mn-content in these rocks as compared to the carbonate-poor ones. Kutnahorite and manganoan dolomite were also detected in XRD powder patterns from the HBIF,

reflecting the high Mn-content of that particular rock unit (see also ¶4.3.1.2).

3.3.2.2 *Siderite*

Siderite is considered to be as common as ankerite in essentially unmetamorphosed BIFs, although the difficulty in distinguishing between various rhombohedral Fe-carbonate facies under the microscope may sometimes lead to wrong estimations regarding their relative abundance (Maynard, 1983). Siderite is commonly present as granules, microspheres, intraclasts, dark microlaminae and very fine-grained blebs and irregular patches, whereas recrystallised varieties are relatively rare (French, 1973; Klein, 1974; Zajac, 1974; Floran & Papike, 1975, 1978; Klein & Fink, 1976; Ewers & Morris, 1981; Haase, 1982; Klein & Beukes, 1989; Beukes & Klein, 1990; Beukes et al., 1990a,b; Carrigan & Cameron, 1990). The fine-grained habit and textural relations of siderite, as well as its common association with chert-greenalite-hematite-(carbon) assemblages, indicates that siderite is probably one of the most primitive mineral species in BIFs that have formed under diagenetic to very low-grade metamorphic conditions (French, 1973).

The determination of the mineral siderite in the study rocks was somewhat problematic. Coarse crystalline siderite is virtually absent from all the carbonate-rich lithologies, in contrast to the observations by Beukes (1983; see also ¶2.2.2.3) that the upper parts of the Hotazel BIF are essentially sideritic. However, characteristic, though weak, siderite peaks were produced in XRD powder diagrams from the greenalite-rich parts of the LBIF unit. It is believed that the abundant dark granules and microlaminae in the lower parts of the LBIF (Figs. 3.3a, 3.5b_{i,ii,iii,iv}) are similar to the sideritic granules and intraclasts observed by Klein and Beukes (1989) in the Kuruman iron-formation and they consist essentially of cryptocrystalline siderite, although it is not impossible that they might have a polymineralic composition. Variable amounts of chert, greenalite, hematite and/or organic carbon may also participate in the

"composite" granules, and any attempt to establish their mineralogical composition without carefully obtained and evaluated electron microprobe data, is highly speculative.

3.3.2.3 *Calcite*

Calcite is a sporadic constituent in most of the major BIF occurrences that have undergone diagenesis to very low-grade metamorphism (Klein, 1983). Apart from the upper parts of the Mara Mamba iron-formation in W. Australia (Klein & Gole, 1981) where abundant medium to coarse-grained calcite coexists with ankerite, all the other BIFs of the world contain calcite in minor to trace amounts. The common medium-grained size and euhedral habit of calcite in BIFs indicates that the latter forms under diagenetic recrystallisation processes, similar to the ones responsible for the coarse crystalline habit of ankerite and magnetite.

Calcite is a common mineral in all the BIF units of this study. Its abundance is reflected by the unusually high contents of Ca (see Tables A1, A2a and Fig. 4.4), and was confirmed by XRD powder diagrams. Calcite occurs as minute bleb-like grains in carbonate-poor lithologies (lower parts of LBIF), either interspersed in a quartz-greenalite matrix or in association with deformed siderite-bearing granules (Figs. 3.3a, 3.5b_{i,ii,iii,iv}). Coarse-grained crystals of calcite in calcite-stilpnomelane- \pm magnetite-(\pm chert) assemblages characterize the carbonate-rich lithologies (Figs. 3.3b,f, 3.4b) and they imply recrystallisation of calcite under diagenetic conditions.

3.3.3 Oxides and sulphides

3.3.3.1 *Magnetite*

Magnetite is the most common Fe-oxide in all major BIF occurrences of the

world. It is commonly medium-grained, well-crystallised, with a subhedral to euhedral habit, and it occurs in continuous bands and laminations, irregular clusters or patches and in concentric textures indicating crystallisation around granules, oolites, etc. (Klein, 1983). Magnetite may have a rather similar grain size to carbonates, which is indicative of their formation under recrystallisation processes related to diagenesis and/or low grade metamorphism. This concept, although still debatable (Klein, *op.cit.*), has been favoured by many authors (Gross, 1973; Dimroth & Chauvel, 1973; Eugster & Chou, 1973; Perry & Tan, 1973; Klein, 1974; Klein & Bricker, 1977; Klein, 1978; Leshner, 1978; Klein & Gole, 1981; Mel'nik, 1982) who consider that the presently observed magnetite represents the product of diagenetic recrystallisation of a precursor material such as "hydromagnetite" ($\text{Fe}_3\text{O}_4 \cdot n\text{H}_2\text{O}$) or mixtures of Fe-hydroxides [$\text{Fe}(\text{OH})_3$ and $\text{Fe}(\text{OH})_2$]. An alternative explanation for the origin of magnetite as proposed by French (1968, 1973), Floran and Papike (1978) and Han (1988) suggests that the mineral owes its origin to low-grade metamorphic reactions that take place at the expense of Fe-silicates (e.g. greenalite), Fe-carbonates (e.g. siderite) or Fe^{+3} -oxides and hydroxides (e.g. hematite). However, Klein and Fink (1976) observed crosscutting relations between coarse-grained magnetite and other coexisting minerals from the Sokoman iron-formation, and they interpreted such textures as a likely recrystallisation product of an earlier "hydromagnetite"-type precursor, rather than as a reaction product of coexisting mineral facies.

Magnetite is the most abundant iron oxide in all the Voëlwater BIF lithologies. It occurs throughout the stratigraphy as subhedral to euhedral crystals, forming bands and laminations in common association with quartz, carbonates and stilpnomelane. Greenalite-rich units may or may not contain any magnetite at all. The main textural characteristic of magnetite is its coarse-grained nature, commonly accompanied by crosscutting relations with both granules in the lower parts of the LBIF unit, and recrystallised granules in higher horizons (Figs. 3.4e,f,g). Overprinting growth of magnetite in the hematite bands of the HBIF indicates recrystallisation of the former under diagenetic and/or very low grade metamorphic conditions.

3.3.3.2 Hematite

Hematite is normally a less abundant Fe-oxide than magnetite in most late-diagenetic to low-grade metamorphic BIFs. When present, it commonly coexists with magnetite but it shows a finer grain size than the latter. It occurs in microbands, laminations and as granules and irregular bleb-like masses. The term "jasper" applies to all the chert-rich lithologies with reddish colour due to the presence of very fine-grained and finely interspersed hematite throughout the rock (Klein, 1983). Hematite is generally considered to be of primary, sedimentary or perhaps diagenetic origin (James, 1954; French, 1973; Dimroth & Chauvel, 1973; Klein & Fink, 1976; Klein, 1978), and its sedimentary precursor to the presently observed crystalline occurrences is probably some kind of ferric hydroxide [Fe(OH)₃], or hydrous ferric oxide (Fe₂O₃.nH₂O) (French, 1973; Klein & Bricker, 1977; Leshner, 1978; Mel'nik, 1982).

Hematite is a minor constituent in all but the HBIF lithologies of this study. The abundance of hematite in the latter rock unit is marked by the characteristic dark-red colour (Fig. 3.4a). In all the other BIF units, hematite occurs as minute inclusions in magnetite indicating possible replacement by the latter, as occasional thin bands in transitional BIF-Mn lithologies, or more seldom as microlaths (specularite?) associated with chert-stilpnomelane-±carbonate-±magnetite assemblages. Minor amounts of very fine-grained hematite may also be associated with greenalite-rich assemblages, as well as with siderite-bearing granules.

3.3.3.3 Pyrite

According to James (1954), pyritic carbonaceous shales/slates from the Lake Superior region with up to 40% pyrite represent typical sulfide iron-formation facies. However, it is unclear if such materials are indeed iron-formations (Klein, 1983). In most sulfide-bearing Proterozoic banded iron-formations of the world,

pyrite is a common but minor constituent (French, 1968; Klein & Fink, 1976; Klein, 1978; Leshner, 1978; Gole, 1980; Klein & Gole, 1981). It may be present in various mineral assemblages and it is usually coarser-grained than the other constituents (e.g. greenalite, siderite, etc), exhibiting a rather euhedral habit (Klein & Fink, 1976). Coexistence of pyrite with pyrrhotite is rare and has been reported mainly from the Mara Mamba iron-formation of the Hamersley Group in W. Australia (Klein & Gole, 1981).

Pyrite is a minor constituent in the rocks of this study. It occurs mainly as fine, subhedral grains in chert-greenalite microbands of the lower parts of the LBIF unit, occasionally as coarser euhedral grains in quartz-ankerite- \pm magnetite assemblages, and in larger amounts in the HBIF unit. Pyrite-rich veinlets are also common in some parts of the stratigraphy but their occurrence is restricted to lithologies near the Mn-horizons and implies overprint by secondary processes. The presence or absence of pyrite in BIF lithologies (including the study rocks) may be of significance in terms of reconstructing and interpreting the palaeodepositional environment of the latter, particularly with respect to the Eh-pH regime of their precipitation.

Fig. 3.3. Mineral occurrences in the Voëlwater BIF. a. Dark, deformed siderite-bearing granules in a very fine-grained, chert-greenalite-calcite- \pm carbon(?) assemblage. b. Dark brown, pleochroic stilpnomelane sprays inside a calcite-ankerite matrix. Note the characteristic fascicular habit of stilpnomelane. c. Felted masses of minnesotaite which have obliterated all original texture of, what used to be, a chert-greenalite assemblage. d. Coexistence of minnesotaite sprays with coarse, rhombohedral ankerite in a quartz- \pm magnetite- \pm pyrite matrix. e. Riebeckite needles in a matrix of microcrystalline quartz- \pm magnetite. f. Carbonate-stilpnomelane-magnetite assemblage. Note the greenish-brown flaky grains in the centre and bottom centre of what is believed to be ferri-annite. g. Ankerite-quartz assemblage. The ankerite is coarse-grained, with an apparent rhombohedral habit. Quartz forms the fine grained matrix with lesser magnetite and occasional pyrite. h. Same as g, but under cross polars. Note the cloudy interiors and clearer edges of ankerite crystals. Width of field of view: (a-h), 8mm.

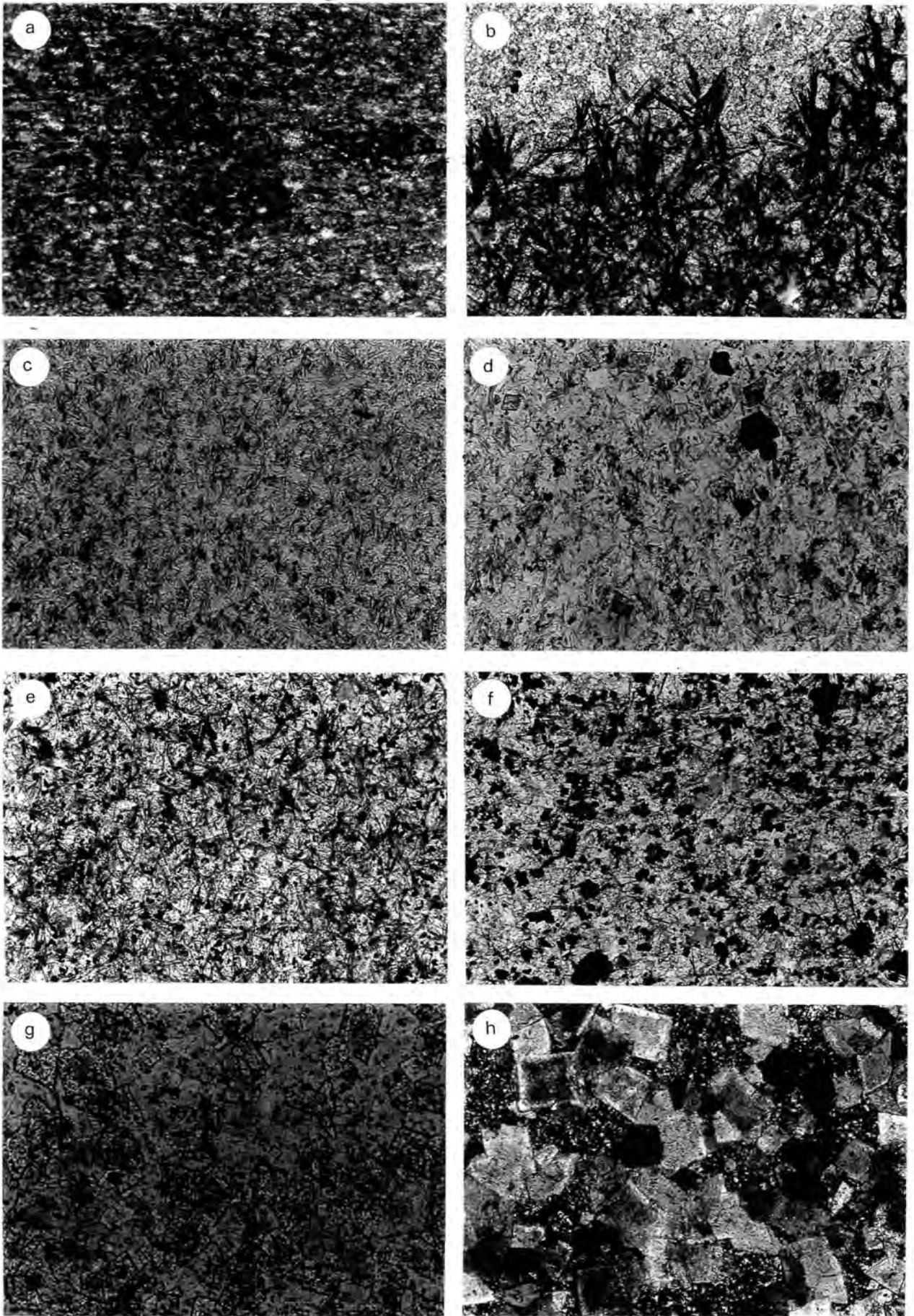


Fig. 3.3

3.4 Textural relations

It is clearly evident from the fore-going mineralogical descriptions that the rocks of this study can be classified in three major lithotypes (respective mineral assemblages are in order of abundance):

-The oxide-rich lithologies which are characterised by the assemblage hematite-magnetite-chert-dolomite-kutnahorite-pyrite- ± minnesotaite- ± greenalite, and are represented by the HBIF unit;

-The silicate-rich lithologies with chert-greenalite-siderite-magnetite-calcite- ± minnesotaite- ± pyrite- ± hematite- ± carbon(?) and abundant, deformed microgranules, which occur at the lower parts of the LBIF, and:

-The carbonate-rich lithologies with quartz-ankerite-magnetite-calcite-stilpnomelane- ± minnesotaite- ± Fe-mica- ± pyrite- ± hematite which characterise the upper parts of the stratigraphy (MBIF and UBIF units), with a (thin) chert-riebeckite-stilpnomelane-carbonate- ± magnetite- ± hematite (specularite) association occurring in the upper parts of the LBIF unit.

Apart from the various scales of banding which is ubiquitous throughout the stratigraphy, all three BIF types exhibit distinct textural signatures which are closely associated with their respective mineral assemblages. The oxide-rich lithologies have essentially no textural significance since they appear dark and dusty under the microscope, due to the presence of large amounts of finely interspersed hematite which could be regarded as of primary origin. The silicate-rich lithologies are generally very fine-grained and the only minerals that may be found in medium- to coarse-grained varieties are magnetite and minnesotaite. The presence of granules in these rocks gives a characteristic textural signature which may very well be directly related to the original primary Fe-precipitates. The carbonate-rich lithologies display apparent recrystallisation effects which are represented by large rhombohedral ankerites, well-crystallized magnetites with a common octahedral habit, calcite mosaics in association with stilpnomelane sheaves and sprays, and rather coarser varieties of quartz.

The distinction between primary and diagenetic textures is somewhat difficult since there is essentially no time-distinction between primary precipitation and diagenesis. The two processes are intimately associated with each other and any attempt to differentiate them, even for study purposes, is doomed to be disputed. However, as was briefly mentioned in the fore-going lines, lithologies with different mineral assemblages from the study area show different degrees of (diagenetic) recrystallisation, even though they belong to the same sedimentary package. It is concluded that any diagenetic effects present in the study rocks depend very much upon the chemical composition and character of the primary precipitate, and, as will be seen in the following lines, the detailed descriptions of the various textural features will directly refer to certain mineral assemblages with which they are commonly associated.

3.4.1 Primary textures

Textural features that may very well be of primary origin are the rhythmic, very-fine-grained hematitic microbands of the HBIF unit. Coarse magnetites in these rocks represent the major diagenetic overprint although other diagenetic textural features such as sinuous, quartz-filled vertical cracks are also present (Fig. 3.4a). The silicate-rich rocks of the lower parts of the LBIF unit have a shaly signature, with alternate dark-green to light-green, regular, sharp bands. These bands are defined by, and correspond to different mineralogical compositions: the darkish bands are granule-bearing as opposed to the light-green ones which consist essentially of microcrystalline greenalite and chert. When magnetite is present, it commonly overprints the granular bands, giving them a dark-grey metallic appearance. The type and regularity of banding, the mineralogical associations and the virtual lack of recrystallisation effects indicate that the silicate-rich rocks were deposited in relatively quiet conditions and have undergone little or no diagenetic recrystallisation processes. It is thus apparent that if any primary textures are present in the study rocks, they are more likely to be related to the granule-bearing, shaly BIFs, than any other lithotype from the study area.

3.4.2 Diagenetic textures and soft-sediment deformation structures

In contrast to the regular, shaly-banded, silicate-rich BIFs, the carbonate-rich lithologies have more irregular, diffuse, grey to dark-metallic bands of various thicknesses. The bands are often characterised by the presence of cross-bedding, pillows, pods, ribbons and other sedimentologically significant features which indicate deposition in a shallower water, agitated environment. Typical diagenetic recrystallisation and replacement textures are abundant in these rocks and are related to certain mineral assemblages. Specifically:

- Rhombohedral ankerite crystals associated with quartz-magnetite-pyrite- \pm minnesotaite assemblages. These ankerites may either be disseminated (Figs. 3.3g,h) or they may form the outer margins of veinlets with a core of microcrystalline quartz (Fig. 3.4d). These textures are found in fairly thick, white contorted carbonate bands and are almost always related to soft-sediment deformation structures (see also Fig. 3.5a).

- Calcite mosaics associated with acicular stilpnomelane (Fig. 3.3b). The calcite is always medium to coarse-grained (Figs. 3.3b, 3.4b) and the stilpnomelane most commonly forms fascicular growth textures (Barker, 1990). These textures consist of bundles of stilpnomelane needles which initiate from nuclei along the contact between calcite and chert-magnetite bands, and then branch slightly, forming characteristic arrangements (Fig. 3.4b).

- Quartz-recrystallisations-replacements. Microcrystalline quartz is often the result of replacement of either primary features (such as granules), or pre-existing minerals. It may be the only product of recrystallisation (Fig. 3.4e) but it may also coexist with diagenetic ankerite (Figs. 3.3g,h, 3.4d,f,g), riebeckite (Figs. 3.3e, 3.4c), and more seldom stilpnomelane. Quartz replacements of granules similar to the ones which characterise the silicate-rich lithologies are typical and common in the carbonate-rich lithologies of this study (Figs. 3.4f,g).

Other characteristic diagenetic features in the Voëlwater BIFs are **stylolites**. A stylolite is an irregular surface within a bed and it is characterised by mutual

interpenetration of the two sides—the columns, pits, and teethlike projections on one side fitting into their counterparts on the other (Blatt, 1982). The seam is made visible by a concentration of insoluble constituents, such as clay or organic matter.

Stylolites in the rocks of this study are closely related to the stilpnomelane-riebeckite associations discussed earlier in this chapter (§3.3.1.4; see also Fig. 3.4h). The orientation of the seams is approximately parallel to the banding, implying that the dissolution was probably caused by an interaction between overburden stress and pore-waters. The Na-rich deriving solutions would form pressure-solution surfaces by dissolving away some part of the original bands and would subsequently flow (or diffuse) and replace pre-existing minerals and textures, giving rise to crystalline quartz-riebeckite-(±magnetite) assemblages (Figs. 3.3e, 3.4c).

Fig. 3.4. Representative textures of rocks from the study area. a. Sinuous quartz vein transecting the hematitic BIF. Similar features have been reported by Simonson (1987), from North American BIFs that have undergone silica cementation and related diagenetic processes. b. Fascicular stilpnomelane needles arranged along the contact between a twinned calcite and a chert-magnetite-carbonate band. c. Grain of unknown mineralogical character now completely replaced by microcrystalline quartz and riebeckite needles. Note preferential riebeckite growth along cleavage(?) planes of the original crystal. d. Quartz-ankerite veinlets in a quartz-carbonate assemblage. The core of the vein consists of microcrystalline quartz and the outer parts of coarse rhombohedral ankerite. Stilpnomelane needles are found in the apophyses of the veins, at the contact with a chert-carbonate-magnetite-stilpnomelane band. e. Granular feature replaced by coarse-grained quartz in a quartz-magnetite-carbonate matrix. These coarser quartz crystals have irregular grain boundaries, indicating high total surface energy due to recrystallisation under very low-grade conditions. f. Granule "ghosts", now totally replaced by microcrystalline quartz. Note the later overprint by rhombohedral ankerite and coarse, subhedral magnetite. g. The same as f, but under cross polars. The granules are now very hard to distinguish due to the intense recrystallisation. h. Stylolite, separating a very fine-grained, chert-carbonate-magnetite-stilpnomelane band from a chert-riebeckite-magnetite one. Width of field of view: (a-g), 8mm; h, 30mm.

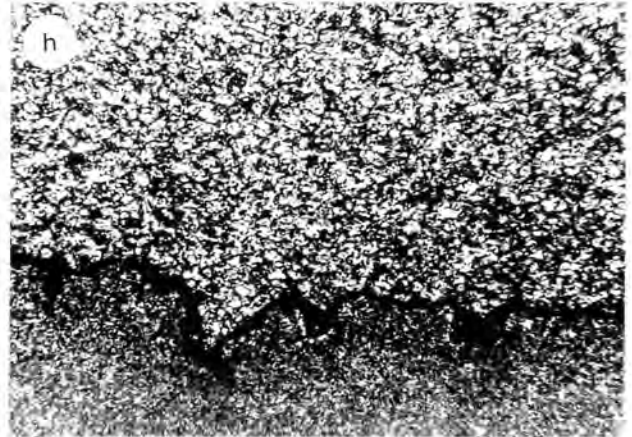
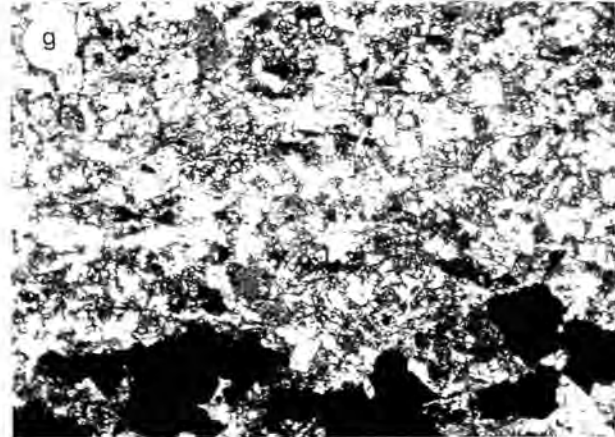
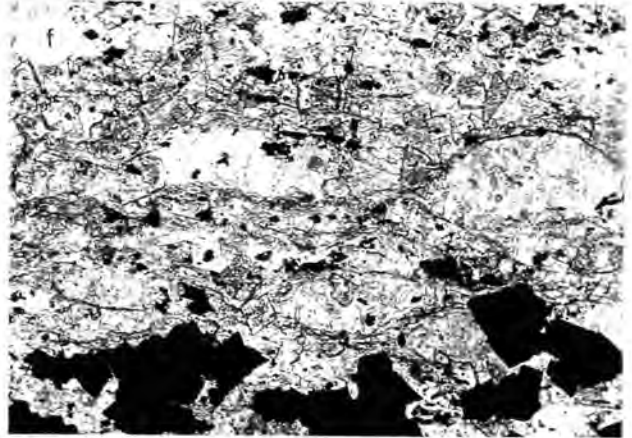
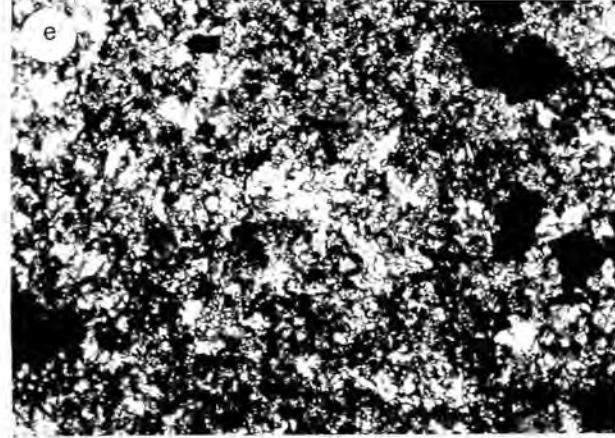
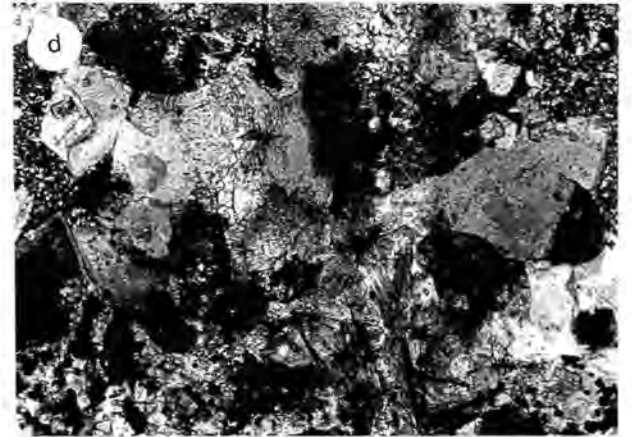
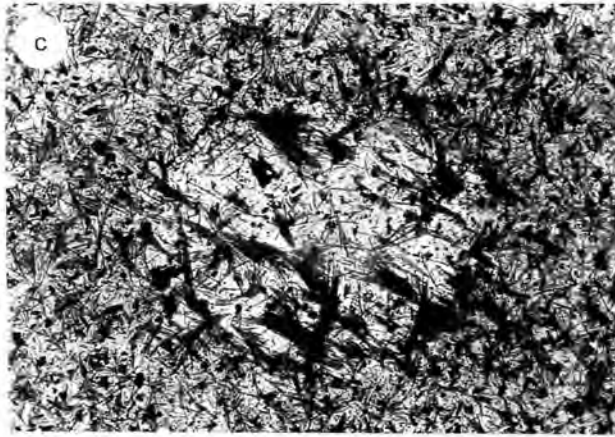
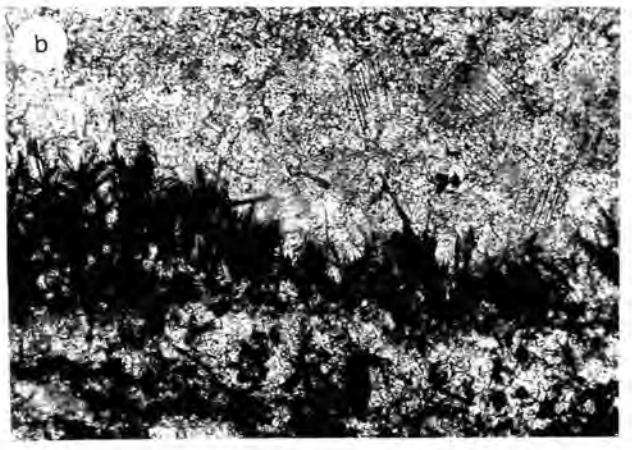


Fig. 3.4

Sedimentary structures related to soft-sediment deformation processes are also common in the carbonate-rich lithologies. They characterise the quartz-ankerite bands and they are clearly visible with the naked eye. Among the structures observed in the study rocks are intraformational breccia, syndepositional folds, boudinage, slump and scour-and-fill structures and microdiapirs (Fig. 3.5a). Similar structures have been observed in several other BIFs of the world (Gross, 1972; Blatt, 1982), and can be interpreted as deformation of noncohesive sedimentary layers or bands (e.g. the quartz-ankerite bands of this study) at the time of, or very shortly after, their deposition, but in any case, before their consolidation. This deformation could result from slumping under the influence of gravity, overloading or unequal loading by sediment, or even from frictional drag (e.g. skin-friction of currents of overflowing fluid or semi-solid material; Reineck & Singh, 1973).

3.4.3 Textural evidence for post-depositional tectonic effects

Evidence for ductile deformation on the Voëlwater BIFs can be found in certain parts of the stratigraphy in the area of study. Specifically, mylonitic zones with shear-sense indicators are abundant in granular lithologies from the LBIF unit, manifesting the presence of tectonic effects which may be of regional significance (thrusting?) in the study area. Some representative textures from these lithologies such as σ structures, possible rolling (δ) structures, "domino" (bookshelf) sliding, etc. (Simpson & Schmid, 1983), are illustrated on Fig. 3.5b.

The main question that arises from the fore-going concerns the timing of the shear deformational processes that caused these structures with respect to the diagenetic and soft-sediment deformation processes in the upper parts of the Voëlwater BIF. As was shown in Figs. 3.4f and g, features with a granular signature are also present in these rocks, but they have now almost completely been replaced by diagenetic quartz-ankerite- \pm magnetite. Any effects of shearing in those recrystallised occurrences is indeed difficult to establish, and it remains

uncertain whether the "post-depositional tectonic effects" of this paragraph are also clearly post-diagenetic, or whether they were initiated at syn-sedimentary times.

3.5 Regional implications

It is a generally accepted view that the iron-formation minerals discussed in the previous paragraphs are late diagenetic products of chemical sedimentary precursor materials (James, 1954; Klein & Fink, 1977; Mel'nik, 1982; Klein, 1983; see also Fig. 3.6). The mineralogical composition of the Voëlwater BIF certainly leaves no doubt as to its origin. What cannot be ascertained in this study is whether the mineralogy of the study rocks remains the same throughout the Kalahari area as a simple function of burial diagenetic processes, or whether the study rocks represent the least affected member of a regional or contact-metamorphic event. The latter possibility requires further investigation that will cover larger areas in Northern Cape, including of course the north-western portion of the Kalahari basin where the Mn-ore has been hydrothermally upgraded. Implications for metasomatic replacement of these ores by deep-seated granitic or syenitic intrusive bodies have been provided by Dixon (1985,

Fig. 3.5. a. Soft sediment deformation structure in carbonate-rich BIF from the study area. This "microdiapir" has probably formed under late-diagenetic conditions but certainly before complete consolidation of the sediment took place. The mechanism for the formation of such features would include: i. burial of fluidised carbonate-sediment under thick overload; ii. compaction, "squeezing" and upward escape of the relatively lighter carbonate-rich fluids through diagenetic cracks; iii. subsequent trapping by the denser overburden; and, iv. growth of coarse ankerite on the edges of the structure, followed by crystallisation of microcrystalline quartz. Width of field of view: 56 mm.

b. Shear-sense indicators in granular, BIF lithologies from the study area, in the form of σ structures (i, iv), possible rolling (δ) structures (ii), and "domino" (bookshelf) sliding (ii, iii, iv). Width of field of view: (i-iv), 8mm; shear sense along the shear plane is shown.

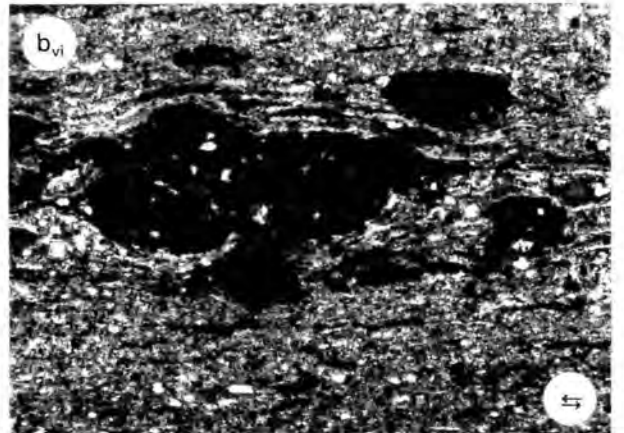
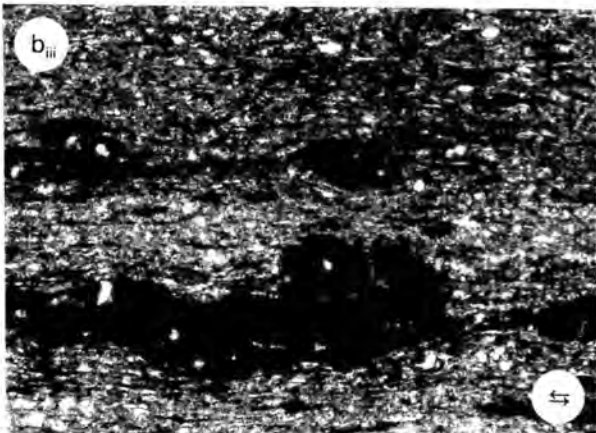
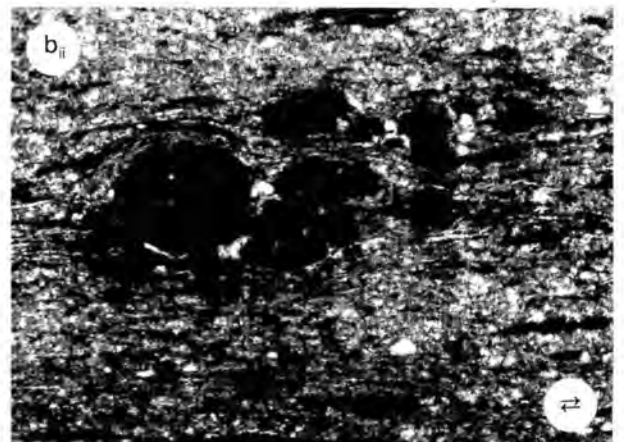
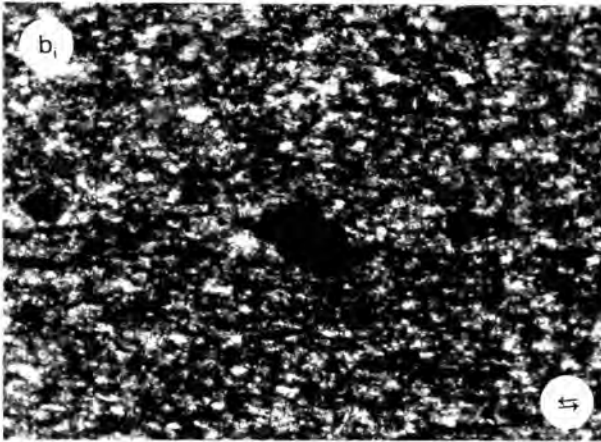
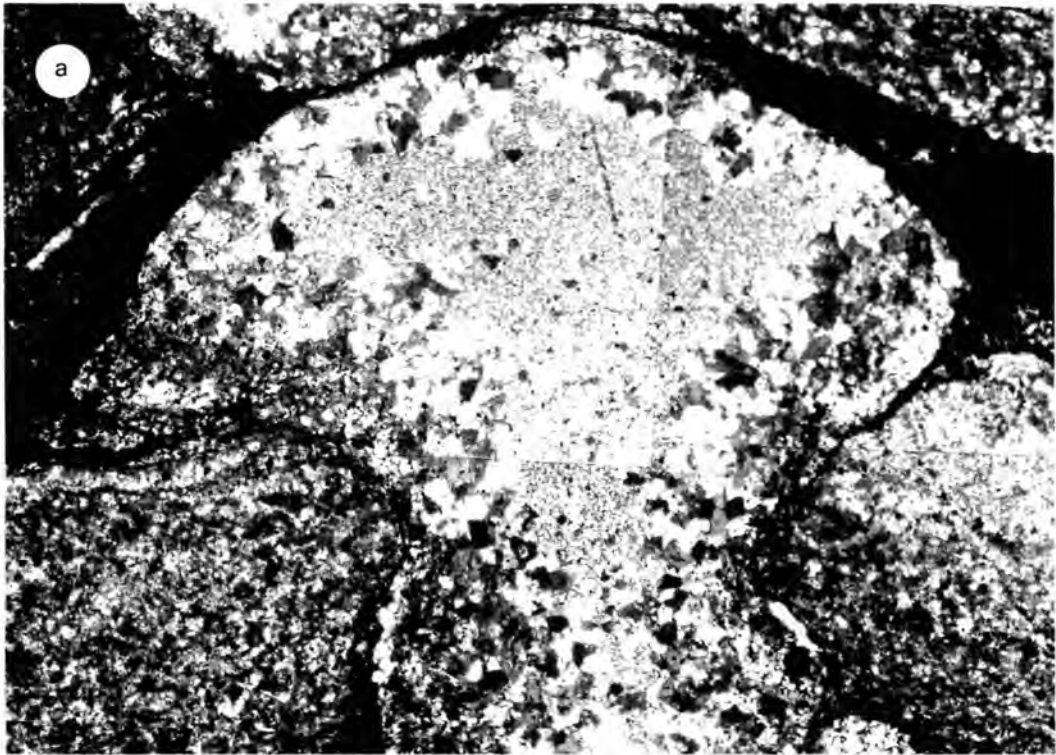


Fig. 3.5

1986, 1989), although little information exists for regional igneous activity in the wider area. The various dykes that transect the Voëlwater rocks cannot have produced such a significant metasomatic effect. Mafic sills in the Penge iron-formation of the Transvaal Sequence, however, are believed to have caused a high-grade metamorphic overprint on the contact metamorphic event related to the intrusion of the Bushveld Complex (Miyano et al., 1987). In this particular case, though, the local metasomatic effect induced by

the sills was largely enhanced by the high temperatures that predominated in the country rocks due to the Bushveld intrusion (op. cit.). In any case, an intrusive body is required in the close proximity of the Kalahari basin to substantiate any metasomatic effect on the Mn-ores, and so far, the Kameel mafic body situated in the Western part of the basin seems to fulfill the required conditions (Wiggering & Beukes, 1987; Beukes, 1993). If this is so, then the Voëlwater BIF may be very similar in regional mineralogical character to the Biwabik and Gunflint BIFs of Minnesota which have been metamorphosed by a basic igneous intrusion (Duluth Gabbro Complex: French 1968; Floran & Papike, 1978).

GRADE OF METAMORPHISM				
LOW	MEDIUM		HIGH	
DIAGENETIC	BIOTITE ZONE	GARNET ZONE	STAUROLITE - KYANITE AND KYANITE ZONE	SILLIMANITE ZONE
Early - Late				
chert	→ quartz			
"Fe ₃ O ₄ · H ₂ O"	→ magnetite			
"Fe (OH) ₃ "	→ hematite			
greenalite				
stilpnomelane				
	ferri-annite			
	talc - minnesotaite			
	Fe - chlorite (ripidolite)			
	dolomite - ankerite			
	calcite			
	siderite - magnesite			
	riebeckite			
	cummingtonite - grunerite (anthophyllite)			
	tremolite - ferroactinolite (hornblende)			
	almandite			
			orthopyroxene	
			clinopyroxene	
			fayalite	

Fig. 3.6. Relative stabilities of minerals in metamorphosed BIFs as a function of metamorphic grade (compiled after James, 1954; French, 1968, Klein, 1978; Floran & Papike, 1978; in Klein, 1983).

4. GEOCHEMISTRY OF THE VOËLWATER BANDED IRON-FORMATION

4.1 Introduction

Many authors have drawn attention to certain aspects of the chemistry of banded iron-formations, such as REE geochemistry (Fryer, 1977a,b, 1983; Graf, 1978; Appel, 1983; Shimizu et al. 1987; Barrett et al., 1988; Jacobsen & Pimentel-Klose, 1988; Dymek & Klein, 1988; Klein & Beukes, 1989; Beukes & Klein, 1990a,b; Derry & Jacobsen, 1990; Danielson et al., 1992; Bau & Dulski, 1992, 1993; Bau, 1993; Bau & Möller, 1993) and stable isotope studies (Becker & Clayton, 1972, 1976; Perry & Tan, 1973; Perry et al., 1973; Dimroth & Kimberley, 1976; Monster et al., 1979; Perry & Ahmad, 1980, 1981; Perry, 1983; Cameron, 1983; Walker, 1984; Gregory, 1986; Kaufman et al., 1990; Beukes et al., 1990a,b; Carrigan & Cameron, 1991). However, considerable lack of geochemical data exists as far as the bulk and trace element composition of these rocks is concerned, and any comparative studies between BIFs from other areas of the world are almost absent from the literature. As it has been highlighted by Davy (1983, p. 333) in his review paper on the chemical composition of Precambrian BIFs: "The problem of establishing and comparing the average compositions of iron-formations is that of lack of data...". Several factors have added up to that problem: secondary processes such as weathering and supergene enrichment, hydrothermal alteration, metamorphism, etc., commonly obscure the primary chemical composition of BIFs. In addition, the banded nature of these rocks always results in severe chemical inhomogeneity, and any sampling procedures should be conducted very carefully in order to attain reliable results. Nevertheless, the chemical characterisation as well as the understanding of the origin of the Voëlwater BIF was approached in this study by means of bulk geochemical data, whereas comparison with other banded iron-formation occurrences was largely based on data essentially supplied by two papers, those of Gross and McLeod (1980) and Gole and Klein (1981). Comparisons with other Fe-bearing lithotypes (e.g. ironstones) as well as with

recent metalliferous sediments are also attempted in this chapter and respective geochemical diagrams are provided therein. It should be stressed, though, that the distinct character of BIFs in terms of age, depositional environment and petrographic signature, was taken under serious consideration before any conclusions or deductions were made. Furthermore, any classification schemes were avoided, and possible genetic implications and modellings will be discussed in detail in the fifth chapter of this study (see §5.2).

4.2 Sample collection, preparation and analytical procedure

Four boreholes (R-65, R-59, R-70 and R-63) situated N-NW of the Mamatwan manganese mine were selected for sampling of the several BIF units present in the stratigraphic column of the Voëlwater Subgroup. These boreholes are aligned on a SSE-NNW direction, in regular intervals of approximately 1000m (Fig. A1). Their selection was based on two facts: i. the boreholes exhibit significant thickness variations of BIF and Mn units in a lateral sense; and, ii. all four boreholes contain the entire succession of the Hotazel formation virtually unaffected by secondary processes. A total of 62 samples was collected, representing essentially all the different BIF lithotypes present in the stratigraphy. The length of the samples was variable, depending on the scale of banding, presence of secondary veining and thickness of the individual rock unit. From these 62 samples, the 35 most homogeneous and at the same time most representative samples were crushed, ground in two stages (swing mill and automatic agate pestle and mortar) and analysed for major and trace elements using X-Ray fluorescence procedures. Major elements (except Na) were determined on fused duplicate lithium tetraborate glass discs prepared after the method of Norrish and Hutton (1969); trace elements and Na were determined on pressed powder pellets. The analyses were done on a Philips PW 1480 X-ray spectrometer at Rhodes University and the results are summarized in Table A1. All analytical runs were calibrated using a variety of international and in-house standards, whereas corrections for dead time, background, spectral line

interference, instrumental drift and mass absorption were made in all determinations.

4.3 Bulk geochemical composition

4.3.1 Major elements

Useful information regarding the Voëlwater BIFs in terms of major element composition can be obtained from the geochemical profiles (Fig. A2). For each one of the selected boreholes, a profile of the distribution of the six most abundant major elements (Fe, Si, Ca, Mg, Mn and Al) was drawn, in order to facilitate comparisons on both a vertical and a lateral sense. Some preliminary conclusions that could be made by a closer examination of these diagrams are summarised below.

-There is an apparent change from silicate-rich to more carbonate-rich lithologies towards younger strata. The transition is considered gradational due to the wide range of CaO contents present in the Voëlwater rocks. However, an Al-K-Na-rich horizon occurring below the middle manganese body and characterised by the abundance of stilpnomelane and riebeckite (Table A1: samples R-70-12, R-63-9; see also ¶3.3.1.4), could be considered as a possible stratigraphic "marker", since it separates relatively carbonate-poor lithologies from carbonate-rich ones. The extent of this "marker" horizon was not possible to determine from the boreholes selected.

-Apart from the significant thickness variation of the Mn and BIF units between the boreholes R-65 and R-59, significant lateral geochemical variations in the form of enrichments or depletions of certain elements were not encountered. Large-scale correlations between the several BIF units are therefore possible from both a geochemical and a mineralogical point of view.

-Mn-enriched lithologies are found in the immediate vicinity of Mn-bodies (R-65-21, R-59-3) but they are most prominent in the hematitic BIF below the

lower Mn-body (R-65-30, R-65-31, R-63-20; see also Table A1). In contrast, the MgO and Al₂O₃ contents remain essentially the same throughout the stratigraphy.

Elements such as K, Na, Ti and P are present in negligible amounts in the rocks of this study. Hence, they have not been included in any of the profiles and they will not be discussed in this section. Additional information regarding the geochemistry of the major elements Si, Fe, Ca, and Mn in the Voëlwater rocks, as well as comparisons with other BIF occurrences of the world, are supplied in the following paragraphs.

4.3.1.1 *Si-Fe-Ca*

From an examination of the major element profiles (Fig. A2), one can deduce that any variation in the bulk chemical composition of the Voëlwater lithologies is entirely dependent upon the changes in the contents of the elements **Si**, **Fe** and **Ca**. The ternary diagram of Fig. 4.1 provides a concise view of the geochemical behaviour of these three elements. A notable feature of the above diagram is the "triangular shape" of distribution of the Voëlwater samples which shows that the three elements are totally interrelated within a distinct compositional field. This diagram also illustrates the difficulty in distinguishing between fields of certain BIF types such as carbonate, silicate or oxide. All samples should therefore be treated as essentially one group, even though they represent more than one mineralogical assemblage.

A better understanding of the inter-element associations between Fe, Si and Ca, can be obtained by means of the diagrams a,b,c and d of Fig. 4.2. The compositions of the three elements are variable, with ranges of 15-55% SiO₂, 0-25% CaO and 25-50% total Fe as FeO. As is shown on the diagram 4.2b, there is an apparent negative correlation between CaO and SiO₂ which verifies the transition from a silicate-rich to a more carbonate-rich environment. Also, the

negative correlations between CaO and FeO (4.2a) and to a lesser extent between SiO₂ and FeO (4.2c), are indicative of a reduction of the amount of Fe from the silicate-rich towards the more carbonate-rich lithologies. The last two negative trends can be integrated and intensified if the FeO content is plotted against the much less variable sum of the CaO and SiO₂ contents (40-55 %), as is illustrated on Fig. 4.2d.

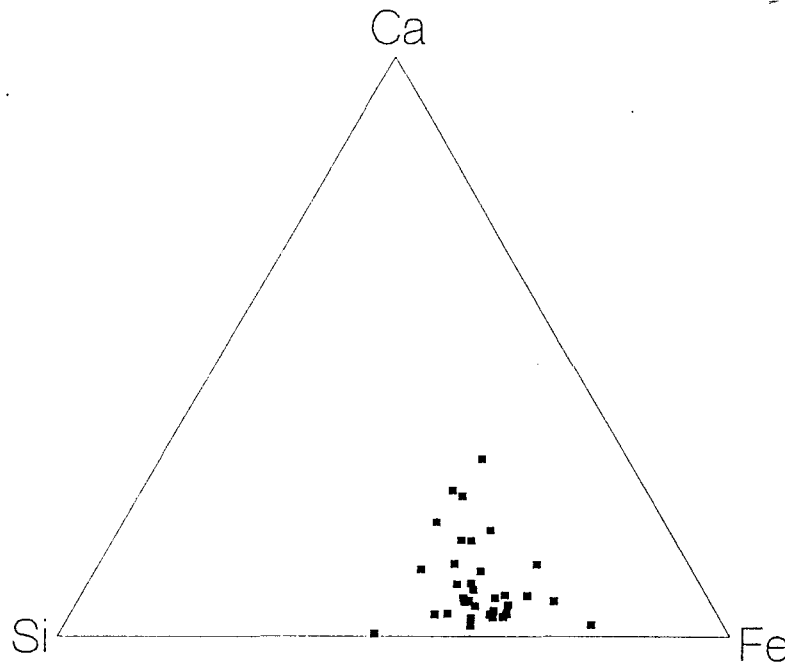


Fig. 4.1. Ternary diagram Ca-Si-Fe illustrating the compositional range of BIF lithologies from this study (filled squares).

Two additional diagrams have been included in Fig. 4.2: The first (4.2e) emphasizes the presence of large amounts of carbonate minerals (particularly calcite) in the Voëlwater BIF, by means of the positive correlation between CaO and LOI (loss on ignition). Even though the CO₂ and H₂O contents are not truly represented by the latter value in any analytical data deriving from XRF techniques due to the oxidation of Fe⁺² to Fe⁺³ during the sample preparation, it appears that it is the content of Ca-bearing carbonate facies that is responsible for most of the loss on ignition (in the form of CO₂) in the Voëlwater rocks. The latter assumption could be particularly valid in the case of the carbonate-rich lithologies which show significant effects of diagenesis and lack of hydrous silicate minerals (no greenalite, little stilpnomelane, occasional minnesotaite)

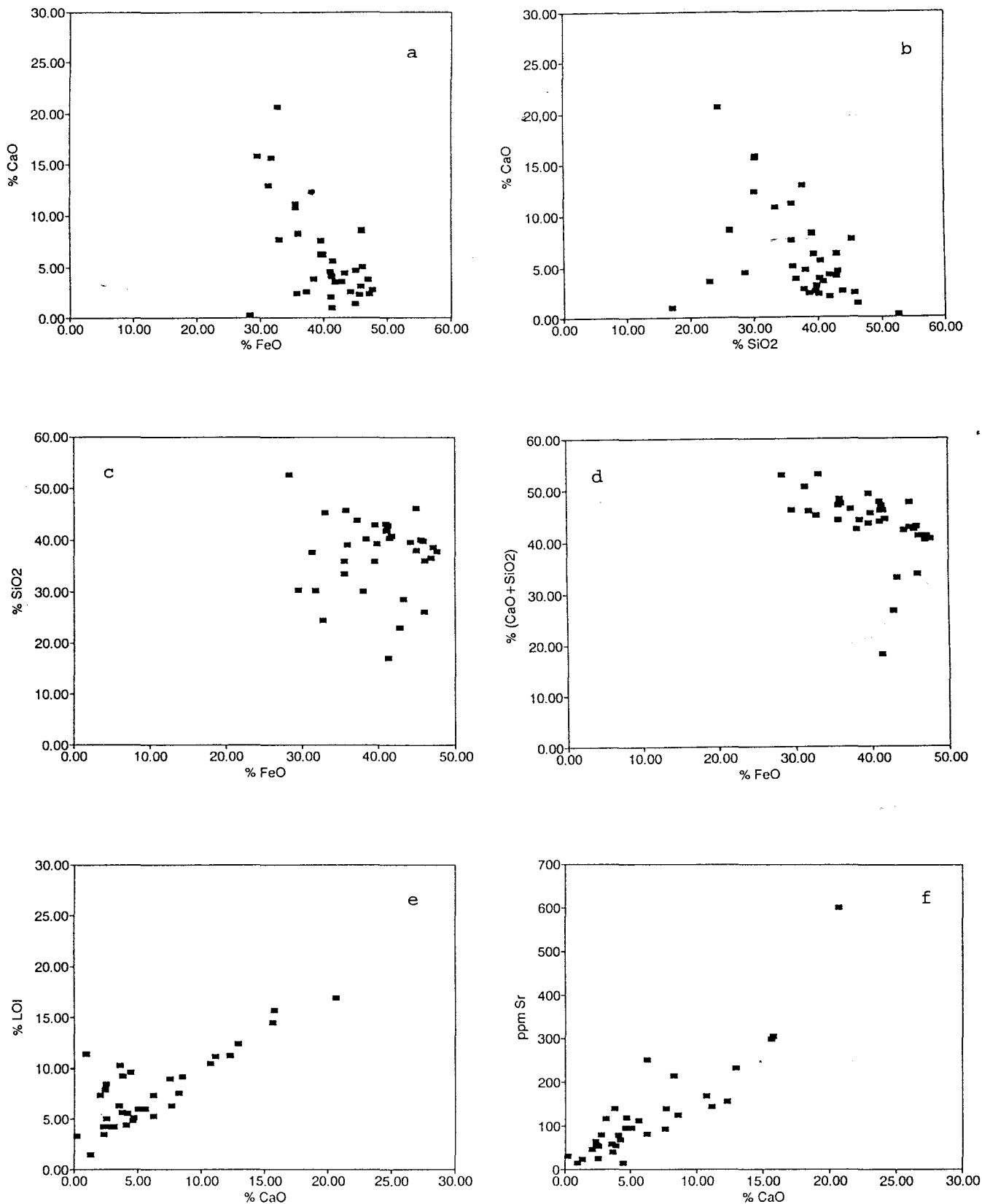


Fig. 4.2. Bivariate diagrams of (a) CaO vs FeO; (b) CaO vs SiO₂; (e) SiO₂ vs FeO; (d) (SiO₂ + CaO) vs FeO; (e) CaO vs LOI; and, (f) CaO vs Sr, for rocks of this study (filled squares).

compared to the silicate-rich horizons. The second diagram (4.2f) manifests the pronounced positive correlation between CaO and Sr, which indicates that the latter element is closely associated with calcium carbonate mineral facies.

4.3.1.2 *Mn*

The bulk of the samples from the study area have essentially low Mn-contents (ranging from 0.04 up to 2.21%), with the highest Mn values normally being found in carbonate-rich samples (Fig. 4.3a). However, three samples collected from the hematitic iron-formation unit below the lower Mn-body (R-65-30, R-65-31 and R-63-20; see Table A1) show significant Mn-enrichment with metal contents up to 18%. This Mn-enrichment is marked by two geochemical trends: the SiO₂ (Fig. 4.3c) and, to a lesser extent, the CaO (Fig. 4.3a) contents are low and decrease slightly as the Mn-content increases. In contrast, the FeO content remains high and essentially constant (Fig. 4.3b). The significance of the diagrams of Fig. 4.3 lies in the geochemical behaviour of Fe and Mn while the hematite-rich BIF unit was laid down: they clearly document that the physico-chemical conditions during the deposition of this particular rock unit were favourable for co-precipitation of the two elements, even when the rates of Mn-deposition were unusually high for BIFs. They imply at the same time, the positive geochemical correlation between Fe₂O₃ and Mn and they offer useful information regarding the palaeodepositional environment of the Voëlwater BIF with respect to its possible modelling.

4.3.1.3 *Chemical comparison with other iron formations*

The average composition of 30 of the analysed samples (Table A1) was used in this study for systematic comparisons with other BIF occurrences of the world. The exclusion of the remaining 5 samples was based on their atypically high values of certain elements, in combination with their limited abundance.

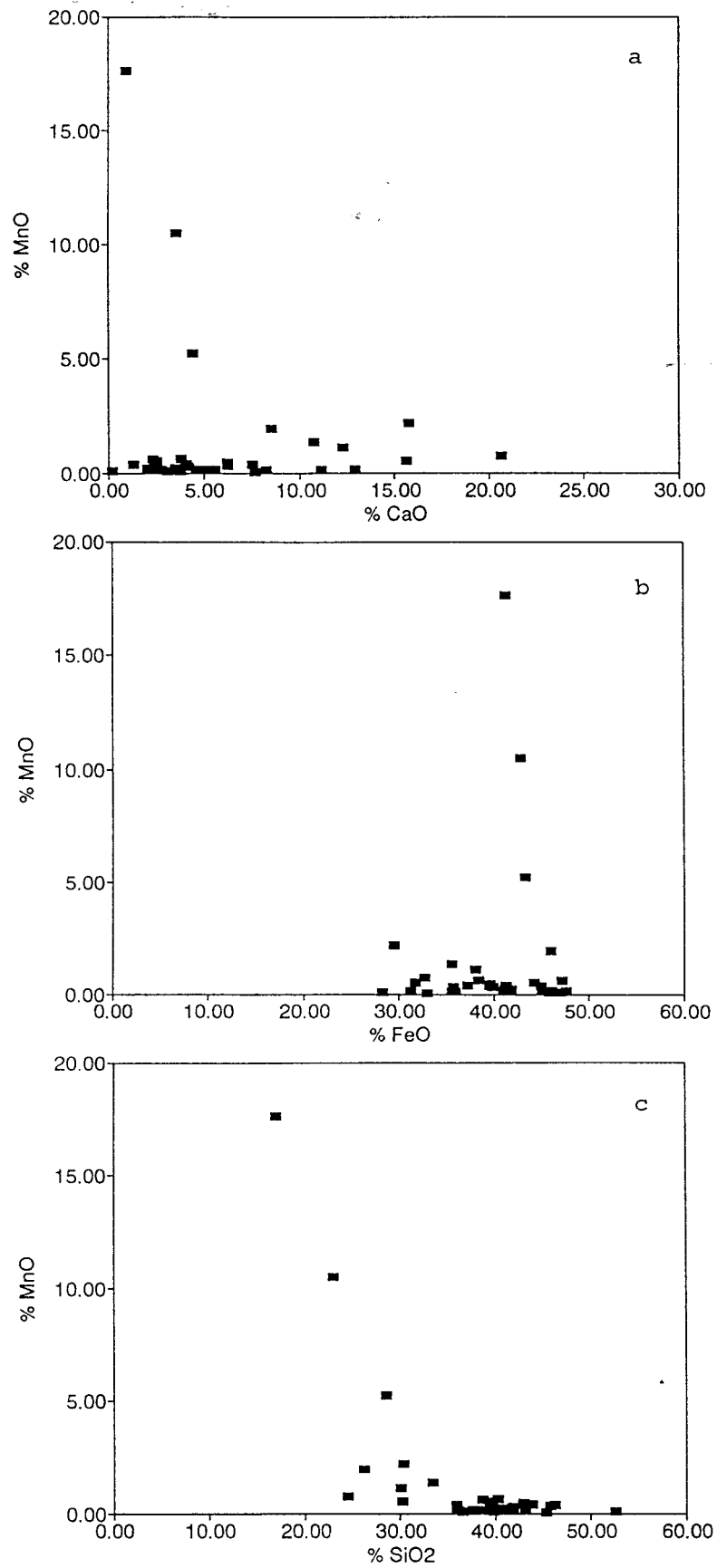


Fig. 4.3. Bivariate plots of MnO vs: (a) CaO, (b) FeO and (c) SiO₂ for samples from the study area (filled squares).

Specifically:

-the samples R-65-30, R-65-31 and R-63-20 from the hematite-rich unit immediately below the lower Mn-body show Mn contents (> 5%) well above the maximum of the rest of the BIF lithologies from the study area;

-the samples R-70-12 and R-63-9 represent a restricted iron-formation unit just below the middle Mn-horizon, and they have unusually high aluminium and alkali-content.

Results for the Voëlwater average are illustrated in Fig. 4.4, together with a field encompassing the range of averages for a variety of other BIFs reported by Gole and Klein (1981; see also Table A2a). Included in this range is the average major element composition of the BIFs of the Asbesheuwels Subgroup in South Africa, as calculated by analytical data reported in the papers by Klein and Beukes (1989) and Beukes and Klein (1990a).

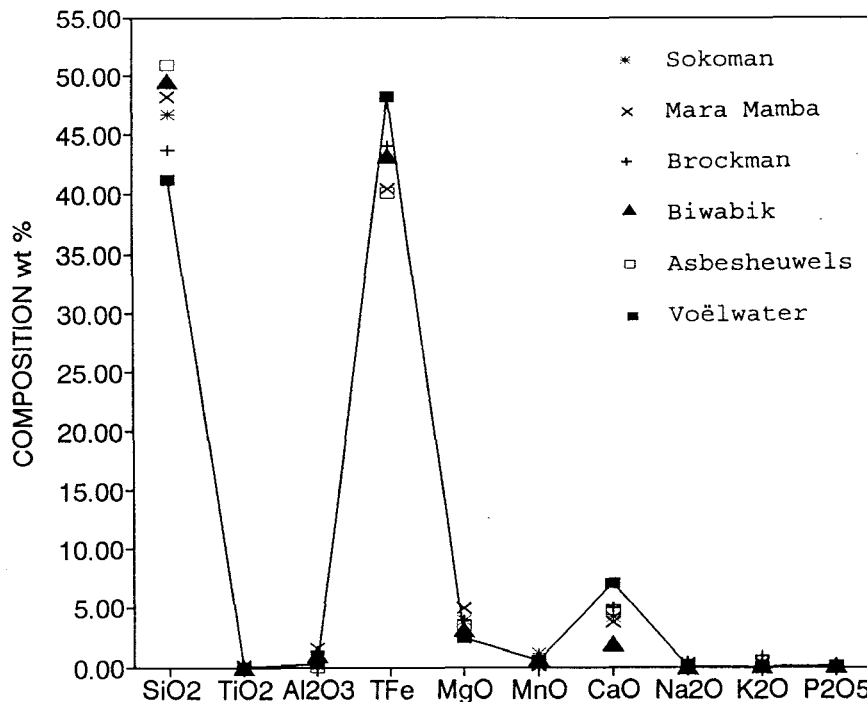


Fig. 4.4. Plot of averaged bulk chemical analyses of banded iron-formations given in Table A2a, as compared to analytical data from this study. The analyses are recalculated to 100% on an H₂O and CO₂-free basis. Total Fe is represented as Fe₂O₃. Data are from Gole and Klein (1981), Klein and Beukes (1989) and Beukes and Klein (1990a).

As is shown on Fig. 4.4, the Voëlwater BIF average has higher Fe(T) (as Fe_2O_3) and CaO and lower SiO_2 and MgO compared to other BIFs. For the remaining oxides the data from this study are well within the ranges reported for other occurrences. It is clearly documented that the Voëlwater BIF is remarkably similar to other Proterozoic BIFs in terms of its average major element composition, a similarity which suggests that the iron-formation of this study was probably formed by processes which were very similar to those that formed other major Proterozoic BIFs of the world.

4.3.2 Trace elements

Geochemical profiles for the 10 most abundant trace elements in the rocks of this study are illustrated in Fig. A2. The Voëlwater rocks are characterised by significant depletion in certain elements (e.g. Co, V), whereas the anomalously high values of Sr and Ba are related to respective high carbonate and Mn-contents, frequently present in the study rocks. In terms of average transition metal contents, comparisons between the Voëlwater BIF and other BIFs of the world were also attempted (Fig. 4.5) with analytical data obtained by various published papers (see Table A2b). Specifically, complete transition metal data for both the Brockman BIF, Australia and average values from several Superior- and Algoma-type BIFs of Canada were obtained by Trendall and Pepper (1977; in Davy, 1983) and Gross and Mcleod (1980), respectively. In the case of the Kuruman and Griquatown BIFs of S. Africa, analytical results for Zn, Ni, Co and Sc were obtained from Klein and Beukes (1989) and Beukes and Klein (1990a), whereas data for Cu, Cr and V were obtained from Hälbich et al. (1993). It should be stressed that several discrepancies were noted in the analytical results published by Klein and Beukes (1989) and Beukes and Klein (1990a), with sometimes unusually high detection limits for certain trace elements (e.g. V) and extraordinarily accurate values for others (e.g. Sc, Co) according to the analytical method employed (XRF). Conclusions based on correlations between the analytical results of this study and this data, therefore, must be guarded.

Nevertheless, as is shown on Fig. 4.5, the compositional pattern of the Voëlwater averages is roughly parallel to the ones corresponding to the Kuruman, Griquatown and Brockman BIFs and to a lesser extent to the Superior-type BIF averages from Canada, suggesting a similarity between the Voëlwater BIF and other typical Superior-type BIFs. In contrast, Algoma-type averages show a markedly different geochemical signature which is characterised by significant enrichment in almost all the elements, particularly Zn, Cu, Ni and Co.

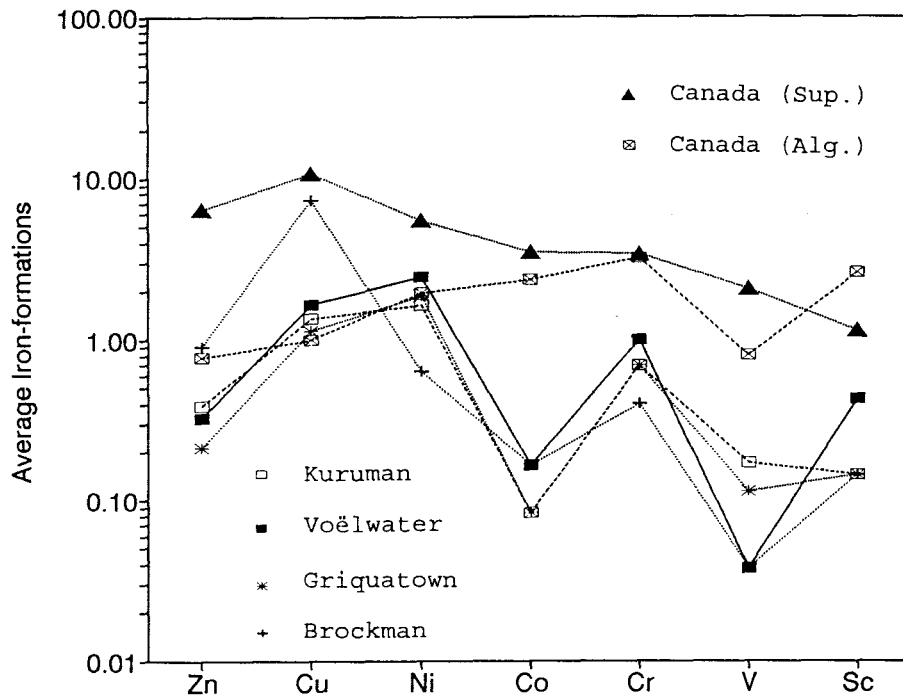


Fig. 4.5. A comparison of average transition metal compositions of the Voëlwater BIF (filled squares), and those characterising the Kuruman and Griquatown BIFs, S. Africa (Klein & Beukes, 1989; Beukes & Klein, 1990a; Hälbich et al., 1993), the Brockman BIF of Australia (Trendall & Pepper, 1977; in Davy, 1983), as well as several Algoma- and Superior-type BIFs of Canada (Gross & McLeod, 1980). Analytical data were normalised using averaged crustal abundances of transition metals, as reported by Shaw (1980).

4.4 Chemical distinction between Fe-bearing sedimentary rocks

4.4.1 Si-(Fe + Mn)-Al

One of the very few ternary diagrams ever devised for the geochemical

distinction between BIFs and Phanerozoic ironstones was proposed by James (1969). From a mineralogical point of view, the main difference between these two lithotypes lies in the kind of silicate minerals present: BIFs normally contain variable amounts of Fe-silicates with negligible Al-content (greenalite, minnesotaite, riebeckite and to a lesser extent stilpnomelane), whereas ironstones consist essentially of two Al-bearing silicate facies, namely **chamosite** and **berthierine** (Young, 1989). It is the difference in the overall content of aluminium that allows for safe geochemical discrimination between these two major categories of ferruginous sediments, as is illustrated in the ternary diagram Si-(Fe + Mn)-Al.

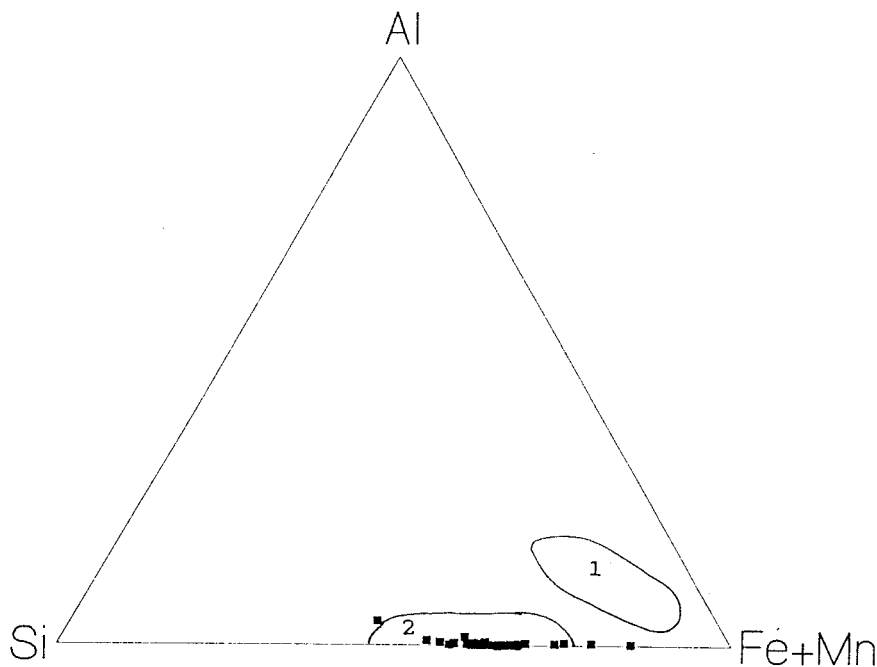


Fig. 4.6. Ternary diagram of Si-(Fe + Mn)-Al showing the fields defined for: (1) ironstones; and, (2) BIFs, by James (1969). Data from the present study are shown as filled squares.

It is clearly documented from the above diagram that lithologies equivalent to Phanerozoic ironstones are completely absent from the Voëlwater BIFs. Samples that do not fall into the field of BIFs could be regarded as "unusually" rich in either Si or (Fe + Mn). However, the writer believes that the position of the field (2) boundaries on the (Fe-Mn) tie-line should be re-defined, since increased geochemical data from various BIF lithologies have been introduced in the literature over the last 25 years.

4.4.2 Fe/Al-Ca/Mg

A significant difference between banded iron-formations and Phanerozoic ironstones is in the CaO content. Proterozoic BIFs have normally low CaO, as against the higher CaO averages for Phanerozoic rocks (Taylor, 1974). Also, similar relation exists as far as Al_2O_3 is concerned (see also 4.4.1). There is, however, little difference in MgO, with respective averages of 2.8% and 2.9% (Lepp & Goldich, 1964). When Ca/Mg and Fe/Al ratios are plotted for comparisons between the two rock-types, two distinct fields can be defined. The first (a) corresponds to high Ca/Mg and low Fe/Al ratios and represents Phanerozoic lithologies, whereas the second (b) shows a reverse correlation and corresponds to chemical analyses from Proterozoic Fe-formations (Taylor, 1974; see also Fig. 4.7). When analytical data from this study are superimposed on the diagram, the Voëlwater rocks plot in the field of BIFs, leaving no doubt about their geochemical character and their similarities with the latter.

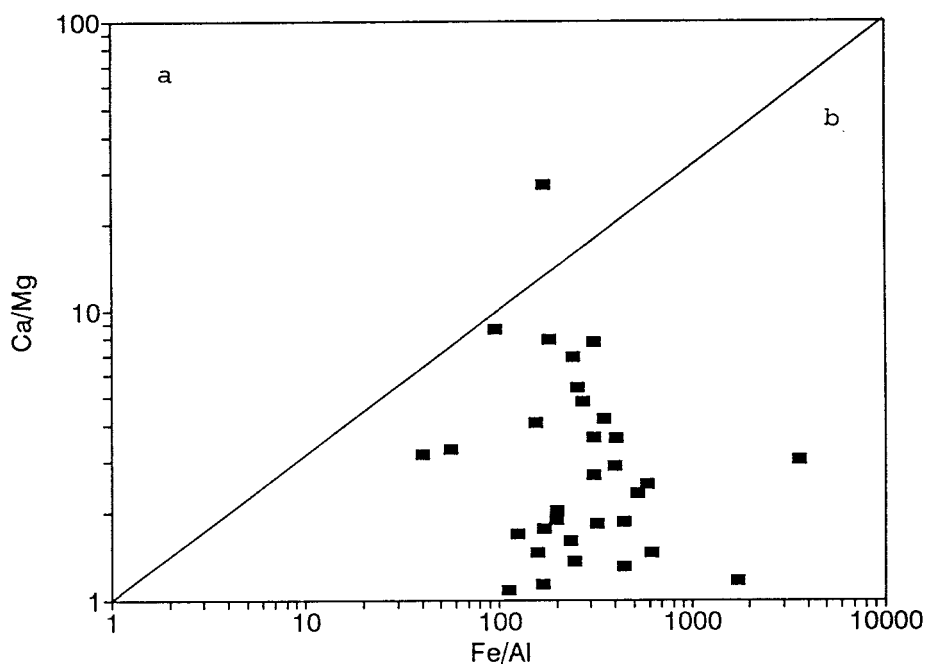


Fig. 4.7. Plot of Ca/Mg and Fe/Al ratios (on log scale) for rocks from this study. Also plotted are the fields of: (a) British Jurassic ironstones (Taylor, 1974); and, (b) Precambrian banded iron-formations (James, 1966; in Taylor, 1974).

4.4.3 Si-Al

Chemical comparison between BIFs, ironstones and several types of ferromanganese deposits such as modern and ancient hydrothermal Fe-Mn deposits, hydrogenous Mn-nodules and Fe-Mn crusts, can be made using the bivariate Si/Al plot. In this diagram (devised by Crerar et al., 1982), the rocks from the study area exhibit a very high Si/Al ratio which can only be compared to the ratios from Superior-type BIFs (after Gross & McLeod, 1980; in Moore, 1989) and hydrothermal deposits (Fig. 4.8). Unlike hydrothermal deposits, ironstones and ferromanganese nodules and crusts of hydrogenous origin have considerably lower Si/Al ratios, depending in each case on the amount of detrital material incorporated in the sediment/rock. Therefore, as is illustrated in Fig. 4.8, a probable chemogenic origin for the Voëlwater BIFs with insignificant detrital input can be clearly established.

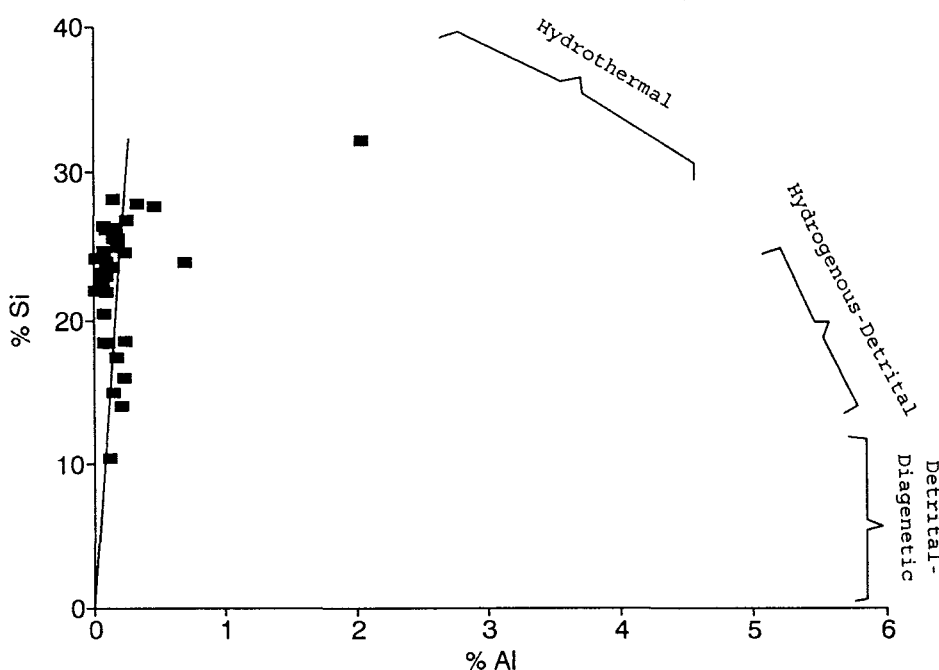


Fig. 4.8. Plot of Si vs Al for BIF lithologies from the study area (filled squares), compared to hydrothermal and hydrogenous-detrital Fe-Mn deposits, and detrital-diagenetic ironstones (after Crerar et al., 1982).

4.5 Comparisons with recent metalliferous sediments

4.5.1 Mn, Fe, Si, and minor metals

Two types of metalliferous sediments are known to occur in the modern oceans (Bonatti et al., 1976; Toth, 1980; Roy, 1981; Marchig et al., 1982):

1. **Hydrothermal deposits**, associated with active rift systems in mid-ocean ridge (MOR) environments. These sediments normally form after a stepwise procedure of: i. circulation of descending seawater in active spreading centres or areas of high heat flow; ii. heating and hydrothermal leaching of tholeiitic basalts; iii. enrichment of the hot brines in various elements and subsequent debouchment on the ocean floor; and, iv. mixing with cold near-bottom seawater and rapid precipitation of iron and manganese hydroxides. The hydrothermal deposits are characterised by strong fractionation between iron and manganese (Bonatti et al., 1976; Toth, 1980) and contents of minor metals (Ni, Cu, Co, etc.) well in excess of normal pelagic sediments but an order of magnitude less than hydrogenous ferromanganese deposits (Crerar et al., 1982).

2. **Hydrogenous (diagenetic) precipitates**, forming under very slow precipitation of iron and manganese hydroxides from seawater. They show low fractionation rates of iron and manganese (Bonatti et al., 1976), and higher concentration of minor metals, due to the extraordinarily high absorption capacity of Fe and Mn hydroxides during slow precipitation (Crerar et al., 1980; in Crerar et al., 1982).

The above-mentioned geochemical differences between recent hydrothermal and hydrogenous sediments can be emphasized by means of the diagrams Fe-Mn-(Ni + Cu + Co)×10 and Fe-Mn-Si(x2), proposed by Bonatti et al. (1972; in Toth, 1980). On the first diagram, the hydrothermal sediments, typically fractionated and relatively poor in transition metals, tend to concentrate at the Fe and Mn apices. In contrast, the hydrogenous sediments, Fe-Mn crusts and Mn-nodules plot in more central fields, indicating that the Fe/Mn ratio in those sediments

averages about unity (Fig. 4.9a). The second diagram compares the relative concentrations of the major components Fe, Mn, and Si, and illustrates that hydrothermal deposits concentrate either on the Mn-apex or on the Fe-Si tie-line, whereas hydrogenous deposits again occupy more central fields (Fig. 4.9b).

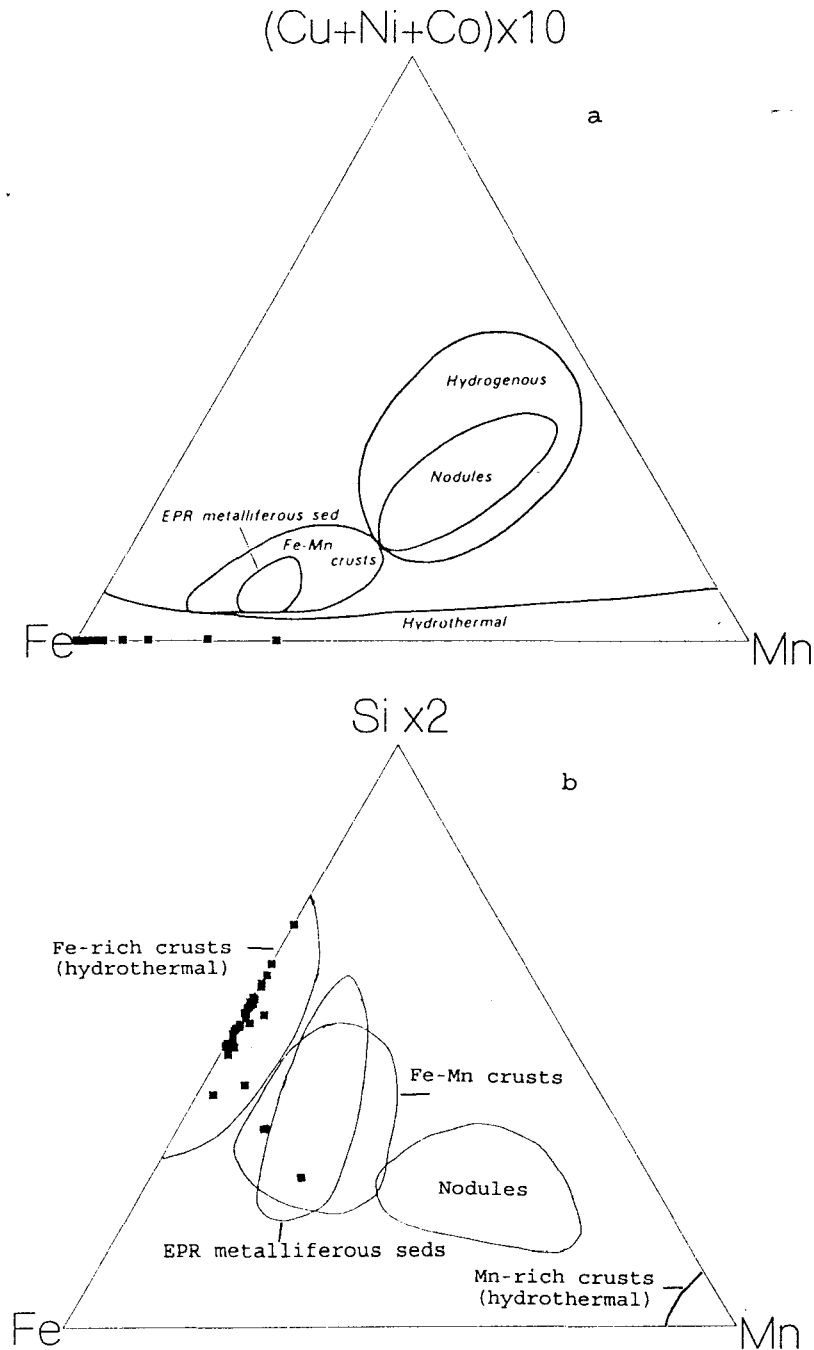


Fig. 4.9. Ternary diagrams of: (a) Fe-(Ni+Cu+Co)x10-Mn; and, (b) Fe-Si(x2)-Mn showing the positions of rocks from the study area (filled squares) relative to the fields of various marine sediments (after Bonatti et al., 1972; in Toth, 1980).

When data from the present study are superimposed on both the diagrams of Fig. 4.9, the vast majority of the samples plot within the hydrothermal fields, indicating that hydrothermal activity of some sort was responsible for the deposition of the Voëlwater BIF. The depletion of certain transition metals (i.e. Co) could either be related to the nature of the hydrothermal component, or to limited scavenging due to high rates of sediment accretion.

4.5.2 Cr and P

Bivariate plots comparing Zr/Cr and Y/P₂O₅ ratios have been devised by Marchig et al. (1982) to distinguish between hydrothermal sedimentary deposits and hydrogenous metalliferous sediments forming under diagenetic processes. In hydrogenous-diagenetic sediments, Cr is bound to the detrital component, thus showing positive correlation to other elements of similar origin such as Zr and Ti. In hydrothermal processes, Cr is partly mobile and its enrichment in hydrothermal sediments is not followed by enrichment of elements deriving from terrigenous sources. In a similar manner, the correlation of P with elements such as Y and REE in hydrogenous sediments is markedly different from the one of hydrothermal precipitates: P and Y or REE correlate positively in sediments of hydrogenous character because they are both carried in the structure of diagenetic biogenous apatite; enrichment of P in hydrothermal precipitates is, in contrast, related to leaching processes that do not provide additional enrichment of Y or REE, rendering any correlation between P and the latter statistically insignificant.

Samples of iron-formations from this study show positive correlation of Cr and Zr, Cr and TiO₂, and P₂O₅ and Y, as is illustrated on Fig. 4.10 (a,b and c respectively). It would be scientifically naive, though, to establish or even assume a hydrogenous source from the above diagrams, since the contents of Cr, Zr and TiO₂ are extremely low. The additional diagram (d) (Zr/Cr vs Y/P₂O₅) of Fig. 4.10, clearly demonstrates the confusion that can be caused by incorrect

evaluation of geochemical data: this diagram has also been devised by Marchig et al. (1982) to intensify the differences between diagenetic and hydrothermal metalliferous sediments, and clearly suggests a hydrothermal origin for the Voëlwater BIF(!). Therefore, the only information that one could extract from the diagrams of Fig. 4.10, focuses essentially on the following two facts: i. the elements Cr, Zr and Ti represent the negligible detrital input that characterised the deposition of the Voëlwater sediments; and, ii. P and Y are hosted in the same mineralogical facies which is probably traces of apatite or xenotime.

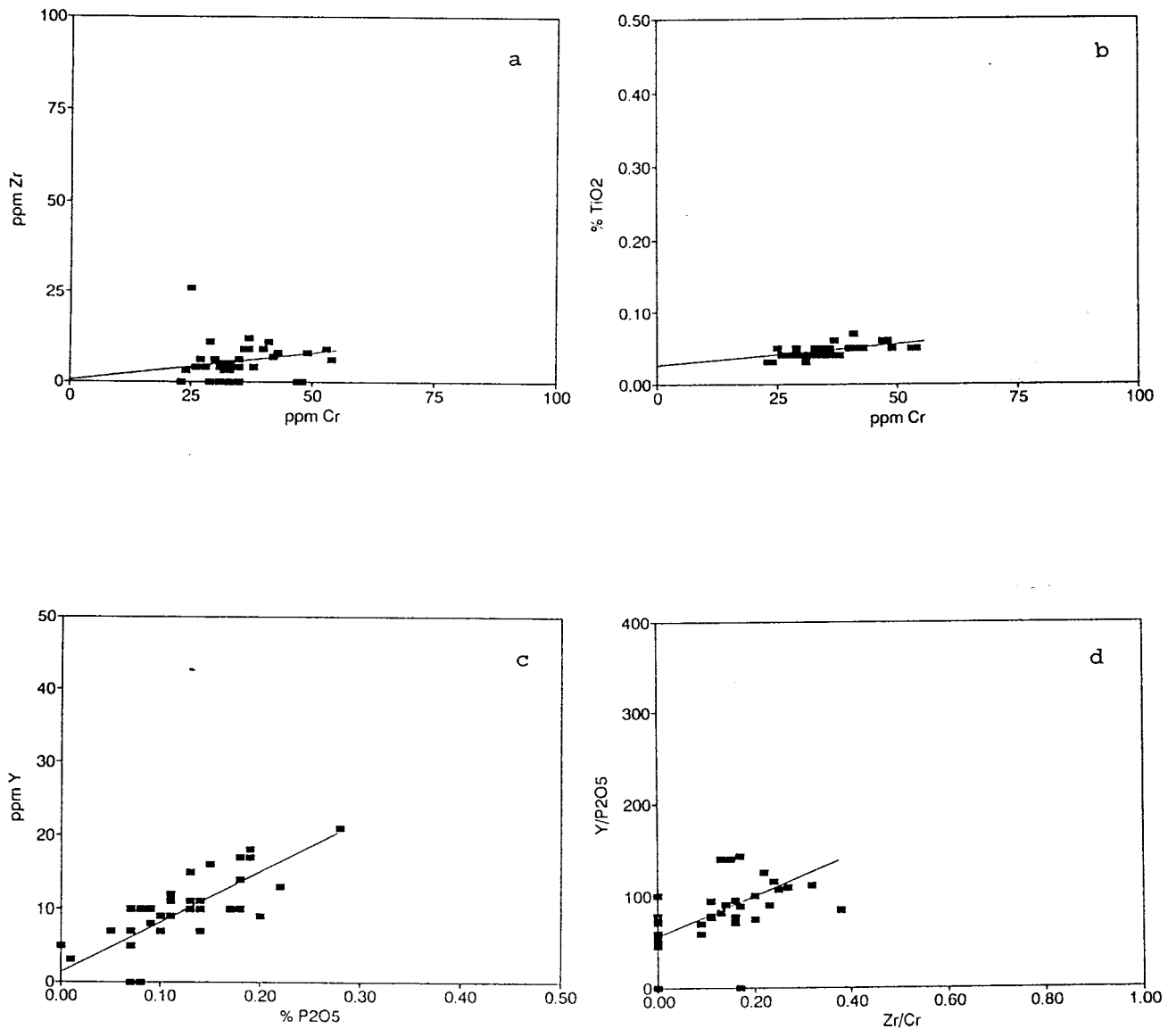


Fig. 4.10. Bivariate plots of: (a) Zr vs Cr; (b) TiO₂ vs Cr; (c) Y vs P₂O₅; and, (d) Y/P₂O₅ vs Zr/Cr, for iron-formations from the study area (filled squares) (after Marchig et al., 1982).

4.5.3 LREE

4.5.3.1 *La vs Ce*

According to Toth (1980), the La/Ce ratio can also be used to distinguish hydrothermal from hydrogenous sediments. The former would have low absolute REE concentrations and depleted Ce content, compared to hydrogenous sediments which are usually enriched in REE and show high Ce concentrations due to the rapid precipitation of Ce from seawater. The BIFs of this study are essentially depleted in both La and Ce (Fig. 4.11) which indicates that hydrogenous processes were insignificant for the formation of the Voëlwater BIF. On the other hand, the analytical data of this study cannot exclude hydrothermal processes, but the La/Ce ratio of 0.5 that characterises the study rocks is significantly lower than the hydrothermal Mn-crusts studied by Toth (similar to the seawater value, approximately 2.8), and it approaches the ratio of ferromanganese crusts from the same study (op.cit., Fig. 5) which show a rather hydrogenous, if not mixed, origin (high transition metal content, moderate Si/Al ratios; op. cit., Fig. 1 and 3 respectively). Therefore, although the possibilities for a hydrogenous origin of the Voëlwater BIF have been eliminated, it is somewhat uncertain whether the relative enrichment of Ce implies a clear hydrothermal origin for the rocks of this study.

4.5.3.2 *Ce anomalies*

Shimizu and Masuda (1977) observed large negative Ce anomalies in deep-sea cherts and they suggested that such anomalies may be used as good indicators of the environment of formation for the latter sediments. Similarly, Crerar et al. (1982) used pronounced negative Ce anomalies in ancient Mn-deposits as strong evidence for a hydrothermal origin. Although only three of the light REE (La, Ce, Nd) were analysed in this study using the XRF technique, comparisons with average, chondrite-normalised, light-REE data for other Precambrian BIFs of the

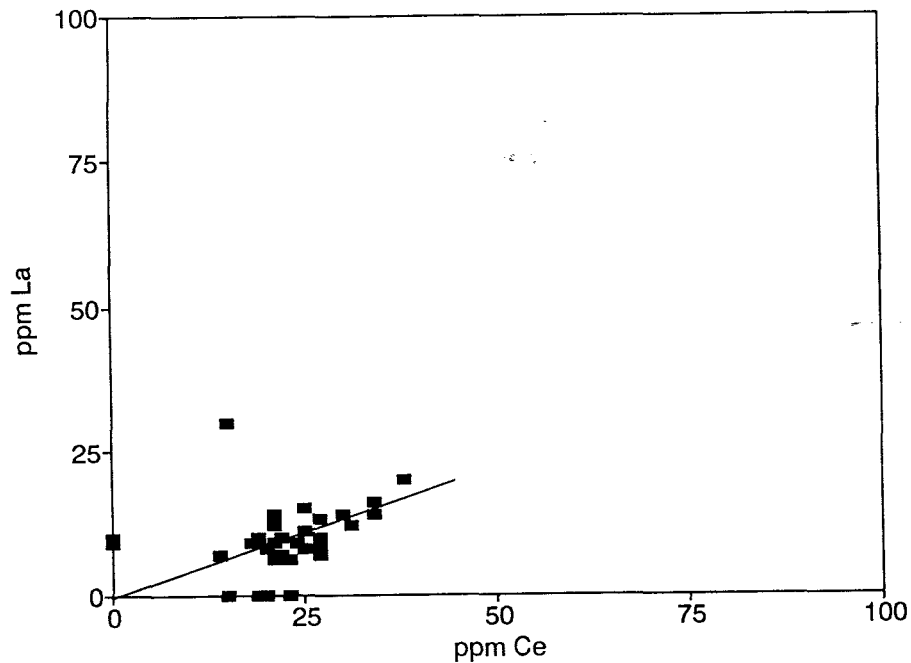


Fig. 4.11. Bivariate plot of La vs Ce for iron-formations from the study area (after Toth, 1980).

world were attempted (Table A3) with the purpose of identifying any prominent Ce anomalies in the study rocks, as well as suggesting possible interpretations regarding their significance. Unfortunately, disagreements between REE data from the same area were frequently encountered and they were probably related to the degree of accuracy of the analytical method employed in each case. Nevertheless, in order to avoid any personal bias and to allow for constructive criticisms, all the available data were plotted and are presented in Fig. 4.12.

As is shown on the diagrams of Fig. 4.12, both the study rocks and all the other BIFs show either no Ce anomalies or relatively minor positive or negative anomalies. No prominent negative Ce anomalies were observed. Tentative conclusions to be derived from this data are that: i. the Voëlwater BIFs show markedly similar LREE patterns to other major, Superior-type BIFs of the world; ii. the Voëlwater sediments were probably formed in a relatively shallow-water environment; and, iii. the LREE fraction of the study rocks may have derived from normal continental drainage and it was not precipitated from seawater during typical processes of chemical sedimentation.

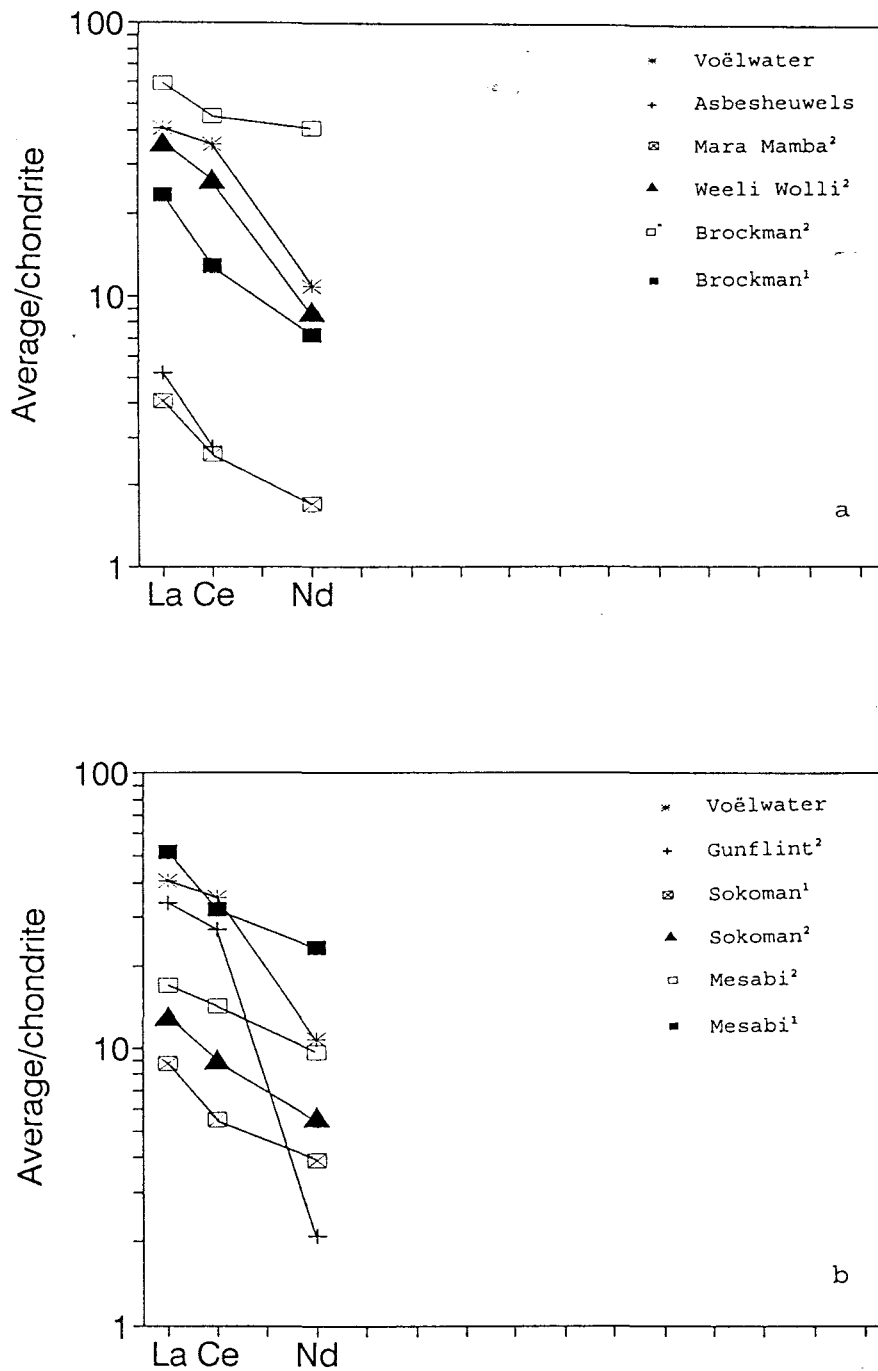


Fig. 4.12. Chondrite-normalised LREE patterns for the study rocks and several other Superior-type BIFs of the world. Data are plotted in two diagrams (4.12a and b) where the average LREE pattern of the study rocks is compared with respective averages of BIFs from S. Africa (Beukes & Klein, 1990a) and Australia (1: Fryer, 1977a; 2: Danielson et al., 1992), as well as with average LREE data of BIFs from Canada and the U.S.A (1: Fryer, 1977a; 2: Danielson et al., 1992). Data were normalised using average chondrite values obtained from Evenson et al. (1978).

4.6 Suggestions for further study

As was shown in the foregoing paragraphs, bulk and trace element geochemistry may provide useful information on several aspects concerning the character and origin of the study rocks. However, further information regarding the conditions of precipitation, origin of, and post-depositional effects on the Voëlwater BIF (diagenesis, metamorphism etc.), can be obtained by means of complete REE and stable isotope data.

Study of REEs in BIFs has the potential to provide significant input into their genesis and in understanding processes that affect them subsequent to their deposition (Graf, 1978; Fryer, 1983). Of particular importance are the implications about the source of metals for BIFs. Several authors have concluded that submarine hydrothermal sources were important or even dominant for the REEs and, by extension, the Fe in BIFs (Appel, 1983; Dymek & Klein, 1988; Jacobsen & Pimentel-Klose, 1988; Shimizu et al. 1987; Klein & Beukes, 1989; Beukes & Klein, 1990a; Danielson et al., 1992; Bau & Dulski, 1993). According to some authors, river systems would have had limited REE input and should be precluded as potential sources, while the mantle would constitute an important source (e.g. Derry & Jacobsen, 1990). Valuable information on the evolution of the Precambrian biosphere-hydrosphere-lithosphere system (Fryer, 1977b; Bau & Möller, 1993), as well as on REE behaviour during precipitation, diagenesis, metamorphism or post-depositional (hydrothermal) alterations of BIFs (Bau & Dulski, 1992; Bau, 1993), have also been obtained by REE studies and they would be of assistance in future considerations.

Becker and Clayton (1972), Jacobsen and Pimentel-Klose (1988) and Carrigan and Cameron (1991), provided evidence from carbon, neodymium and oxygen isotope studies respectively for the origin of BIFs. Dimroth and Kimberley (1976) used stable isotope evidence for the presence or not of atmospheric oxygen in the Precambrian, whereas Perry (1983) suggested that oxygen isotopic compositions of BIFs may reflect the temperature and oxygen isotope

composition of the Precambrian oceans. Oxygen and carbon isotope ratios for several mineral facies in BIFs have also been used to estimate conditions of (burial) metamorphism (Becker & Clayton, 1976; Perry & Ahmad, 1981). Gregory (1986), for example, conducted studies on fluid-rock interaction during metamorphism of BIFs using oxygen isotope systematics on quartz-magnetite pairs. The primary and diagenetic controls of isotopic compositions of iron-formation carbonates can also be determined by means of carbon and oxygen isotopes. Specifically, variations in the chemical composition of primary and diagenetic carbonates, primary changes in the isotopic composition of the water column beneath which the BIFs were formed, oxygen-isotopic exchange between carbonates and coexisting mineral phases, or post-depositional thermal processes such as iron-dependent oxidation of organic carbon (Perry & Tan, 1973; Perry et al., 1973; Walker, 1984), might be reflected by isotopic compositions of carbonates (Beukes et al., 1990a,b; Kaufman et al., 1990). Finally, sulfur isotope studies on BIFs have also been conducted in the past (Monster et al., 1979; Cameron, 1983), and they have primarily supplied implications on the origin of Precambrian BIFs.

5. DISCUSSION: THE GENESIS OF THE VOËLWATER Fe-Mn SEDIMENTS

5.1 Genesis of BIFs

The Precambrian banded iron-formations of the world have been the object of intensive and long-continued investigations, mainly because of their unusual nature, their restriction in time and their overwhelming economic significance. Particularly, the origin and significance of this enigmatic rock type has been a tantalising as well as stimulating area of research for many geologists throughout the years. Although various concepts about the origin of BIFs have been discussed in a voluminous literature for more than a century, the genesis of these scientifically fascinating rocks remains highly controversial, and apart from the fact that the bulk of banded iron-formations represent typical chemical sediments, there are many other issues on which there is still no consensus. Misconceptions exist mainly because of the inadequate description and documentation of stratigraphy and lack of recognition of the diversity in lithological facies that is characteristic of banded iron-formations (Gross, 1991). Also, the impossibility of applying actualistic comparisons for many of the characteristic features of banded iron-formations, as well as the obvious fact that comparable iron-formations may have formed under rather different conditions could be the reasons for the lack of a uniform genetic model (Eichler, 1976).

Among the various genetic models proposed for the genesis of Superior-type banded iron-formations (terrigenous, volcanogenic-exhalative, biogenic, etc.), there are certain hypotheses that have recently gained considerable currency. It is unavoidable that the brief review of the forthcoming paragraphs will revolve around these particular theories-tenets for most serious students of iron-formations. The principal points for discussion about the genesis of BIFs will be the following:

1. palaeodepositional environment;

2. source and transportation of iron and silica; and,
3. physico-chemical conditions of precipitation, including information on:
 - the atmosphere and oceans in the Precambrian;
 - the role of organisms; and,
 - proposed genetic modellings.

5.1.1 Palaeodepositional environment

It is widely accepted that banded iron-formations were deposited in relatively shallow-water marine settings, probably in partly barred, stable, continental-shelf basins of sometimes enormous dimensions (Becker & Clayton, 1972; Trendall, 1973a,b,c,d; Beukes, 1973; Drever, 1974; Loughheed, 1983; Garrels, 1987). In some cases the proposed depositional basins are regarded as open environments (frequently referred to as oceans, e.g. Button et al., 1982), even though they are restricted from terrestrial input (Gross, 1980; Beukes, 1983; Morris & Horwitz, 1983; Holland, 1984; Simonson, 1985). The unusual tectonic and environmental stability that characterised those basins, coupled by the apparent absence of clastic contamination, possibly corresponds to a polar or desert environment (e.g. James & Trendall, 1982). Many BIF depositional basins have been depicted as barred lagoons which held off terrestrial debris and permitted an undisturbed sedimentation in a quiet, shallow water environment (Dimroth, 1976; Chauvel & Dimroth, 1974). Fresh-water lakes (Govett, 1966), or playa-lake complexes (Eugster & Chou, 1973) have also been proposed as possible environmental settings, suggesting an evaporitic origin for banded iron-formations. Similar evaporitic settings have also been favoured by Trendall (1973b,d), Dimroth (1976), Garrels (1987) and Kimberley (1974; in Holland, 1984), the latter suggesting that Proterozoic banded iron-formations represent a likely replacement product of aragonite muds. Nevertheless, the possible evaporitic character of BIFs has been strongly disputed by various authors (e.g. James & Trendall, 1982; Morris & Trendall, 1988), on the grounds of primarily sedimentological, as well as petrographic and geochemical evidence.

5.1.2 Sources and transportation of iron and silica

The source of Fe and Si in the major BIFs of the world has not yet been clearly established. With the exception of Holland (1973, 1984) who suggested that the Precambrian oceans could account for a possible source of Fe provided that they contained a few mg/l of dissolved iron, all the other hypotheses refer to either a terrigenous or a volcanogenic derivation. Metasomatic, magmatic or even cosmic processes have also been invoked (e.g. Alexandrov, 1973), but they have limited applications and their validity is conjectural.

One of the first authors who favoured a terrigenous origin for Fe and Si was Gruner (1922). He suggested that the two elements derived from a large landmass of greenstone lavas and basalts, and were carried to the depositional basin as organic colloids, or absorbed by them. Sakamoto (1950) also suggested that Fe and Si might be derived from a landmass under conditions of mature weathering and lateritisation. Similar hypotheses on terrestrial weathering sources for Fe and Si (with or without additional contribution by volcanic sources) were also proposed in the papers by Govett (1966), Lepp and Goldich (1964), Pride and Hagner (1972), Alexandrov (1973), Garrels et al. (1973) and Drever (1974), until recently when Hälbig et al. (1993) suggested a detrital origin for the BIFs in Griqualand West, S. Africa.

A terrigenous source is inconsistent with the several sedimentological constraints introduced by Simonson (1985), but the most important constraint on any hypothesis appears to be the sheer magnitude of BIFs. As Holland (1984) pointed out, very large drainage systems would be required to provide the necessary amounts of Fe and Si, combined with unusually high capacity to dissolve and carry the two elements, either on the surface or underground. The existence of such conditions in the Precambrian seems very unrealistic, particularly when compared to presently operating river systems. In addition, the physicochemical mechanisms known to separate Fe and Si from any sediment load (dissolution, ionic or colloidal migration) bear strong limitations, and are not

expected to have been effective enough to supply the required amounts of those elements to the Precambrian depositories (Mel'nik, 1982).

A volcanic origin of Fe and Si was first suggested early this century by van Hise and Leith (1911). They concluded that the two elements derived by dissolution of submarine basalt flows or basic volcanic rocks from hot solutions, hot or cold meteoric waters, or seawater. Goodwin (1956) also considered a volcanogenic source of Fe and Si in the Gunflint iron-formation. He stated that there is a direct and sympathetic relation between BIFs and lavas/pyroclastics, with a cyclical coordination of volcanism and sedimentation in a larger and more significant sense. Gross (1965) concluded that the main source of the Fe and Si must be related to volcanogenic processes. He considered that the widespread distribution of iron-formations, their composition and minor element content, and association with such a diversity of rock types and depositional environments could not be accounted for by weathering processes alone, and that volcanogenic processes offered a more likely alternative. Trendall and Blockley (1970) opted for volcanism as the most likely source of Fe in the Hamersley Basin, and they used the presence of fragmental tuffs as strong evidence for volcanic input. Brooks (1977), using evidence from Archaean variolites suggested that Fe may either be partial-melt mantle derivative, or alternatively, the product of chemical degradation of variolitic lavas. Morris and Horwitz (1983) invoked derivation of Fe and Si from pulsed outputs of a large oceanic rift or hot-spot under anoxic conditions, possibly supplemented by normal continental drainage. Simonson (1985) favoured volcanogenic-exhalative processes as the source of Fe and Si since all the other proposed models are at odds with his sedimentological constraints. Klein and Beukes (1989) suggested a hydrothermal source of Fe and possibly Si for the BIFs of the Transvaal Sequence, which is presumably related to contemporaneous volcanic activity. Kimberley (1989b) suggested deep weathering accompanied by hydration of new crust or late diagenesis of sediments as the source of cherty iron-formations, the latter including the Superior-type BIFs (Kimberley, 1979, 1989a). According to the same author, non-cherty iron-formations are related to

exhalative processes along continental margins and seismic pumping of seawater through ophiolite-bearing sedimentary piles. Finally, Morris (1993) in the most recent genetic model for the deposition of the BIFs of the Hamersley Group in W. Australia invokes a volcanic source of Fe and Si directly related to mid-ocean ridge (MOR) or hot-spot activity. The advantage of the volcanogenic sources is that they generally seem more feasible for the migration of Fe and Si by means of hot acid solutions which, particularly under the low O₂ conditions of the Precambrian oceans, may have carried substantial amounts of both Fe⁺² and ionic-colloidal Si-complexes (Mel'nik, 1982).

5.1.3 Conditions of precipitation

5.1.3.1 *The atmosphere and oceans in the Precambrian*

The evolution of the atmosphere and oceans has been the subject of numerous studies in the past (e.g. Cloud, 1972; Walker, 1977; Walker et al., 1983; Holland, 1984) which focused particularly on the rise of atmospheric oxygen and the history of carbon dioxide concentrations. Although it is beyond the scope of this study to discuss the various approaches in examining these problems, a brief reference to the currently accepted ideas is regarded necessary.

Previous hypotheses have suggested that the oxygen content of the Precambrian atmosphere, particularly at Early Archaean times, was considerably lower (if not absent) than that of today (e.g. Cloud, 1973; Mel'nik, 1982). However, certain authors (e.g. Cloud et al., 1982) have concluded that the first appearance of oxygen-producing photosynthetic organisms early in Earth history was probably responsible for the rise of the Precambrian atmospheric oxygen levels and for the evolution of the atmosphere-ocean system in general. The concept that the atmosphere was oxidizing in at least some periods of the Precambrian has been established primarily on the grounds of geochemical (e.g. C and O isotopes: Dimroth & Kimberley, 1976) and pure geological evidence (e.g. existence of

ferric iron in sedimentary rocks, early "red beds", sea and groundwater sulfate, etc.: Clemmey & Badham, 1982). Furthermore, Fe-Ti correlations in Precambrian sediments have shown that Fe was neither substantially added to, nor significantly redistributed in those rocks and therefore it did not greatly affect the near-surface redox cycle or atmospheric oxygen levels (Kump & Holland, 1992). However, there is still uncertainty as to whether the atmosphere was oxygenic as far back as the Archaean, or whether it characterised certain periods of the Precambrian as part of an evolutionary cycle. Walker et al. (1983) and Kasting (1987) concluded that there was an apparent switch from a reducing atmosphere in the Archaean to an oxidising one in the Early Proterozoic which was marked by a decrease in the occurrence of detrital pyrite and uraninite and an increase in the occurrence of redbeds. Clemmey & Badham (1982) and Holland (1984) have disputed such an interpretation and they believe that the paucity of Archaean redbeds is related to diagenetic alteration or to a lack of suitable environments in which they could have formed. Furthermore, it has been argued that the survival of uraninite is kinetically possible under O_2 partial pressures of up to 4×10^{-3} bar, whereas palaeosol data show no obvious change in oxidation state between 1.5 and 3.0 Ga ago, indicating that the postulated increase in pO_2 near 2.4 Ga ago may not have occurred.

Irrespective of the atmospheric conditions in the Archaean, most workers agree that the Early Proterozoic atmosphere was oxidizing (e.g. Towe, 1983). Nevertheless, the widespread occurrence of banded iron-formations indicates that anoxic (reducing) conditions prevailed in the deep oceans at that time, as the genesis of these rocks is thought to require lateral transport of ferrous iron in solution (Holland, 1973; Mel'nik, 1982; Ewers, 1983). This fact is in accordance with the three-stage model for the evolution of atmospheric oxygen proposed by Kasting (1987; see also Fig. 5.1). Kasting concluded that oxygen was essentially absent from the Earth's atmosphere and oceans prior to the emergence of a photosynthetic source, probably during the Early Archaean (**reducing stage**). During the Early Proterozoic the atmosphere and surface ocean were apparently oxidising (deposition of oxidised surface deposits or "redbeds"),

while the deep ocean remained reducing (**oxidizing stage**). The regulation of atmospheric pO_2 during this stage was probably related to the presence of mantle-derived Fe^{+2} , an assumption which, if valid, may have important implications for the source and genesis of BIFs, and particularly the Voëlwater Fe-Mn association (see also ¶5.3). The establishment of oxidising conditions in the deep oceans was marked by the disappearance of BIF approximately 1.7 Ga ago and permitted atmospheric oxygen to climb to its present level (**aerobic stage**). O_2 concentrations may have remained substantially lower than today, however, until well into the Phanerozoic.

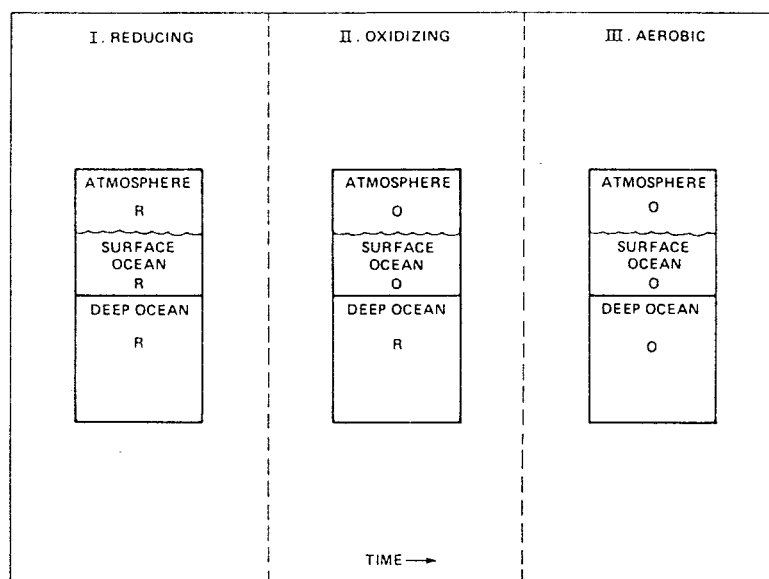


Fig. 5.1. Schematic diagram showing the three expected stages in the evolution of atmospheric oxygen. "O" indicates oxidising conditions; "R" indicates reducing conditions (after Kasting, 1987).

Finally, Kasting (1987) stated that CO_2 concentrations were substantially higher in the Archaean than today and that the climate was much warmer. Periods of extensive glaciation during the Proterozoic indicate that the climate at these times was relatively cool. Kasting (op. cit.) concluded that in order to be consistent with climate models, a decline in the CO_2 partial pressures is assumed, although this may be inconsistent with paleosol data which implies that pCO_2 did not change appreciably during that time.

5.1.3.2 *The role of organisms*

The possible role of organisms in the deposition of iron-formation has been considered by various authors. Mancuso et al. (1971) identified biogenic structures from the Negaunee iron-formation that resemble fossil algae and may have been at least partly responsible for the deposition of Fe. Cloud (1973) concluded that the precipitation of Fe and Si was generated by microorganisms that depended for survival on a supply of oxygen-depressing ferrous iron in the ambient waters. LaBerge (1973) suggested that organisms such as bacteria or algae may have been silica precipitators and he concluded that at least some of the chert in iron-formations was biologically precipitated. Similarly, Klemm (1979) suggested that silica-secreting organisms enhanced the precipitation of silica-rich microbands in the BIFs of the Transvaal Sequence in S. Africa. In contrast, Button et al. (1982) argue the possibility that silica-secreting organisms existed in the Precambrian, but they suggested that heterotrophic microbes may have directly contributed to the deposition of Fe-hydroxides, as many bacteria do today (see also §5.1.3.3).

Nevertheless, the importance of microorganisms in the deposition of BIFs still remains conjectural. According to Nealson (1982), many bacteria oxidise and deposit iron oxides and hydroxides, but it is unknown whether or not bacteria form extensive natural iron precipitates, although they are almost always associated with such precipitates. The physiology of iron-oxidising bacteria is not well understood and this precludes extrapolation to pre-Phanerozoic sedimentary iron deposits. Nealson (op. cit.) also stated that bacteria that catalyse iron oxidation indirectly by altering environmental conditions may have been important in the formation of ancient iron deposits, but this notion is hard to assess without accurate information regarding environmental conditions at the time of iron-ore deposition.

The possibility that early diagenesis is a consequence of the metabolic activities of bacteria has been strongly suggested by Walker (1984) in the light of carbon

isotope evidence from BIFs. Recent investigations have also shown that metal reducing microbial organisms (e.g. the bacterium *Shewanella putrefaciens*) can grow anaerobically by coupling carbon oxidation to the dissimilatory reduction of Fe and Mn, and may have some relevance to our understanding of the formation and diagenetic modification of BIFs (Lovley et al., 1987; Myers & Nealson, 1988a,b; Nealson and Myers, 1990). The initial iron in these sediments is believed to have been in the form of Fe^{+3} which was subsequently reduced by those

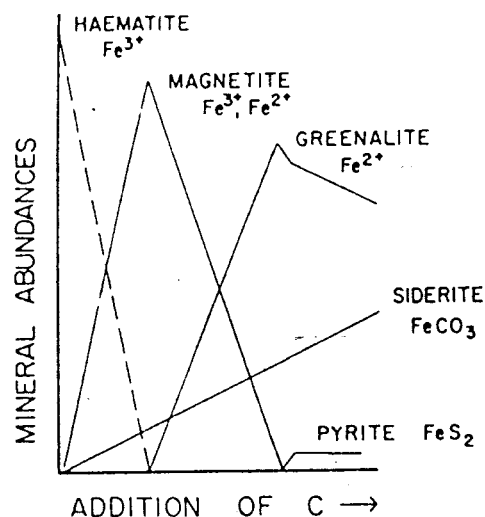


Fig. 5.2. Effects of suboxic diagenesis of increasing amounts of organic C on the mineralogy of BIFs, as a result of progressive reduction of Fe^{+3} to Fe^{+2} (after Walker, 1984).

microorganisms, releasing at the same time isotopically light carbon from organic carbon oxidation. As a result, the preserved ratio of Fe^{+3} to total iron in these processes is a product of early suboxic diagenesis, and it does not represent the true primary ratio. The generally low concentration of organic carbon in BIFs is explained as a consequence of the early diagenetic oxidation of an initially much larger amount of carbon by the oxidized iron of the formations themselves. Finally, the oxide, silicate, and sulphide facies of iron-formations may reflect a response of the sedimentary system to the early diagenetic alteration of progressively larger amounts of reduced organic carbon (Fig. 5.2). The oxide facies contains both Fe^{+2} and Fe^{+3} , the silicate facies contains principally the Fe^{+2} form, and the sulphide facies contains Fe^{+2} and sulphide that is presumably the product of bacterial sulphate reduction.

5.1.3.3 Genetic modelling of BIFs

In recent years, genetic models for the large-scale deposition of BIFs have been approaching common ground, although consensus is still remote. The various

modern ideas explain the genesis of BIFs as a result of upwelling currents in a "stratified ocean". Most of the upwelling BIF paradigms assume modern oceanic circulation based on the conceptual three-layer model, with a thermo-pycnocline zone separating the cold dense multilayered deep waters from an upper wind-mixed warm-layer (Morris, 1993). The deep waters would act as potential reservoirs of dissolved Fe^{+2} which would have derived from submarine hydrothermal sources. Convective upwelling currents driven by MOR or hot spot activity would result in mixing of the lower and upper oceanic water-layers, giving rise to the precipitation of Fe-Si-rich sedimentary layers (bands). The mineral-chemical nature, thickness and alternation trends of these layers would be largely dependent upon the interplay of several processes such as seasonal changes, eustatic movements, storm mixing of seawater layers, bacterial activity, contemporaneous volcanism, diagenesis, etc. The upwelling theory has been described in various ways over the last 20 years, and its "evolution" through the most representative genetic models presented in several publications during that period is summarised herein.

Drever (1974) was one of the first to suggest that iron-formations could have formed in stratified, shallow-water marine conditions (Fig. 5.3), with iron transported to the oceans in detrital sediments and silica transported in solution. He concluded that if atmospheric P_{O_2} was significantly lower than at present and biological productivity was comparable to present-day values, the entire oceans below the thermocline would be anaerobic ($f_{\text{O}_2} \approx 10^{-70}$), while the surface mixed zone would be relatively oxidising. The supply of Fe^{+2} to the oceans in sediments was much greater than the supply of dissolved sulfate. Under anaerobic conditions, all the sulfur would be precipitated as pyrite, and Fe^{+2} would build up in solution until siderite saturation was achieved (≈ 10 ppm Fe^{+2}). When the anaerobic deep water welled up onto a shallow platform, the dissolved Fe^{+2} would be oxidised to goethite, and slight evaporation would cause precipitation of amorphous silica or magadiite. Siderite would be formed where the supply of organic carbon was sufficient to maintain anaerobic conditions at the sediment-water interface. Silica-secreting organisms are

assumed to have been absent, and an oceanic pH value of 7.7 or lower (perhaps caused by a slightly higher atmospheric P_{CO_2}) would be required to prevent sepiolite precipitation. Quantitative calculations show that hydrogen ion released by oxidation of Fe^{+2} and precipitation of goethite would be sufficient to prevent precipitation of calcite when the water is evaporated sufficiently to deposit a weight of SiO_2 equal to the weight of Fe_2O_3 precipitated by oxidation of Fe^{+2} . Apart from the direct consequences of lowered atmospheric P_{O_2} , slightly increased P_{CO_2} , and the absence of silica-secreting organisms, the chemistry and thermal structure of the oceans 2 b.y. ago could have been identical to those of the present-day, shallow-water carbonate depositional environments.

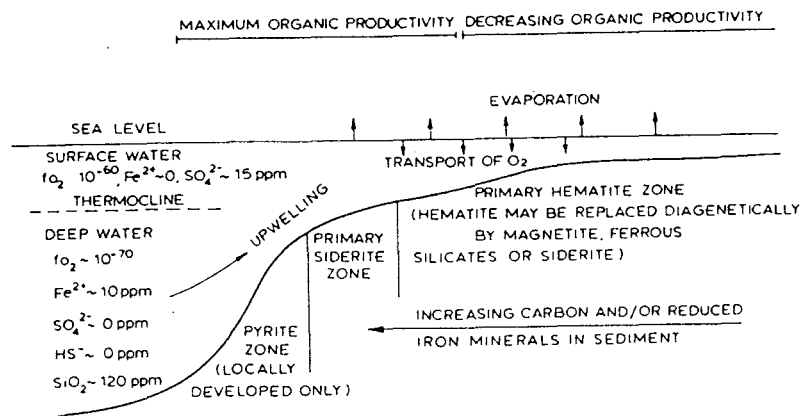


Fig. 5.3. Idealised depositional environment of a banded iron-formation. The term "hematite" includes all ferric oxides and hydroxides (after Drever, 1974).

Button et al. (1982) proposed a two-layer oceanic environment (an upper oxic and a lower anoxic) for the deposition of BIFs. They concluded that even relatively low concentrations of dissolved Fe^{+2} in the deep ocean would, because of the immense volumes involved, have constituted an enormous reservoir of the metal. According to the above authors, source is no longer a problem; Fe would derive from terrigenous and submarine sources over a longer period of time. Absence of organisms such as protists (diatoms-radiolarians) or animals (sponges) that deplete silica from solution caused accumulation of silica in the

Precambrian oceans, building to concentrations close to saturation with amorphous silica. Thus, there could have been an essentially continuous rain of silica-rich precipitate onto the ocean floor. Large scale precipitation of Fe in the BIFs began when deep Fe-rich waters reached newly developed shallow continental-margin basins and shelves by means of upwelling mechanisms similar to the ones that produced the major manganese deposits of the Phanerozoic (Frakes & Bolton, 1984, 1992) and the phosphate deposits in the present oceans. Generation of oxygen in the upper layer of the ocean could be explained by photosynthetic mechanisms involving cyanobacteria in the photic zone although non-biological photo-oxidation and photolytic dissociation of water vapor cannot be excluded. Seasonal changes would explain the cyclicity of Fe-rich and Fe-poor bands. Also, heterotrophic microbes may have directly contributed to Fe-deposition in the form of Fe-hydroxides, as many "Fe-bacteria" do today. Such organisms may have thrived at the shallow sediment-water interface, utilising oxygen and small amounts of organic matter (both provided by photoautotrophs) in the precipitation of Fe (+ Mn).

Francois (1986) stressed that photosynthesis was not required to precipitate BIFs. He proposed that a three-layer ocean had existed in the Early Proterozoic (mixed layer, thermocline and deep-water reservoir). Fe^{+2} would have been transported by diffusion and upward advection (upwelling) from the deep-water reservoir (which was saturated with respect to siderite and had a temperature of $5^{\circ}C$) to the mixed layer, throughout the thermocline. The latter is characterised by a linear decrease of temperature with depth and an approximate thickness of 1000m (Fig. 5.4). Transformation of the Fe^{+2} to $FeOH^{+}$ would have taken place in the mixed layer which would have been 100m thick and would have had a temperature of $20^{\circ}C$. Photo-oxidation of $FeOH^{+}$

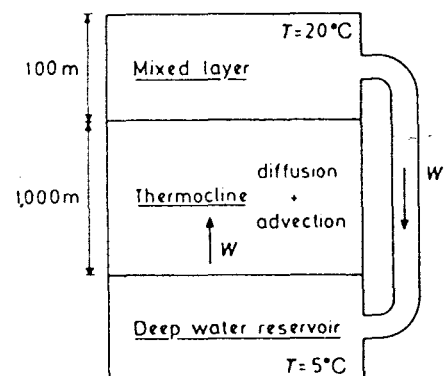


Fig. 5.4. Vertical structure of the ocean in the model for the deposition of BIFs (after Francois, 1986); w is the advective velocity.

would have followed, giving rise to Fe^{+3} particles. In this model, it is assumed that no reduction of Fe^{+3} takes place in the thermocline, so that there is no production or sink of Fe^{+2} in this layer. Some Fe^{+3} may, nevertheless, be reduced to Fe^{+2} in the deep water as it has been suggested by other workers (e.g. Walker, 1984). According to Francois (1986) the above mechanism was able to produce large amounts of banded iron-formation deposits such as the BIFs of the Hamersley Group in W. Australia.

Klein and Beukes (1989) suggested that the BIFs of the Transvaal Supergroup in S. Africa were laid down in a depositional basin with a stratified water column (Fig. 5.5). During a regressive stage, the surface waters were the site of much organic carbon productivity and the locus of cryptalgal limestone and intraclastic limestone deposition, with deposition of pyritic carbonaceous shale at somewhat greater depth (below the chemocline). During a transgressive stage of the basin, the deeper waters acted as the site for iron-formation deposition. These deeper waters were depleted in organic carbon and enriched in dissolved ferrous iron relative to the shallow water mass, with continued availability of oxygen along the chemocline separating the two water masses. Deposition of chert-rich units would have been triggered in the lower surface waters (above the photic zone) as a result of supersaturation with respect to SiO_2 . The hydrothermal source of the iron (and probably the SiO_2) in the iron-formation would have been a very dilute hydrothermal input in the deep ocean waters, as concluded from mixing calculations of REE values for modern Atlantic Ocean water and hydrothermal solutions from the East Pacific Rise.

Carrigan and Cameron (1991) proposed that the Gunflint iron-formation of Minnesota, was deposited in a stratified water column with anoxic bottom water. The depositional basin had restricted communication with the open ocean and was affected by distal volcanism. Hydrothermal activity associated with the volcanism provided a large source of dissolved iron, and possibly silica, which helped buffer O_2 and sulphate in water to low levels. Low concentrations of sulphate limited the generation of H_2S that would otherwise have restricted the

solubility of iron. During periods of increased hydrothermal activity, the anoxic/oxic water boundary moved upwards, permitting transport of iron to a shallow shelf, where it was precipitated as siderite, iron hydroxides, iron silicates or pyrite, depending on physicochemical conditions. The transition to the overlying limestone marks a decrease in hydrothermal activity with a contraction of the redox boundary.

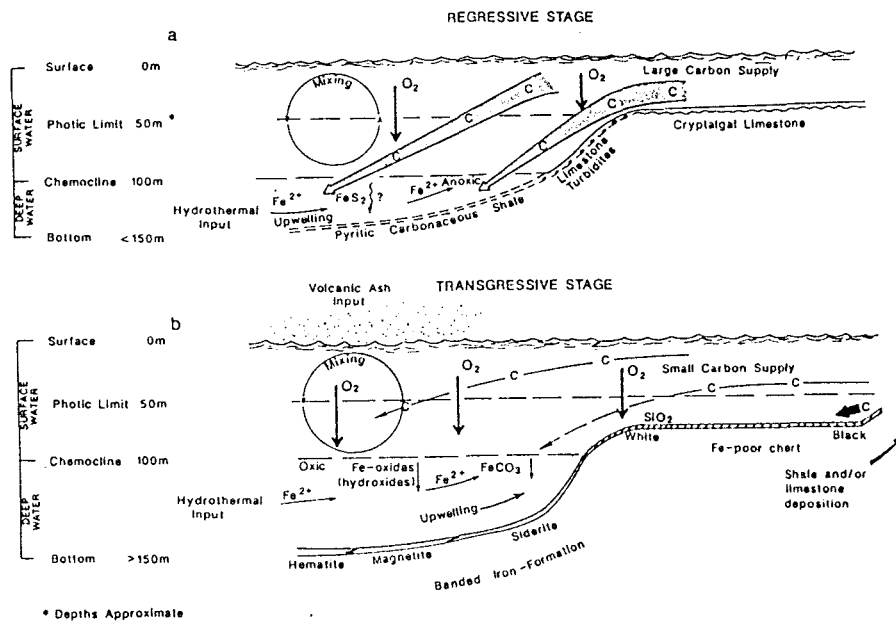


Fig. 5.5. Schematic depositional environment for iron-formation deposition and that of associated lithofacies in a marine system with a stratified water column in (a) a regressive stage, and (b) a transgressive stage. In (a) the photic zone reaches the floor of the deep shelf, allowing for cryptalgalaminated limestone deposition. In (b) the photic zone is considerably above the floor of the deep shelf, causing the deposition of various iron-formation facies and chert. The thick arrows labeled C (carbon) in (a) represent high carbon productivity and supply, and the narrow arrows in (b) represent much less carbon productivity and supply. The vertical depth scale is based upon the basinal reconstruction of Klein et al. (1987) (after Klein & Beukes, 1989).

Finally, **Morris** (1993) proposed a model for the deposition of BIFs of the Hamersley Group in W. Australia whereby the supply of materials can be accommodated by the interaction of two major oceanic supply systems: i. surface currents; and, ii. convective upwelling from MOR or hot spot activity, both modified by varied input of pyroclastic material (Fig. 5.6). The surface

currents were saturated in silica and carried minimal iron due to photic precipitation, but were periodically recharged by storm mixing. Precipitation from them gave rise to the banded chert-rich horizons, whose regular and finely laminated iron/silica distribution resulted from seasonal meteorological influences. Precipitation from convection driven upwelling of high iron solutions from MOR or hot-spot activity periodically overwhelmed the delicate seasonal patterns of the surface currents to produce the iron-dominated mesobands. A wide range of intermediate mesoband types in the Hamersley BIFs resulted where the deep water supply was modified by varied MOR activity, or by partial blocking of upwelling waters by surface currents. During these periods of oxide-dominated BIF, silica was deposited from saturated solution mainly by evaporative concentration, and iron by oxidation due to photolysis and photosynthetically produced oxygen. Superimposed on these supply differences was the varying effect of fine aluminous ash from distal volcanic sources, changing the meteorological and depositional conditions.

5.2 Genesis of the Voëlwater BIF-Mn sediments

Before any discussion about the formation of the Voëlwater BIF and Mn-sediments commences, it is necessary to summarize the petrographic and geochemical results of this study, together with information from previous research activities in the study area:

1. The stratigraphic succession in the Voëlwater subgroup of sediments encompasses three Mn-intercalations within a BIF unit, the latter comprising: i. a lower hematite-rich horizon; ii. a silicate-rich horizon between the lower and middle Mn-bodies, and; iii. a carbonate-rich horizon which occurs between the middle and upper Mn-bodies and above the upper Mn-body.
2. The minerals that make up the various lithotypes in the Voëlwater BIF, viz. chert (quartz), magnetite, hematite, greenalite, minnesotaite, stilpnomelane,

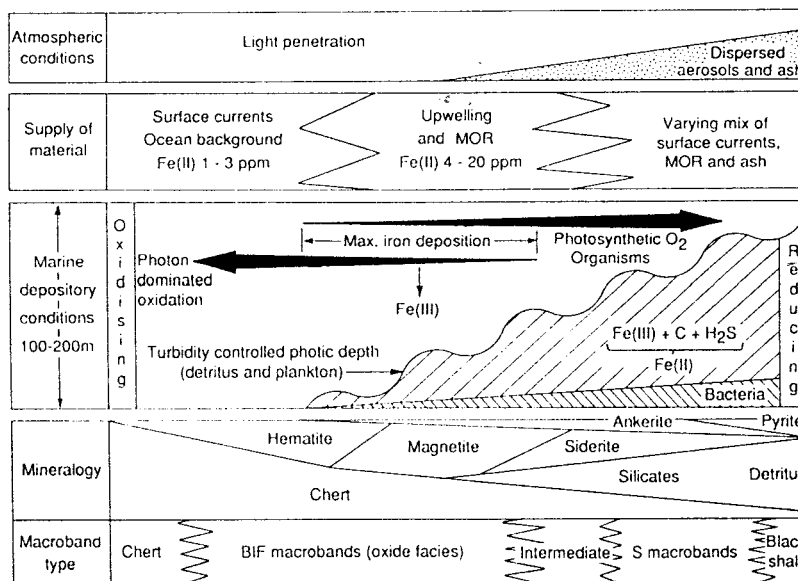


Fig. 5.6. A summary of the main features of the genetic model for BIF and associated sedimentary rocks in the Hamersley Group (after Morris, 1993). Atmospheric conditions are modified by volcanic emissions. Supply of materials is (1) from surface ocean currents, giving rise to hematite varves, interrupted periodically by (2) high iron supply from upwelling currents and MOR hydrothermal output, both modified by (3) fine ash from distal sources. Photic depths are controlled by seasonal changes, and turbidity in the water and atmosphere. Precipitation of iron is primarily by oxidation in the photic zone, and the precipitate consolidates as ferric oxide; or is modified by partial reduction to form magnetite (2 ferric/1 ferrous); or is substantially reduced, dependant on the organic supply, augmenting iron in the sub-photic zone and leading to the precipitation of ferrous-rich compounds. Increasing volcanism improves the nutrient content of sea-water for organic growth, but also adds limits to growth by curtailing the amount of available light, leading to S macroband (chert-carbonate-silicate BIF with shaly bands) deposition. Maximum organic supply with minimum oxidation results in black shales. The mineralogical distributions are qualitative.

riebeckite, Fe-mica, calcite, ankerite, siderite and pyrite, are typical of Superior-type BIFs that have undergone late diagenetic to low-grade metamorphic effects. Textural evidence has shown that certain mineral facies in the study rocks may represent the direct consolidated analogues of sedimentary precursors (e.g. greenalite and siderite), whereas others appear to be diagenetic products of the latter (e.g. magnetite and ankerite).

3. From a geochemical point of view, the study rocks exhibit striking similarities with several other Superior-type BIFs of the world. Geochemical differences that may be of particular importance are the higher Ca and Fe, and lower Si contents of the Voëlwater BIF. The high Mn-content in certain lithologies is attributed to their transitional character with respect to the Mn-orebodies of the study area.

4. Finally, the Mn-units that are interbedded with the Voëlwater BIF in the study area consist essentially of braunite ($\text{Mn}^{+2}\text{Mn}^{+3}_6\text{SiO}_{12}$) and kutnahorite [$\text{Ca}(\text{Mn},\text{Mg})(\text{CO}_3)_2$], with lesser amounts of hausmannite (Mn_3O_4), jacobsite (MnFe_2O_4), bementite [$(\text{Mn}_5\text{Si}_4)_{10}(\text{OH})_6$], friedelite [$(\text{Mn},\text{Fe})_8(\text{Si}_6\text{O}_{15})(\text{OH},\text{Cl})_{10}$], calcite, hematite, and traces of pyrochroite [$\text{Mn}(\text{OH})_2$] and feitsknechtite (beta- $\text{MnO}\cdot\text{OH}$) (Kleyenstuber, 1984; all the minerals represent diagenetic products of sedimentary precursors). The chemistry of the Mn-ores is relatively simple and is characterised by low silica (approx. 4%: free quartz is absent; all the silica is bonded in the braunite structure) and high carbonate content, the latter reflected in the CO_2 content of 12 to 16 per cent which makes the ore virtually self-fluxing (Kleyenstuber, 1984; Nel et al., 1986).

5.2.1 The depositional model

It is probably impossible to establish any genetic model for the formation of the Voëlwater chemical sediments on the basis of the above-mentioned data alone. Previously proposed models for the genesis of other major BIFs of the world may, however, be of particular assistance for constructive suggestions. It appears that all the genetic models already discussed (see ¶5.1.3.3) agree in certain points, such as the existence of a reducing oceanic environment with a stratified water column in the Early Proterozoic. The anoxic, deep-waters in such oceans would have acted as reservoirs for large amounts of Fe^{+2} which would have derived from deep-seated hydrothermal agents related to mid-ocean ridge (MOR) or hot-spot activity. The upper oceanic layer would have been characterised by surface currents saturated in silica and would have carried

minimal iron due to photic precipitation. Precipitation of this layer would have given rise to chert-rich bands under quiet conditions. Periodic storm mixing would have resulted in recharging of the surface waters with Fe^{+2} , and subsequent precipitation of Fe/Si laminations, the distribution of which was largely controlled by meteorological influences. Convection-driven upwelling mechanisms would have had a similar depositional effect but they would have been characterised by more intense Fe-precipitation which overwhelmed the above-described delicate seasonal patterns and led to the deposition of Fe-dominated bands of variable thicknesses, depending each time on the grade and extent of the associated MOR or hot-spot activity.

Precipitation of Fe may have taken place partly in the form of Fe^{+2} as a direct precipitate in a deep-water anoxic environments, and partly as Fe^{+3} , the product of photosynthetic and/or photolytic oxidation of upwelled Fe^{+2} in the surface waters. With regard to the Voëlwater rocks in particular, the precipitation of manganese can be explained in a similar manner, but in that case (as will be shown later on) slightly higher redox conditions would be required. Suboxic diagenesis probably due to bacterial activity in the deeper waters (Froelich et al., 1979) would have led to the formation of Fe-mineral facies containing primarily Fe^{+2} , and in a lesser extent Fe^{+3} (e.g. greenalite, stilpnomelane, magnetite, etc.). Such a notion, however, does not clear up the origin of minerals such as greenalite which may be either a typical diagenetic product under moderately high reducing conditions, or a direct Fe^{+2} -precipitate, although the latter seems more likely due to the common fine-grained textural character of the mineral. Bacterial-induced diagenesis also requires the presence of significant amounts of organic carbon in BIFs which has not yet been observed (Gole & Klein, 1981). A possible explanation for this organic carbon deficiency in BIFs could be related to the early diagenetic oxidation of large amounts of the former by the oxidized iron (and manganese) of the formations themselves (Walker, 1984; see also ¶5.1.3.2). Unfortunately, organic C determinations or carbon isotope studies were not conducted during this study, and therefore no conclusions can be made as to the role of organic matter in the diagenesis of the Voëlwater sediments.

5.2.2 Applications of Eh-pH systematics

Eh-pH diagrams for iron and manganese species may provide useful implications regarding the physicochemical conditions of deposition of BIFs and, consequently, the Voëlwater Fe-Mn rocks (Brookins, 1988; see also Fig. 5.7). These diagrams have been constructed on the basis of direct observations on the geochemical behaviour of primary iron and manganese precipitates. However, petrographic (textural) evidence has shown that most of the mineral facies described in BIFs represent the possible products of diagenetic overprint on the initial Fe-rich (and Mn-rich as in the Voëlwater case) sediment. Such diagenetic mineral facies are abundant in the study rocks and the associated Mn-ores (e.g. ankerite and magnetite of the BIF lithologies; braunite and kutnahorite of the Mn-bodies) and therefore, the information extracted from these phase diagrams must be cautiously evaluated. Nevertheless, on the assumption that the original compounds constituting the primary iron and manganese sediments are (after Mel'nik, 1982):

1. amorphous hydroxides of Fe and Mn: $\text{Fe}(\text{OH})_3$, $\text{Fe}(\text{OH})_2$, $\text{Mn}(\text{OH})_2$;
 2. amorphous SiO_2 and CaCO_3 , and:
 3. finely dispersed crystalline magnetite (Fe_3O_4), greenalite [$\text{Fe}_3\text{Si}_2\text{O}_5(\text{OH})_4$] and siderite (FeCO_3), with subordinate amounts of Fe-sulphides (pyrite, \pm pyrrhotite),
- one can deduce that the deposition and diagenetic modifications of the study rocks have been largely controlled by the redox potential in the palaeodepositional basin. Small scale fluctuations of, primarily, the Eh conditions could explain the nature and distribution of banding in the study rocks, whereas the coexistence of certain minerals in the bands themselves (e.g. magnetite and hematite) may have been related to kinetic factors. As an example, the formation of alternate bands of (chert + greenalite) - magnetite can be readily demonstrated by slight redox changes in a predominantly alkaline and reducing depositional environment (see Fig. 5.7). One of the disadvantages of phase diagrams however, is the fact that they usually do not incorporate all the possible mineral species that may be found in natural environments. This is typically the case in the study rocks where the introduction of CaCO_3 and SiO_2 in the carbonate-rich

BIF-lithologies and the Mn-ores respectively has played a major role in the presently observed mineralogical and geochemical character of these rocks. As a result, the conditions for the formation of minerals such as ankerite and braunite cannot be directly estimated, and only the fact that they most likely represent diagenetic products of sedimentary precursors can lead to certain assumptions. In the case of braunite for instance, it can be confidently suggested that the initial sediment that gave rise to its formation was largely composed of amorphous silica and a Mn-rich precursor. The nature of the latter is difficult to resolve particularly when it is well-documented that braunite may represent a late diagenetic product of various Mn-bearing facies (Roy, 1981). One possibility could be that braunite is a diagenetic product of MnO₂ polymorphs such as the ones found in Mn-nodules and crusts in the present day marine basins (e.g. todorokite, birnessite, vernardite, etc.). However, this seems rather unlikely since the redox conditions in the Proterozoic oceans were much more reducing than those of today, even though the upper parts of them were in contact with an oxidising atmosphere. Another more feasible possibility is that the braunite has derived from diagenetic recrystallisation of a pyrochroite-type precursor [Mn(OH)₂] which precipitated directly from the anoxic bottom waters of the depositional basin, with additional introduction in the system of SiO₂ from the surface waters. A similar mechanism can also be proposed for the genesis of Fe-bearing minerals such as greenalite, provided that the latter represents a diagenetic mineral facies formed at the expense of Fe(OH)₂ and not a primary precipitate. Yet, there are questions regarding the formation of Fe-facies in BIFs that still need to be resolved, such as:

1. whether the original Fe-sediments precipitated in the form of Fe⁺³ compounds as a result of upwelling of Fe⁺² in the upper, mixed oceanic layers; or:
2. whether they formed partly as Fe⁺³ compounds but together with additional contribution of direct Fe⁺²-bearing precipitates from the bottom, anoxic ocean waters.

The effects of early and late stage diagenesis on both these two alternatives, particularly with regard to the Fe⁺²/Fe⁺³ ratio presently observed in BIFs, certainly restricts any considerations to the range of speculation and conjecture.

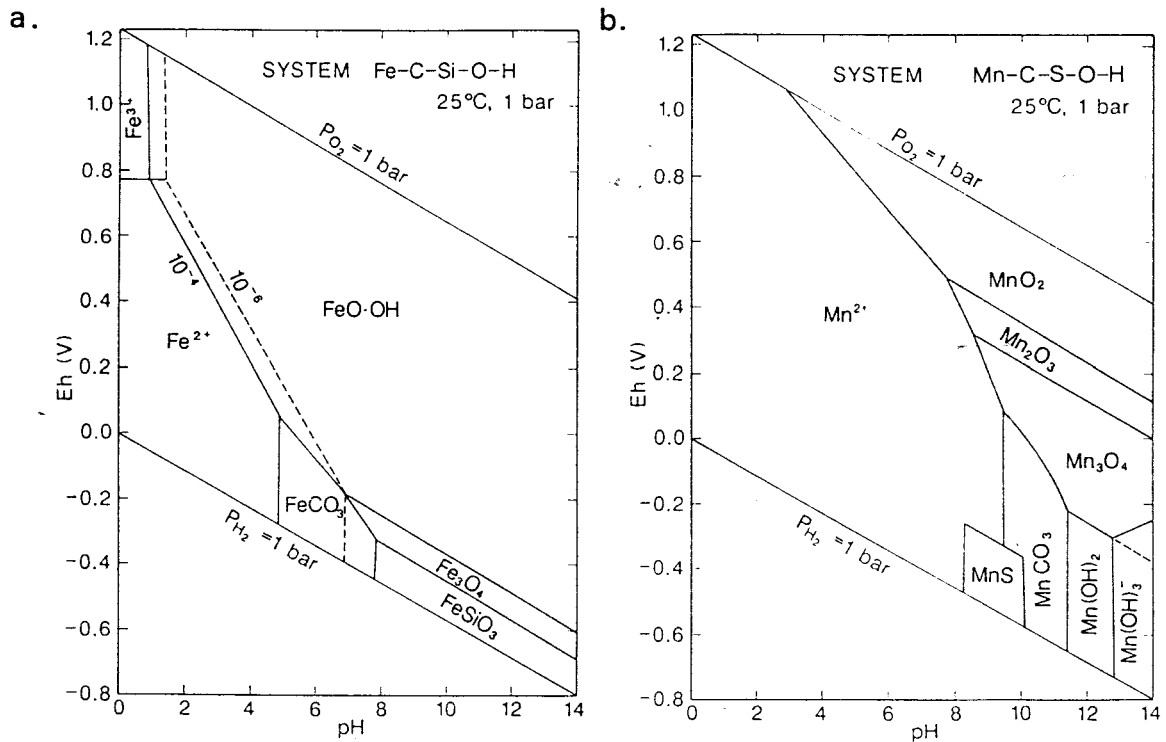


Fig. 5.7. a. Eh-pH diagram for part of the system Fe-C-Si-O-H. Assumed activities for dissolved species are: Fe = 10^{-6} , Si = 10^{-3} , C = 10^{-3} . Goethite and magnetite assumed as Fe³⁺ solid phases. b. Eh-pH diagram for part of the system Mn-C-S-O-H. Assumed activities for dissolved species are: Mn = 10^{-6} , C = 10^{-3} , S = 10^{-3} (after Brookins, 1988).

Changes of the redox conditions on a much larger scale could have accounted for the alternating BIF-Mn horizons of the study area. Such changes were probably also critical for the antithetic variation in thickness between those horizons in certain boreholes (Fig. A1; see also §5.2.3), and they may have been attributed to a combination of certain factors, such as tectonic instability, eustatic changes and the possible presence of palaeotopographic irregularities in the depositional basin. While, for example, the thick, carbonate-rich Mn-beds would have formed extensively in relatively shallow waters, the deposition of such sediments in somewhat deeper parts of the basin would have been restricted and, after some period of time, inhibited, as the critical redox boundary between Fe and Mn precipitation was reached (see also Fig. 5.8). As a consequence, BIF would subsequently have been laid down, thus causing the significant lateral facies changes presently observed. It should be stressed that

the processes that led to the formation of the Voëlwater Fe-Mn sediments were characterised by remarkable fractionation effects on the deposition of the two elements, with most BIF lithologies carrying virtually no Mn, and Mn-ores being characterised by sometimes high Mn/Fe ratios (Nel et al., 1986).

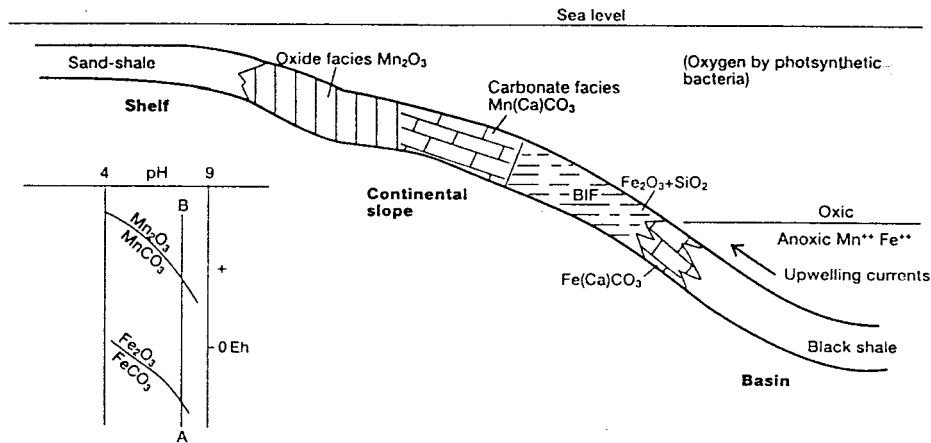


Fig. 5.8. Model for deposition of Mn and BIFs from upwelling anoxic waters (after Button et al., 1982; modified after Cannon & Force, 1983, in Schissel & Aro, 1992).

5.2.3 Considerations of local significance

Although the area covered in this study represents only a minor segment of the entire Kalahari basin, some important conclusions can be drawn from the foregoing discussion. For that reason, a NNW-SSE section (Fig. 5.9) was constructed using detailed loggings of the four selected boreholes, with the purpose of illustrating the lateral trends in the various Voëlwater lithologies between the presently operating Mamatwan mine and the non-operating Smartt mine (for details, see also Fig. A1). As is shown on Fig. 5.9, a significant lateral variation in the thickness of both the lower Mn-body and the LBIF exists over a rather short distance (more subtle thickness variations were also observed in the overlying BIF-Mn units but they cannot be satisfactorily depicted in Fig. 5.9). What is even more important is the fact that this main variation is characterised

by an antithetic relation between the two beds which, in terms of mineralogical composition, corresponds to the lack of a well-developed silicate-rich BIF in the LBIF unit (see ¶3.3), when the latter overlies thick portions of the lower Mn-horizon. This fact indicates that a dramatic increase in the deposition of Mn-sediment occurs in a SSE direction, which may be attributed to the presence of, for example, a preserved domal feature in the palaeodepositional basin, or it could simply be related to southward shallowing of the latter. On the other hand, the decrease in thickness of the lower Mn-horizon in the northern parts of the Kalahari area (e.g. the thickness of the lower Mn-body at Wessels mine attains a thickness of approximately 5 m; Kleyenstuber, 1991) may be related to respective deepening of the depositional basin towards that direction. It should be added that the shearing features observed in the granular, greenalite-rich lithologies of the LBIF unit and their possible recrystallised equivalents in the upper, carbonate-rich lithologies (see also ¶3.4.3 and Figs. 3.3a, 3.4f,g and 3.5b_{i,ii,iii,iv}) may very well reflect syn-diagenetic deformational processes induced by an interaction of mechanisms such as slumping/sliding, compressional or tensional stress and deep burial of H₂O-rich argillaceous Fe-sediment. The above, if combined with the afore-mentioned thickness variations and the consistence in the overall thickness of the Voëlwater sedimentary package, could reflect the operation of intense syn-sedimentary (growth) faulting in the depositional basin which may or may not be related to other tectonic processes that pre-dated or post-dated the deposition of the Voëlwater sediments (e.g. rifting or thrusting). However, if the growth-faulting invoked represents a later expression of intense, localised geotectonic and associated volcanic activity which took place prior to the deposition of the Voëlwater sediments, then there is a good indication that economic manganese-deposits with "Mamatwan-thicknesses" (> 40m) may now be resting on top of major lava piles which might correspond to palaeosites (foci) of increased submarine volcanism. Any of the above possibilities, however, may be confirmed or questioned by means of further prospecting, with the additional aid of regional geophysical data.

It is therefore not imperative that post-Voëlwater faulting or thrusting should be

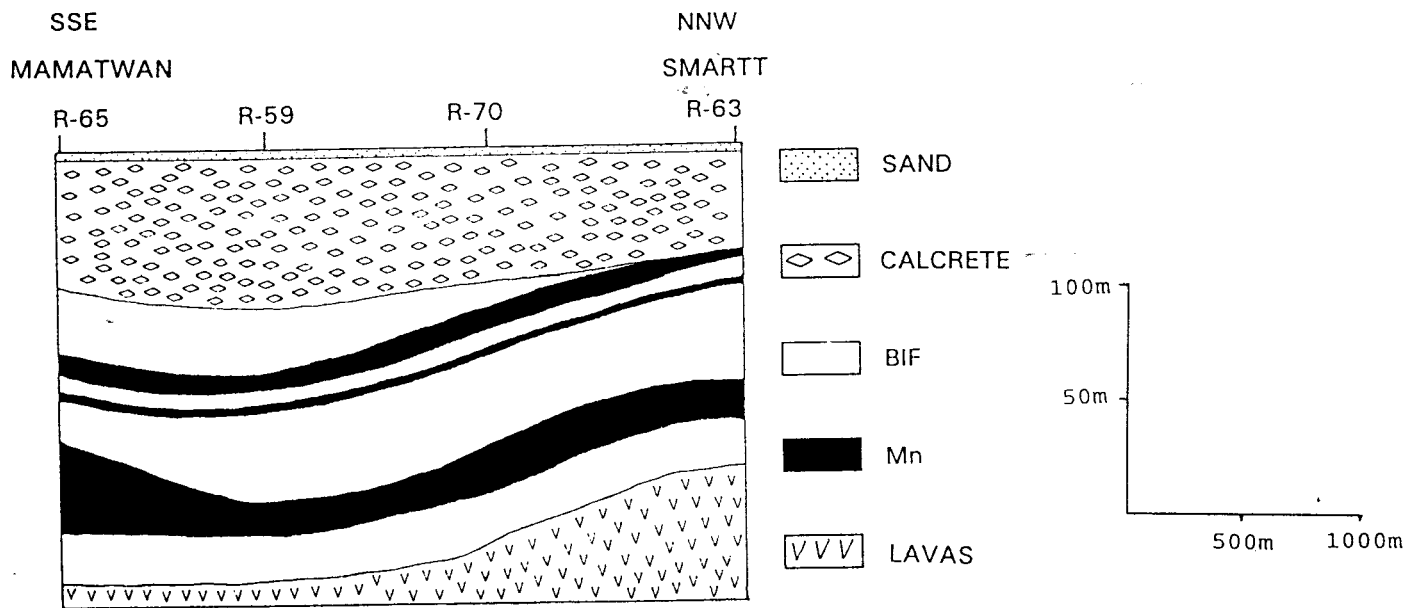


Fig. 5.9. NNW-SSE section between the Mamatwan (operating) and Smartt (non-operating) Mn-mines of the Kalahari Manganese Field (see also Fig. A1).

invoked in order to explain any lateral variations in thickness over a short distance, although post-depositional tectonism can certainly not be excluded as an important process in the Kalahari field. It is apparent that the same amount of chemical sediment precipitated in those parts of the basin which are situated in the vicinity of Mamatwan mine, particularly with regard to the lower Mn-body and the LBIF unit. Also, no duplication of strata due to thrusting was observed, although as has already been mentioned, evidence of mylonitisation (shearing) clearly exists, particularly in the silicate-rich lithologies of the LBIF unit (see, ¶3.4.3). The strong recrystallisation and soft-sediment deformation features observed in the upper, carbonate-rich parts of the Voëlwater BIF are probably related to differential effects of diagenesis in a strongly carbonaceous environment and they cannot be correlated with any tectonothermal effects due to the (possible) existence of proximal, overlying thrust sheets. However, it has been well-documented that thrusting processes have affected a significant portion of the Kalahari basin in the north-western parts (e.g. Black Rock Mn-

mine; Beukes & Smit, 1987), and they may very well have contributed to the hydrothermal upgrading of the respective Mn-ores (e.g. Kleyenstuber, 1984) by supplying the required hydrothermal fluids, without necessarily the addition of a magmatic heat source. Nevertheless, as was also stressed in ¶3.5, there is still controversy as to whether the metasomatism that characterises the NNW parts of the basin should be ascribed to purely tectonometamorphic processes of local significance, regional burial metamorphic processes with variable effects in certain areas, or simply thermal metamorphism induced in the proximity of an igneous intrusion. The results of this study have shown that even if the shearing observed in several lithologies of the study area is indeed related to thrusting, then no reason exists why there should not be any metasomatic effect on the Mn-ores in the southern portions of the Kalahari basin. Up until now, no hydrothermally enriched Mn-ores have been found in the area around Mamatwan mine, and this fact may constitute an additional indication for the existence of intense tectonism and, possibly, associated magmatism that affected primarily the north-western parts of the Kalahari basin.

5.2.4 Broad-scale geotectonic implications

It is important to note that the occurrence of the large Mn-deposits of the Kalahari Field in direct association with the Voëlwater BIF, may be of particular significance to the global evolutionary trends that characterised the Precambrian. This lithological association is found in the youngest member of BIF deposition of the Transvaal Sequence in Southern Africa and marks a transition from BIF to carbonate deposition (Mooirdraai dolomite sequence). The latter transition completes a major carbonate (Campbellrand dolomites) → BIF (Kuruman-Griquatown-Voëlwater stages) → carbonate (Mooirdraai dolomites) chemical sedimentary cycle in the Griqualand West Sequence which was interrupted by essentially two major events:

1. a glacial(?) event (Makganyene diamictite), and
2. a volcanic event (Ongeluk lavas).

From a broader perspective, it could be suggested that the above cycle may reflect respective changes in the wider geotectonic regime, the O₂ and CO₂ contents of the atmosphere and oceans, as well as shifting of the climatic conditions that characterised the Early Proterozoic geology of S. Africa over a significant period of time. The Transvaal Basin in Griqualand West seems to offer an excellent opportunity for further considerations in that respect. It appears that with the passing of time, lithospheric stretching (rifting?) - changed the depositional environment from a shallow carbonate platform where the Campbellrand dolomites were deposited, to relatively deeper environments which triggered the deposition of large amounts of microbanded BIFs (Kuruman stage). Subsequent gradual shallowing of the depositional basin (perhaps related to continuous filling of the depository with chemical sediment) would have been reflected by the deposition of granular BIFs (Griquatown stage). The atmospheric-oceanic-climatic conditions during that period would have switched from a warm, CO₂-rich regime to a cooler, CO₂-poor one, with no appreciable change in the oxygen budget of the atmosphere which remained oxidising. Particularly in the Transvaal-aged rocks of S. Africa strong evidence exists for an oxidising atmosphere in the Early Proterozoic, such as the occurrence of hematite-bearing palaeoweathering profiles (Wiggering & Beukes, 1990; Holland & Beukes, 1990) and extensive "red beds" (Truswell, 1990a). The deeper parts of the oceans however, would have been characterised by stabilisation of anoxic conditions which are necessary for the preservation of significant amounts of Fe⁺² in solution. The gradual atmospheric cooling would have played an important role to the prolonged precipitation of SiO₂-rich BIFs (the Asbesheuwels BIFs have average silica contents in excess of 50%; see also Table A2a, ¶4.3.1.3 and Fig. 4.4) by means of supersaturation of surface waters, whereas the culmination of this cooling event would have corresponded to the deposition of glacial diamictite sediments (Makganyene stage).

Further lithospheric stretching related to a mantle plume episode or hot-spot activity, would have caused intense geotectonic activity in the form of rifting and associated volcanism (Ongeluk stage). This resulted in a dramatic change in

the conditions of BIF deposition at least in certain parts of the Griqualand West sub-basin, which was possibly related to uplift and subaqueous extrusion of large amounts of andesitic lavas. The physicochemical conditions would have changed appreciably, with shallowing of the depositional basin and respective shifting of the redox conditions which gave rise to the rapid deposition of large amounts of Mn-bearing BIF (HBIF unit) and carbonate-rich manganese sediment. Shortly after the cessation of the Ongeluk volcanic episode, (thermal?) subsidence would have followed which resulted in further shifting of the redox conditions and deposition of microbanded, silicate-rich BIF. Filling of the depositional basin by continuous accumulation of chemical sediment was probably coupled by further contemporaneous tectonic instability, in order to account for the two subsequent cycles of carbonate-rich BIF and Mn deposition in a progressively shallower depositional environment.

During the deposition of the Voëlwater sedimentary package, the CO₂ content of the atmosphere would possibly have increased and the climate would have become progressively warmer. The above two factors could explain the relatively lower silica and higher iron and carbonate content of the Voëlwater rocks which represent a rather transitional type of BIF towards carbonate-bearing lithologies. From that point of view, the Voëlwater Fe-sediments may represent one of the, globally, very last members of Superior-type BIF deposition, since they were probably formed just before carbonate sediments assumed a far more increasing importance on the Early Proterozoic shelves (Frakes, 1979). This fact may be of major significance as far as the timing of Mn ore-formation is concerned, for it indicates that the conditions that favoured the deposition of Mn in direct association with Proterozoic BIFs may have characterised an important evolutionary boundary of the Precambrian era. This boundary is marked by the disappearance of BIFs after about 2200 m.y. ago and the subsequent increase of carbonate rocks (Fig. 5.10), and corresponds to a major transition from an "oxidising" to an "aerobic" atmosphere which came into existence when the last vestiges of ferrous iron were swept out of the deep oceans (Kasting, 1987; see also ¶5.1.3.1).

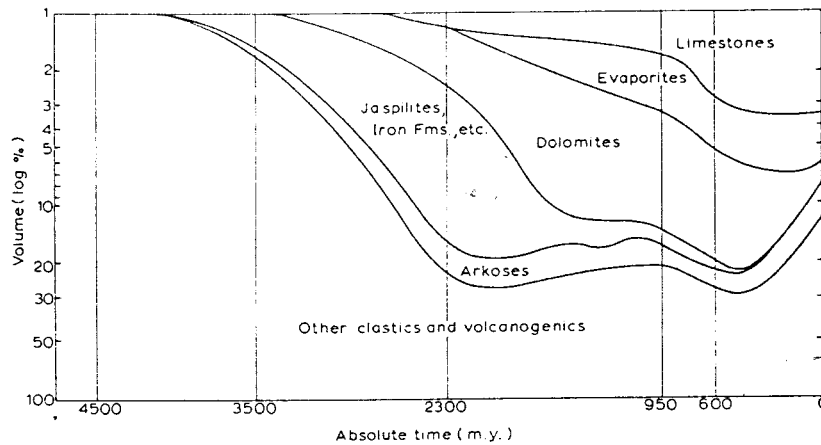


Fig. 5.10. Estimates of abundances of sedimentary rock-types (log-scale) throughout Earth history (modified after Ronov, 1964; in Frakes, 1979).

5.2.5 Suggestions for exploration

The importance of the foregoing discussion lies in the future exploration of areas which may carry large, BIF-hosted Mn-deposits. Specifically, in any Precambrian sedimentary basins of the world where Superior-type BIFs occur, economic Mn-ores should be expected in the uppermost (youngest) BIF members, provided that the latter grade up to carbonate lithologies in an upward-shallowing and essentially undisturbed chemical sedimentary sequence. Prerequisites for such a sequence should be:

1. a sufficient build-up of manganese concentrations in the depositional basin during prolonged precipitation of chert-rich BIFs, and coupled with negligible intermediate deposition of carbonate-bearing sediments;
2. contemporaneous geotectonic activity in the form of rifting and, possibly, associated submarine volcanism. Large-scale rifting processes in shallow-water carbonate platforms would have been necessary for the development of deep-water basinal environments, which caused the extensive deposition of BIFs. However, in a more advanced rifting system which may be reflected by the subaqueous extrusion of tholeiitic lavas, geotectonic activity in the form of episodic uplifts and subsidences would have switched accordingly the conditions

of BIF deposition. As a result, the rapid precipitation of BIF - carbonate-rich Mn-sediment cycles would have been enhanced, provided that the conditions for extensive carbonate deposition could not be sustained. It should be noted that the presence of extrusive volcanics offers an additional expression for the existence of such a geodynamic regime but it is certainly not required, since it is not necessary for the entire process.

Nevertheless, the possible source of Fe and Mn may cause further complications. For example, in the case of the Voëlwater sediments it has been suggested that the BIF and the Mn orebodies are directly associated with the underlying Ongeluk volcanics. Geochemical evidence that could support such a notion exists in the study area, mainly in the form of unusually high values of certain trace elements (e.g. Ba and Co; see also Table A1, samples R-65-30, R-65-31, R-63-20) in the lower BIF unit (HBIF; see ¶3.3), which is found immediately above the Ongeluk volcanics. Although this fact could be considered as a good indication of volcanogenic-exhalative processes, it is difficult to estimate the grade and extent of such processes, as well as its effect on the deposition of the Voëlwater chemical sediments. Furthermore, direct associations between Superior-type BIFs and volcanic rocks have not been extensively found in other major BIF occurrences of the world, and it is therefore uncertain whether:

1. the Fe and Mn of the study rocks derive from a common volcanic source;
2. the two metals have a common, but not volcanogenic-exhalative origin; or,
3. the Mn has an exhalative origin, and its precipitation "interrupted" the deposition of typical BIF, with the Fe deriving from a different source.

Irrespective of the origin of Fe, if the Mn has a direct volcanic origin then any BIFs which directly overly submarine extrusive rocks should be explored as possible host-rocks for potential Mn-mineralisation. If that is the case, then the above-mentioned exploration suggestions could be considered inadequate, if not invalid. Nevertheless, the writer will leave this matter open to criticism, particularly after the origin of the study rocks has been discussed in the following paragraphs.

5.3 The origin of the Kalahari Mn-deposits

5.3.1 Previous hypotheses

The origin of the manganese deposits in the Kalahari area has been the object of continuous debate for more than thirty years. The various genetic theories suggested can be outlined in two major groups, namely **replacement** models and **volcanogenic** models.

Replacement models: Theories about a replacement origin for the major Mn-deposits of the Kalahari were particularly favoured until the late 1970's. One of the pioneers of the replacement hypothesis was Frankel (1958) who suggested that the Mn-orebodies of the Voëlwater Subgroup formed under replacement of limestones by manganese deriving from weathering of the Campbellrand dolomites. A similar concept was proposed by Boardman (1964), who concluded that Mn was liberated from the same source (i.e. Campbellrand dolomites) and replaced Mn-rich calcareous units. Epigenetic metasomatic replacement of banded iron-formations was the mechanism supported by J. de Villiers (1960) for the formation of the Kalahari Mn-deposits, whereas replacement of BIFs by deep-seated magmatic emanations was also envisaged by P.R. de Villiers (1970). Although the various replacement hypotheses leave several questions unanswered (e.g. how can the cyclicity of the BIF-Mn units be described by replacement processes, particularly when it is well documented that the contacts between the two lithologies are sedimentary and gradational? if the Campbellrand dolomites were the source for the Mn, where did the Fe and Si for the BIFs derive from? which magmatic source in the entire Griqualand West area could have caused such an enormous metasomatic effect?), they have not yet been abandoned as possible genetic mechanisms. The latest version of the replacement theory was introduced by J.E. de Villiers (1983, 1990), who describes the origin of the Mn-ores as products of hypogene replacement processes at the expense of BIFs. This model was proposed on the basis of mainly mineralogical investigations, and suggests a close genetic relation

between the Mn-deposits in the Kalahari field and the Mn-ores of the Postmasburg area in Griqualand West.

Volcanogenic models: Beukes (1973) first introduced the idea that the Kalahari Mn-deposits may be genetically related to the underlying Ongeluk volcanics. This concept was overlooked by Söhnge (1977), who suggested that the volcanic rocks of the Ventersdorp Sequence were the source for the Mn, together with deeply weathered surrounding lithologies. Also, according to Söhnge (op. cit.) the Mn-sediments were precipitated under the influence of large-scale bacterial activity. Nevertheless, a volcanogenic-sedimentary model which associates the Ongeluk lavas with the Voëlwater sedimentary package was subsequently developed and established in the mid-1980's (Beukes, 1983; Kleyenstuber, 1984, 1985; Nel et al., 1986; Beukes, 1986a,b; Beukes & Kleyenstuber, 1986) and at present, it is believed that it represents the most likely genetic mechanism for the deposition of the Kalahari Fe-Mn sediments.

5.3.2 The currently accepted model

Volcanogenic-sedimentary Mn and Fe-Mn deposits are known to occur throughout the geological record. They are intimately associated with volcanic rocks (mainly spilites and diabases) and tuffs and they are hosted in chert (jasper), siliceous shale and siliceous carbonate formations that usually intergrade in a common volcanic series (Roy, 1981). Their modern equivalents are found in areas of active volcanism in present-day marine basins such as the Mid-Atlantic, Mid-Indian and Pacific-Antarctic ridges, the East Pacific Rise and the Galapagos Rift. The process for the formation of volcanogenic-sedimentary deposits is now very well understood and it has been described by numerous authors (e.g. Bonatti et al., 1976; Lalou, 1983). It briefly involves leaching of Fe, Mn, Si and minor metals from hot basalts by descending seawater in areas of high heat flow or mid-ocean ridge (MOR) activity, and subsequent debouchment of the modified hydrothermal fluids on the sea-floor, followed by rapid

precipitation of iron and manganese hydroxides. Apart from the Fe-Mn oxides, other deposits related to these processes include several types of massive sulfides ("stockwork-disseminated" type, massive "black-smoker" type, stratified "Red-Sea" type) and metal silicates, which can be effectively classified according to the timing of the hydrothermal discharge (Bonatti, 1983).

The presence of the Ongeluk volcanics in direct contact with the Voëlwater chemical sediments provides a tempting prospect for the source of Fe, Si and Mn in the latter rocks. Kleyenstuber (1985) noted several similarities between the Voëlwater association and volcanogenic-sedimentary deposits described by Park (1946) and Shatskiy (1964), and reviewed by Roy (1981). These similarities were established on the grounds of lithostratigraphic correlations between the various Voëlwater lithologies and a typical ophiolitic complex associated with Mn-bearing sedimentary rocks. However, it appears that the differences between the regional geological setting in the Kalahari area and the ophiolitic association are much more striking than the similarities suggested by Kleyenstuber (1985). Specifically:

1. An ophiolitic complex as described by Coleman (1977) has not been identified in the Kalahari area as yet. Kleyenstuber (1985) suggests that highly serpentinised ultramafic bodies intersected by drilling near the Botswana Border could account for the ultramafic sequence, which is probably represented by the Molopo Farms Complex. However, recent investigations have revealed that the Molopo Farms Complex is similar in tectonic setting, age and size to the Bushveld Complex (Gould et al., 1987; von Gruenewaldt et al., 1987; Wilhelm et al., 1990) and it is thus younger than the Transvaal sediments and Ongeluk volcanics (Fig. 5.11). Moreover, there is uncertainty regarding the presence of any gabbroic lithologies in the Kalahari area, and the typical diabasic sheeted dyke complex which characterises the upper parts of almost all ophiolitic complexes certainly cannot be correlated with the various dykes that transect the Voëlwater rocks, neither volume- nor age-wise. Unfortunately little is known about the Kameel mafic intrusion (Wiggering & Beukes, 1990; Beukes, 1993)

which is situated in the western part of the Kalahari basin, particularly with regard to its exact tectonic setting. However, the fact that Beukes (1993) suggests that this igneous body might have been responsible for the hydrothermal (metasomatic) alteration of the Kalahari Mn-ores (Wessels-type ores) is an indication that the Kameel intrusion is probably post-Transvaal in age. The writer believes that until further information becomes available regarding any mafic magmatic lithological occurrence in the wider area of Northern Cape, it would be very hypothetical to invoke the presence of a completely "blind" ophiolitic sequence which might have been genetically associated with the Ongeluk lavas. Such a hypothesis becomes even more conjectural since the general absence of typical ophiolites between 2.6-1.2 Ga has been well-established (Glikson, 1981), in addition to the fact that the Ongeluk volcanics have already been described in the literature as continental-type tholeiitic andesites (Sharpe et al., 1983).

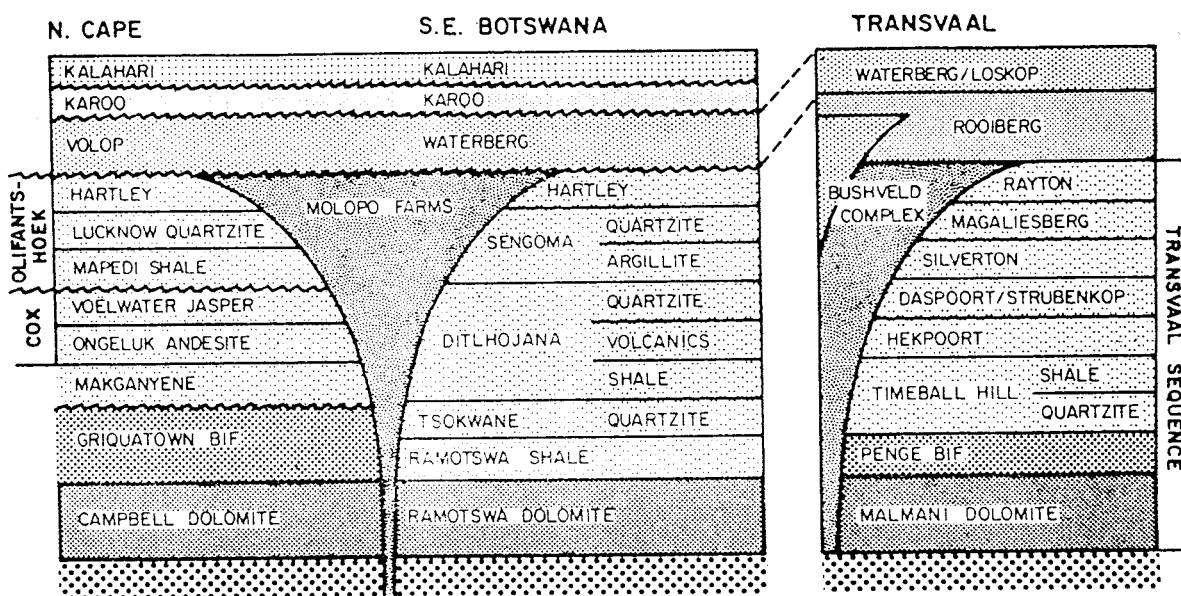


Fig. 5.11. Schematic section through the Molopo Farms Complex area, illustrating the relationship between the complex and the surrounding country rocks. The relation of the Bushveld Complex to the country rocks is shown for comparison (after von Gruenewaldt et al., 1987).

2. It has been well documented in the foregoing chapters that the host rocks of the major manganese deposits of the Kalahari are typical Superior-type BIFs or,

as the writer suggested in the first chapter of this study, BIFs s.s. Although it has always been attempted to treat BIFs s.s. like any other type of Fe-bearing sediment irrespective of age, tectonic setting or origin (e.g. Gross, 1983, 1990), it has been clearly established that rocks of this type mark a restricted time span in the geological record and they are completely absent from geologically younger areas. The mineralogical and geochemical character of these rocks is distinctly different from any other type of chemical sediment, and any systematic comparisons or uniformitarian assumptions must always take this fact under serious consideration. Therefore, it is strongly argued herein that the Voëlwater BIF does not bear any similarity with cherts associated with ophiolitic sequences, which may or may not carry economic Mn-deposits. This correlation was also attempted by Kleyenstuber (1985) to note the similarities between the Kalahari Mn-deposits and other volcanogenic-sedimentary prototypes, but it overlooked some important facts:

-Manganiferous cherts in ophiolitic "melanges" (term commonly used to describe the chaotic structures in volcano-sedimentary sequences of ophiolitic affiliation) represent essentially the consolidated equivalents of radiolarian oozes (radiolarian cherts, radiolarites, radiolarian jaspers, etc.). These rocks have simple mineralogy and chemistry and they bear little or no iron as compared to BIFs s.s. The reason for the very high Mn/Fe fractionation ratio in these cherts is the fact that essentially all the iron leached by the underlying basaltic pile precipitates as pyrite (often rich in Cu) veins and stringers in the basalts and before the hydrothermal fluids debouch on the ocean floor, forming characteristic stockwork-type sulfide deposits (Cyprus-type ores).

-Ophiolite-bearing manganiferous sequences are mostly known to occur at the Jurassic-Cretaceous boundary, although examples of Palaeozoic and Cenozoic age are also common (Roy, 1981). Manganese-rich lenses of small dimensions are commonly hosted in radiolarian cherts in these sequences, with typical examples the manganiferous cherts of the Franciscan assemblage in the U.S.A. (Crerar et al., 1982), the Apennine ophiolites and associated Mn-deposits of Italy (Bonatti et al., 1976) and the Mn-occurrences of the Orthrys ophiolitic

complex, Greece (Tsikos, 1991). The characteristics of these manganese ores are their very small size which often renders them uneconomic, as well as their simple mineralogical composition which is represented essentially by one mineral (braunite). The above are in contrast with the age and lithological character of the Voëlwater BIF, as well as with the enormous dimensions and mineralogy of the Kalahari Mn-ores which carry significant amounts of Mn-carbonate (kutnahorite).

Irrespective of the applicability or not of the ophiolite-model, the question that arises from any volcanogenic hypothesis is whether subaqueous leaching of large volumes of basaltic rocks could account for the genesis of the giant Kalahari Mn-ores and associated BIFs, or the genesis of BIFs s.s. in general. Under ideal circumstances, and using mathematical calculations and formulae involving: i. intense heat-flow and/or high ocean-floor spreading rates over long-term periods; ii. submarine extrusion of large basaltic masses; iii. interaction with seawater under high water-rock ratios; and iv. high rates of sediment accumulation, it could be argued that leaching of the Ongeluk lavas could indeed have provided the necessary Fe-Mn and Si for the formation of the Voëlwater BIF and Mn sediments. Similar conditions are believed to have existed in the Precambrian, with higher temperatures in seawater-basalt systems combined with higher water circulation through hot oceanic crust, which resulted in extensive leaching and larger Fe-flux to the oceans than at present (Mottl & Holland, 1978; Fryer et al., 1979; Seyfried & Janecky, 1985). This mechanism has been suggested to describe the origin of all the BIFs s.s. of the world, has been based largely on REE systematics (Jacobsen & Pimentel-Klose, 1988; Derry & Jacobsen, 1990) and is almost identical to the convection-cell models that describe the genesis of modern Mn-deposits in mid-ocean ridges (e.g. Bonatti et al., 1976; see also Fig. 5.12).

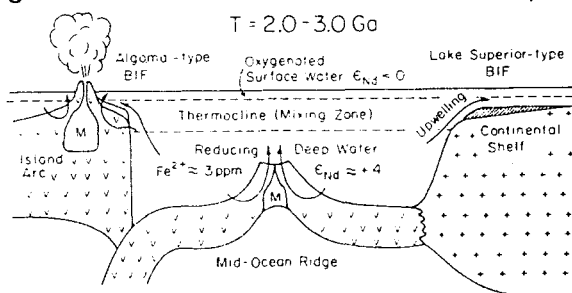


Fig. 5.12. According to Jacobsen and Pimentel-Klose (1988), the required Fe⁺² for the genesis of BIFs would have derived from hydrothermal convection in active mid-ocean ridges.

Due to the presence of pervasive alteration (Schutte & Cornell, 1990; Schutte, 1992), hyaloclastites, and abundant quartz-epidote-carbonate-pyrite stringers in the Ongeluk lavas, it is fairly evident that leaching of the latter rocks has occurred to some extent. However, several authors have argued that even in areas where conditions like the above mentioned have existed, the resultant deposits are small in size and the concentration of Mn is sporadic, corresponding to irregular pulses of contemporaneous hydrothermal activity. The deposits in Olympic Peninsula, for example, although they are associated with major volcanic piles are relatively small in size, reflecting the restricted supply of metals through the endogenous process (Roy, 1981). Therefore, more effective hydrothermal processes than simple convection models as proposed by Bonatti et al. (1976) and Bischoff and Dickson (1975), are needed to explain the origin of such vast amounts of Fe and Mn that gave rise to the giant deposits of the Kalahari.

5.3.3 A possible alternative

It is a well-established fact that the Precambrian era characterises a period of the geological record which was marked by unusual, and sometimes unique, geological phenomena. On a global scale, the "once-only" development of BIFs s.s. should be mentioned as a representative example. The Proterozoic geological record of Southern Africa in particular is characterised by the development of large intracratonic basins (e.g. Transvaal, Witwatersrand) which host the biggest Au and Mn deposits of the world, the intrusion of the largest layered complex on earth (Bushveld igneous complex and the associated ore-deposits: Cr, PGE, V, etc.), as well as the presence of unusually widespread volumes of sub-continental andesitic volcanics (Ventersdorp, Ongeluk and Hekpoort stages). The above facts may bear strong implications regarding possible tectonic settings during the Proterozoic eon and their evolutionary trends in a broader geotectonic perspective. They also offer ground for reassessment of the various genetic models which relate magmatism or volcanism with ore-forming processes, such

as the model for the genesis of the Kalahari Mn-ores.

The metallogenesis of S. Africa during the Early Proterozoic is closely related to the global-scale tectonic processes occurring at that time (Hutchinson, 1981). Proterozoic tectonism was dominated by rifting of continental crust, accompanied by mafic magmatism. Particularly in the Early Proterozoic, the rift displacement was mainly vertical and formed major, asymmetrical yoked basins (e.g. Witwatersrand). Evolution of this tectonic setting resulted in lateral-rift displacement at Mid-Proterozoic times, followed by global expansion and, probably, subsequent formation of deep oceanic basins which separated the major rifted continental blocks. The lateral separation along the rifts continued and, by Late Proterozoic time, evolved into the familiar Phanerozoic plate tectonics involving major lateral interaction of oceanic and continental crustal plates.

How does the genesis of the Kalahari Mn-deposit fit into such an evolutionary geotectonic cycle? Unfortunately, little information can be provided in this study to support an individual genetic model that would shed light to all the controversies. From the fore-going chapters and previous studies, the possibility that the Voëlwater Fe-Mn chemical sediments had a terrigenous source was minimised. Replacement hypotheses also seem to leave several inexplicable aspects. On the other hand, the volcano-sedimentary model has failed to offer an alternative genetic mechanism, mainly because it was based on unsuccessful correlations, misinterpretations and considerable lack of data. One genetic concept, however, that has not been extensively discussed in the literature has been proposed by Böstrom (1973, 1976a,b; in Roy, 1981) and Böstrom et al. (1976; in Roy, 1981). According to these authors, degassing during differentiation of primitive pyrolite into peridotite and basalt (a process which is extensively occurring at depth along the active ridges) should account for the supply of Fe, Mn and other minor metals in the modern oceans, in the form of CO₂-rich emanations. These elements are now incorporated in sediments that show significant enrichment in Fe, Mn, Ba, V, U and As and depletion in Al, Ti

and Th. The high (Fe + Mn)/Al ratio in these sediments is not characteristic of products of hot springs in basaltic areas, since Fe and Al cannot be effectively fractionated by leaching processes (op. cit.). Furthermore, basalts from DSDP cores show only negligible alteration and, therefore, only minimum leaching (Scott & Hajash, 1976). Thus, seawater-basalt reactions in active ridge areas cannot produce the characteristic Al-poor, Fe-Mn-rich sediments and a deep-seated source is considered necessary.

If such a mechanism is postulated for the Kalahari case, then one can explain the negligible contents of Al and Ti in the Voëlwater Fe-Mn sediments. The Ongeluk lavas do no longer need to be the ultimate source for the Fe and Mn: the two metals, (and possibly the Si) could derive from deeper sources, in amounts largely dependent on the composition of the upper mantle and, possibly, lower crust. Partial melting of the latter would produce large volumes of magma, the degassing of which would bear a significant volatile component. The magma generation and the subsequent upward movement of the separated volatiles would have been triggered in areas of high temperature-high density, by rifting which may have been characterised by vertical displacement, as it has been envisaged for the Early Proterozoic. Evidence of the rift-associated magmatism would have been the submarine extrusion of the Ongeluk lavas, covering large areas of the Transvaal depositional basin, although no direct surface expression of the magmatic source has been identified as yet. Whether the magmatic emanations had the capacity to remove certain amounts of metals as they were passing through surrounding lithologies, and carry them to the depository is debatable. It is also uncertain whether any interaction existed between these emanations and other fluid phases in shallower depths such as diagenetic fluids from permeable (unconsolidated?) sedimentary packages. A combination of magmatic-related processes and hydrothermal agents related to burial metamorphism should also not be excluded. The cyclicity of the BIF-Mn bodies would have been controlled purely by shifting in the physicochemical conditions of precipitation in the depositional basin, related to both exogenous and endogenous processes.

It is not the first time that degassing processes have been suggested as possible genetic mechanisms for either Precambrian BIFs or Mn-deposits. Lambert and Groves (1981) concluded that degassing and sea-floor alteration could account as possible sources of Fe and Si in BIFs. From a different standpoint, deep-seated magmatic emanations were invoked to have acted as agents of epigenetic replacement that formed the Kalahari Mn-ores at the expense of BIFs (P.R. De Villiers, 1970; see also ¶5.3.1). Derivation of Fe and Si due to mantle volatilisation is also in good accordance with recent models for the genesis of BIFs (Beukes & Klein, 1989; Kimberley, 1989b; Morris, 1993). The source of Fe (and Si) in these models is believed to be hydrothermal and directly related to MOR activity. However, volcanic rocks associated with possible rifting processes have only rarely been found in most major BIF occurrences of the world, and Mn in these rocks is also absent (see also ¶1.2). Hypotheses to explain the lack of Mn in BIFs s.s. have been suggested (e.g. dissimilar effects of photo-oxidation on Fe and Mn precipitation, Anbar & Holland, 1992; very low atmospheric pO_2 in the Precambrian to stabilise a Mn^{+4}/Mn^{+2} redox boundary, Bau & Möller, 1993) but a satisfactory explanation is still needed to account for the lack of Mn in all but the Voëlwater BIFs s.s., if the foregoing model is indeed valid. As has already been stressed, a factor that may have played a very important role in the genesis of the Kalahari Mn-ores (irrespective of source of metals or origin) is the transitional character of the associated Voëlwater BIFs which probably reflects a major but gradual change in the entire lithosphere-hydrosphere-biosphere system of the Early Proterozoic (see ¶5.2.4). However, if the pervasive alteration of the Ongeluk lavas in the Kalahari area is indeed related to extensive leaching of Fe, Mn, Si, Ba etc., then it could also be suggested that deep-seated hydrothermal agents with high initial Fe and Si contents could have become more enriched in Mn, (+ Fe, + Si) from leaching of the hot lavas, resulting in the relatively high Fe-contents of the Voëlwater BIFs and the associated Mn-deposits. Such a possibility, however, implies a mixed origin for the Voëlwater sediments, is also highly hypothetical and requires further investigation.

6. SUMMARY AND CONCLUSIONS

The banded iron-formations of the Voëlwater Subgroup represent the youngest members of BIF-deposition in the Transvaal Sequence in Griqualand West. They are interbedded with the giant Kalahari Mn-deposits, an association which, in terms of metallogenetic significance, renders the Voëlwater rocks-unusual in the geological record.

Mineralogical and textural studies on the various Voëlwater BIF lithologies showed that the latter are the possible diagenetic-low metamorphic products of Fe-rich sedimentary precursors deposited in an anoxic and relatively deep water environment. Certain mineral facies may be directly related to the original sediment (e.g. greenalite) whereas others exhibit characteristic diagenetic features (e.g. ankerite). The precipitation of the initial sediment would have largely taken place as a result of photo-oxidation and/or photosynthesis of Fe^{+3} (although direct, deep-water precipitation of Fe^{+2} in the form of Fe-silicates and Fe-carbonates cannot be excluded), during periodic storm mixing of anoxic bottom ocean waters saturated in Fe^{+2} with surface waters saturated in silica. This process would have given rise to alternate Fe-Si laminations, whereas Fe-rich bands of variable thicknesses would have been formed due to convection upwelling mechanisms driven by mid-ocean ridge or hot-spot activity of various grades. The degree of diagenetic processes that affected the original precipitate may have been closely associated with the rate of contemporaneous organic carbon productivity in the palaeoenvironment of deposition. The precipitation and diagenesis of the Mn-sediments could be described accordingly, but under moderately higher redox conditions.

Soft-sediment deformation structures are abundant in the carbonate-rich lithologies of the study area. They are found exclusively in association with certain mineral assemblages (i.e. chert-ankerite bands) and they characterise the post-depositional but syn-diagenetic history of the initial sediment. Post-

depositional features which might be related to important tectonic processes (e.g. thrusting) were also identified in granular, greenalite-bearing lithologies but their significance in ore-formation processes with respect to the study area remains somewhat conjectural.

Bulk chemistry studies provided useful information regarding the geochemical character of the study rocks. The high Ca and Fe and low Si content in the upper BIF lithologies of the Voëlwater Sequence corresponds to their transitional character towards shallow-water carbonate rocks (Mooibraai dolomites). Comparisons with other major BIF occurrences of the world confirmed that the Voëlwater BIF is a typical example of Superior-type BIF. Also, correlations with the geochemistry of recent metalliferous sediments suggest that the study rocks are not detrital in origin, but they are probably related to some sort of submarine hydrothermal input which was, nevertheless, not necessarily similar to the hydrothermal systems that characterise the modern, active mid-ocean ridges.

Anomalously high values of certain trace elements (e.g. Ba) were recognised in the lowermost BIF lithologies which directly overlie the Ongeluk lavas. However, due to the sheer magnitude of Proterozoic BIFs and particularly the Kalahari Mn-deposits, the possibility that typical convection-cell models which operated in submarine volcanic sequences could have acted as important suppliers of Fe and Mn has been questioned. Instead, large-scale magmatic processes in the form of partial melting, differentiation and associated degassing of the upper mantle have been proposed in this study as major contributors to the initiation of BIF-related hydrothermal activity. Later modification (enrichment) of the ascending, mantle-derived hydrothermal agents by low-temperature fluids related to, for example, dewatering of sedimentary packages, may have played a critical role to the entire process.

Although by far the largest, the Kalahari Mn-deposits are certainly not the only ones that characterise the Proterozoic eon. Precambrian Mn-ores are found in association with various lithotypes such as sandstones-claystones, black shales,

carbonates and iron-formations (Roy, 1976, 1992). In a review of the major Proterozoic iron and manganese deposits, Schissel and Aro (1992) concluded that the Voëlwater Fe-Mn association is similar to:

1. the Fe-Mn-deposits of the Minas Series, Brazil; and,
2. the Fe-Mn-ores of the Noamundi-Group, India.

This possible similarity was stressed but not discussed in the first chapter of this study (see ¶1.2). However, it appears from the limited literature available that many differences exist between the study rocks and the above deposits. Firstly, in both these areas of the world, the Mn-mineralisation is not interbedded with BIF as in the case of the Kalahari ores. The Proterozoic Mn-beds of Minas Gerais are directly associated with carbonaceous sediments in a transition at the top of the *Caue itabirite*. The latter is an Fe-rich sedimentary rock unit which consists of chert, hematite and magnetite but lacks Fe-silicates and Fe-carbonates (Van N. Dorr, 1973a), thus showing little mineralogical resemblance to Superior-type BIFs. On the other hand, the Mn-ores of India overly hematite-rich cherts known as *banded hematite jaspers* and are hosted in manganiferous shales and interbedded dolomites (Banerji, 1977). These hematitic rocks have also been described as Superior-type BIFs but this is in contrast to their age (1100 m.y.) and mineralogical character (no Fe-silicates or Fe-carbonates have been reported; Banerji, op. cit.). Finally, in terms of mineralogy, both the Brazilian and the Indian ores are clearly of supergene origin (pyrolusite, psilomelane and manganite), and little is known about the possible enriched "protores".

Conclusively, the uniqueness of the Voëlwater lithological association emphasised in the introductory paragraphs of this study could be further supported. Nevertheless, it is important to note once again the significance of carbonate sedimentation in the metallogenesis of Mn in the Precambrian. A possible explanation for the close correlation of Proterozoic manganese with carbonate sediments could be the role of organic carbon in diagenetic processes, particularly of BIF sedimentary sequences. According to Morris (1993), if organic carbon has indeed played a role in BIF diagenesis (as it has been previously

suggested; see ¶5.1.3.3) then a good reason exists why manganese, an essential component in the mechanism of modern photosynthesis, tends to concentrate in carbonate rather than oxide minerals. There are several cases of such Proterozoic manganese-carbonate associations: the previously discussed ore-deposits of Minas Gerais, Brazil, though different in mode and occurrence from the Voëlwater rocks, constitute a representative example (Van N. Dorr, 1973a), and so do the Proterozoic carbonate-bearing Mn-ores of Ghana, Ivory Coast and Upper Volta (Roy, 1981). A few rhodocrosite-bearing Mn-ore occurrences of the Noamundi Group in India (Banerji, 1977) are also associated with dolomites, but probably the best examples are found in the Transvaal Sequence of S. Africa where apart from the Kalahari deposits, minor Mn-occurrences are associated with stromatolitic limestone/dolomite bioherms of the Heynskop Formation, with manganese being concentrated in diagenetic ankerites (Dirr & Beukes, 1990; Beukes, 1993).

The determination of the origin of the Kalahari Mn-deposits certainly requires detailed studies on various aspects of ore-formation which would not have been covered within the confines of the present study. The previously-made suggestion that Mn and other metals which are enriched in modern "active ridge sediments" may have, at least partly, a juvenile origin has been based on the light of geochemical and geophysical evidence such as the high heat-flow values on ocean ridges, the recognition of anomalous ^3He in the deep sea, or because many of the enriched elements in those sediments are excess volatiles from the upper mantle (e.g. B, As, Cd, Hg), or have very large ionic radii (e.g. Ba, U) (Horn and Adams, 1966; Clark et al., 1969; Elderfield, 1977). However, such an approach has been criticised because it does little to improve our understanding of sediment genesis. As Krauskopf (1967) pointed out: "correct though it may be... it merely transfers the area of ignorance from the ore deposit to a magma... and our information about magmas is so very limited that we can neither check the hypothesis nor use it to make predictions. Building hypotheses in this manner is a harmless pastime, but it contributes little to our knowledge of ore deposition" (from Elderfield, 1977).

It is probably beyond any doubt that the geometry of magmatic intrusions has direct influence on hydrothermal activity at mid-ocean ridges (Brikowski & Norton, 1989). However, magmatic volatilisation as a direct agent for ore-forming process is a concept that certainly requires further evaluation. Unfortunately, any processes that are related to magma generation can only be indirectly approached (e.g. deductions based on the amount and type of metals from analyses of volcanic gases, since no satisfactory means are available of analysing volatiles from cooling magmas), and there are always severe limitations to such treatments. Our knowledge of volatilities is useful only in showing that: i. Fe and Mn can, theoretically, be separated from a magma on the basis of volatility and can be transported in significant amounts at high temperatures; ii. some gross fractionation may occur of metals that can be transported with iron and manganese (e.g., As and Pb), and those that cannot (e.g., Ag and Au) (Elderfield, 1977). However, the amount of metals that can be transported as volatiles falls off dramatically with decreasing temperature and is unimportant for most metals below 400°C (Barnes & Czamanske, 1967). As a result, the mechanisms that operate to transport metals of magmatic origin may change considerably in the intermediate and lower temperature ranges by interaction between volatiles and other hydrothermal phases, and may very well resemble low-temperature volcanogenic processes, thus preventing the distinction of any magmatic contribution of Mn and Fe to marine sediments. It is important to note that such interactions between magma chambers and hydrothermal systems located on mid-ocean ridge axes have been well documented, and they involve exsolution of magmatic volatiles into those systems as well as incorporation of the hydrothermal systems into the magma chamber by digestion of altered roof rocks (Nehlig, 1993).

From the fore-going facts it could be confidently suggested that large-scale magmatic processes in the form of magma convection, underplating, differentiation and associated degassing (Fyfe, 1990) may have played a very important, though indirect, role to the genesis of ancient deposits of hydrothermal-sedimentary affiliation. This concept may have had particular

applicability in the Precambrian of Southern Africa which was characterised by endogenous processes with orders of magnitude considerably higher than in other areas of the globe. It is hoped that one of the contributions of this study will be to stimulate further research that will look into the Kalahari Mn-deposits from a much broader perspective, with special emphasis on any direct or indirect evidence for possible interaction between shallow and/or deep-seated hydrothermal systems.

7. ACKNOWLEDGEMENTS

I would like to thank SAMANCOR for giving me the opportunity to undertake such a challenging research project in my first scientific endeavour in South Africa. A great thank-you to Mr Rick Arnot for his invaluable support and understanding during my stay in Hotazel, as well as to the secretary Mrs C. Ferreira and the geologists Dr. I.E.E. Williams, N. Bleeker, C. Lathy and S. van der Merwe, for their continuous assistance over a "hot" three-month period in the dry and remote Kalahari Manganese Field.

Working under the supervision of Prof. J.M. Moore has been one of the greatest benefits during my first two years in South Africa. His constructive discussions, criticisms and scientific arguments were essential and critical for the completion of this study. I would like to sincerely thank Prof. Moore for always keeping his door open for my endless queries (it became an everyday practice in the last three months of this study), and putting up with my frustration during a period and uncertainty for the future.

I am indebted to all the members of the academic staff of the Geology Department at Rhodes University. They have always been helpful and keen to listen to my problems, and supply me with their valuable suggestions. A great thank-you to Prof. H.V. Eales, Prof. R.E. Jacob, Prof. J.S. Marsh, Prof. N. Hiller, Dr. R.W. Harris and Mr. C.A. Mallinson. I am also thankful to Mrs C. Davies and Mrs S. Brooks (Departmental and Exploration Geology secretaries respectively), Mr J.R. Hepple (technical officer) and Mr A. Roman, Mr L.W. Morgan, Mr A. Visagie and Mr M. Stonestreet (scientific assistants), for allways being prepared to assist me in all these matters that were beyond their responsibility.

I would also like to thank all the ex- and current members of the postgraduate team here at Rhodes for their individual contributions throughout my studies. A special thank-you to Dr. J. Stiefenhofer, Dr. W. Meier, Dr. R. Elias, P.A. Kerber,

C.M. Williams, H. Holland, S. Frost, S. Smith, P. Hoyle, B.D. Coxon, I. Gendall, M. Skead, C. Gapara, G. Dwyer, S. Mujdrlica, R. Boelema, K. Hartmann, P. Mann, P. Schoeman, C. Breedt and C. Chikusa. I wish them all the best in their future careers.

I am gratefully indebted to the Head of the Geology Department at the University of Athens and ex-supervisor of my Honours project, Prof. S. Skounakis, for promoting my visit to South Africa for postgraduate studies. For the same reason, I would like to extend my warmest appreciation to Prof. K. Sideris, Ass. Prof. M. Stamatakis and Dr. K. Papavasiliou, as well as to Mr. V. Galanopoulos from the Institute of Geological and Mineral Research (I.G.M.E), Athens, Greece.

This study would not have been possible without the contribution of my beloved parents Niko and Sotiria. It would be inappropriate to say that their assistance was only in the form of financial input. Money is worth nothing compared to the moral support, encouragement and motivation that they offered me so bountifully all these years.

Last, but not least, I would like to thank my best friends Mr and Mrs Anetos for their warm hospitality and invaluable support over the last two years, as well as to my girlfriend and best mate Carla Flint for her patience and understanding, and for always being there when the times got tough.

Working on the Voëlwater banded iron-formations was indeed a daunting task for a young geologist with essentially no experience in Precambrian Geology. My studies in Greece provided me with a considerable background on all these aspects of the Earth Sciences that are related to presently active plate tectonics. However, my visit to South Africa certainly prompted my scientific skills to a considerable level, by covering an enormous gap in my knowledge of Precambrian geology and metallogenesis. There is nothing left to say than that I am really looking forward to doing further research in this geologically fascinating country.

8. REFERENCES

- Acharya, S., Amstutz, G.C., and Sarangi, S.K., 1982, Diagenetic crystallisation and migration in the banded iron-formations of Orissa, India, in: *Ore Genesis: The state of the Art*, eds., G.C. Amstutz, A. El Goresy, G. Frenzel, C. Kluth, G. Moh, A. Wauschkuhn, and R.A. Zimmermann: Special Publication of the Society for Geology applied to Mineral Deposits, No. 2, pp. 442-451.
- Alexandrov, E.A., 1973, The Precambrian banded iron-formations of the Soviet Union: *Econ. Geol.*, v. 68, pp. 1035-1062.
- Altermann, W., and Hälbich, I.W., 1990, The Tectogenesis of Proterozoic banded iron-formations on the south-western Kaapvaal Craton: Abstracts, *Geocongress '90*, *Geol. Soc. S. Afr.*, pp. 192-195.
- Anbar, A.D., and Holland, H.D., 1992, The photochemistry of manganese and the origin of banded iron-formations: *Geoch. Cosm. Acta*, v. 56, pp. 2595-2603.
- Anderson, G.J., 1970, The Marquette District, Michigan, in: *Ore deposits of the United States*, ed., J.D. Ridge: *Am. Inst. Min. Met. & Petr. Eng., Graton-Sales vol.*, v. 1, pp. 508-517.
- Appel, P.W.U., 1983, Rare earth elements in the Early Archaean Isua iron-formation, West Greenland: *Prec. Res.*, v. 20, pp. 243-258.
- Ayres, D.E., 1972, Genesis of iron-bearing minerals in banded iron-formation mesobands in the Dales Gorge Member, Hamersley Group, Western Australia: *Econ. Geol.*, v. 67, pp. 1214-1233.
- Banerji, A.K., 1977, On the Precambrian iron-formations and the manganese ores of the Singhbhum Region, Eastern India: *Econ. Geol.*, v. 72, pp. 90-98.
- Barker, A.J., 1990, *Introduction to metamorphic textures and microstructures*: Blackie, (USA: Chapman & Hall), 170 p.
- Barnes, H.L., and Czamanske, G.K., 1967, Solubilities and transport of ore minerals, in: *Geochemistry of Hydrothermal Ore-Deposits*, ed., H.L.

- Barnes: Holt, Reinhard and Winston, New York, pp. 334-381.
- Barrett, T.J., Fralick, P.W., and Jarvis, I., 1988, Rare-earth element geochemistry of some Archaean iron-formations north of Lake Superior, Ontario: *Can. J. Earth Sci.*, v. 25, pp. 570-580.
- Bau, M., 1993, Effects of syn- and post-depositional processes on the rare-earth element distribution in Precambrian iron-formations: *Eur. J. Miner.*, v. 5, pp. 257-268.
- Bau, M., and Dulski, P., 1992, Small-scale variations of the rare-earth element distribution in Precambrian iron-formations: *Eur. J. Mineral.*, v. 4, pp. 1429-1433.
- Bau, M., and Dulski, P., 1993, Distribution of rare earth elements in Precambrian sedimentary Fe-, Mn-, and P-deposits: Extended abstracts, 16th Colloquium of African Geology, Swaziland, v. I, pp. 27-28.
- Bau, M., and Möller, P., 1993, Rare earth element systematics of the chemically precipitated component in Early Precambrian iron-formations and the evolution of the terrestrial atmosphere-hydrosphere-lithosphere system: *Geoch. Cosm. Acta*, v. 57, pp. 2239-2249.
- Becker, R.H., and Clayton, R.N., 1972, Carbon isotopic evidence for the origin of a banded iron-formation in Western Australia: *Geoch. et Cosm. Acta*, v. 36, pp. 577-595.
- Becker, R.H., and Clayton, R.N., 1976, Oxygen isotope study of a Precambrian banded iron-formation, Hamersley Range, Western Australia: *Geochim. Cosm. Acta*, v. 40, pp. 1153-1165.
- Belevtsev, Ya.N., 1973, Genesis of high grade iron-ores of Krivoy-rog type, in: *Geness of Precambrian Iron and Manganese deposits: Proc. Kiev Symp. 1970, UNESCO Paris*, 382 p.
- Beukes, N.J., 1973, Precambrian iron-formations of Southern Africa: *Econ. Geol.*, v. 68, pp. 960-1004.
- Beukes, N.J., 1978, Die karbonaatgesteendes en ysterformasies van die Ghaap-Groep van die Transvaal-Supergroep in Noord-Kaapland. PhD thesis (unpubl.), Rand Afrikaans University, Johannesburg, 580 p.
- Beukes, N.J., 1979, Litostratigrafiese onderverdeling van die Schmidtsdrif-

- Subgroep van die Ghaap-Groep in Noord-Kaapland: *Trans. Geol. Soc. S. Afr.*, v. 82, pp. 313-327.
- Beukes, N.J., 1980a, Lithofacies and stratigraphy of the Kuruman and Griquatown iron-formations, Northern Cape Province, South Africa: *Trans. Geol. Soc. S. Afr.*, v. 83, pp. 69-86.
- Beukes, N.J., 1980b, Stratigrafie en litofasies van die Campbellrand-Subgroep van die Proterofitiese Ghaap-Groep, Noord-Kaapland: *Trans. Geol. Soc. S. Afr.*, v. 83, pp. 141-170.
- Beukes, N.J., 1980c, Suggestions towards a classification of, and nomenclature for iron-formation: *Trans. Geol. Soc. S. Afr.*, v. 83, pp. 285-290.
- Beukes, N.J., 1983, Palaeoenvironmental setting of iron-formations in the depositional basin of the Transvaal Supergroup, South Africa, in: *Iron-Formations: Facts and problems*, eds., A.F. Trendall and R.C. Morris: *Developments in Precambrian Geology 6*, *Els. Sci. Pbl.*, 558 p.
- Beukes, N.J., 1984, Sedimentology of the Kuruman and Griquatown iron-formations, Transvaal Supergroup, Griqualand West, South Africa: *Prec. Res.*, v. 24, pp. 47-84.
- Beukes, N.J., 1986a, The Transvaal Sequence in Griqualand West, in: *Mineral Deposits of Southern Africa*, eds., C.R. Anhaeusser and S. Maske: *Geol. Soc. S. Afr.*, v. 1, pp. 819-828.
- Beukes, N.J., 1986b, Sedimentology, structure and mineral deposits of Transvaal-Aged basins: *Excursion Guidebook, Geocongress '86*, *Geol. Soc. S. Afr.*, 48 p.
- Beukes, N.J., 1987, Facies relations, depositional environments and diagenesis in a major Early Proterozoic stromatolitic carbonate platform to basinal sequence, Campbellrand Subgroup, Transvaal Supergroup, Southern Africa: *Sed. Geol.*, v. 54, pp. 1-46.
- Beukes, N.J., 1993, A review of manganese deposits associated with the Early Proterozoic Transvaal Supergroup in Northern Cape Province, South Africa: *Extended abstracts, 16th Colloquium of African Geology, Swaziland*, v. 1, pp. 37-39.
- Beukes, N.J., Kleyenstuber, A., and Nel, C., 1982, Volcanogenic-sedimentary

- cycles in the Kalahari Manganese Field: Abstracts, Sedimentology '82, Geol. Soc. S. Afr., pp. 93-97.
- Beukes, N.J., and Dreyer, C.J.B., 1986, Crocidolite deposits of the Pomfret Area, Griqualand West, in: Mineral Deposits of Southern Africa, eds., C.R. Anhaeusser and S. Maske: Geol. Soc. S. Afr., v. I, pp. 911-921.
- Beukes, N.J., and Kleyenstuber, A.S.E., 1986, Sedimentology, diagenesis and hydrothermal alteration of the Kalahari manganese deposit, Transvaal Sequence, Griqualand West: Extended abstracts, Geocongress '86, Geol. Soc. S. Afr., pp. 497-500.
- Beukes, N.J., and Smit, C.A., 1987, New evidence for thrust faulting in Griqualand West, South Africa: implications for stratigraphy and the age of red beds: S. Afr. J. Geol., v. 90(4), pp. 378-394.
- Beukes, N.J., and Klein, C., 1990a, Geochemistry and sedimentology of a facies transition-from microbanded to granular iron-formation-in the Early Proterozoic Transvaal Supergroup, South Africa: Prec. Res., v. 47, pp. 99-139.
- Beukes, N.J., and Klein, C., 1990b, Sedimentology and geochemistry of Early Proterozoic storm-dominated deposits in a transition zone from microbanded Kuruman to granular Griquatown iron-formation, Griqualand West: Abstracts, Geocongress '90, Geol. Soc. S. Afr., pp. 50-52.
- Beukes, N.J., Klein, C., Kaufman, A.J., and Hayes, J.M., 1990a, Carbonate petrography, kerogen distribution, and carbon and oxygen isotope variations in an Early Proterozoic transition from limestone to iron-formation deposition, Transvaal Supergroup, South Africa: Econ. Geol., v. 85, pp. 663-690.
- Beukes, N.J., Klein, C., Kaufman, A.J., and Hayes, J.M., 1990b, The palaeoenvironmental implications of carbonate petrography, kerogen distribution and carbon and oxygen isotope variations in the Early Proterozoic transition from Cambellrand limestone to Kuruman iron-formation deposition in Griqualand West: Abstracts, Geocongress '90, Geol. Soc. S. Afr., pp. 53-55.
- Bischoff, J.L., and Dickson, F.W., 1975, Seawater-basalt interaction at 200°C

- and 500 bars: implications for origin of sea-floor heavy metal deposits and regulation of sea-water chemistry: *Earth Plan. Sci. Lett.*, v. 25, pp. 385-397.
- Blake, R.L., 1965, Iron phyllosilicates of the Cuyuna district in Minnesota: *Amer. Min.*, v. 50, pp. 148-169.
- Blatt, H., 1982, *Sedimentary Petrology*: W.H. Freeman & Co., 564 p.
- Blockley, J.G., Trendall, A.F., and Thorne, A.M., 1989, Early Precambrian crustal evolution and mineral deposits, Pilbara Craton and adjacent Ashburton Trough, in: *Origin and Evolution of Sedimentary Basins and Their Energy and Mineral Resources*, ed., R.A. Price: *Geophysical Monograph 48, IUGG v. 3*, pp. 159-167.
- Blockley, J.G., and Myers, J.S., 1990, Proterozoic rocks of the Western Australian Shield-geology and mineralisation, in: *Geology of the Mineral Deposits of Australia and Papua New Guinea*, ed., F.E. Hughes: *Austr. Inst. Min. Metall.*, v. 2, *Monograph No. 14*, pp. 607-616.
- Boardman, L.G., 1941, The Black Rock manganese deposit in the south-eastern Kalahari: *Trans. Geol. Soc. S. Afr.*, v. 44, pp. 51-60.
- Boardman, L.G., 1964, Further geological data on the Postmasburg and Kuruman manganese ore deposits, Northern Cape Province, in: *The Geology of some ore deposits in Southern Africa*, ed., S.H. Haughton: *Geol. Soc. S. Afr.*, v. II, pp. 415-440.
- Bonatti, E., Zerbi, M., Kay, R., and Rydell, H., 1976, Metalliferous deposits from the Apennine ophiolites: Mesozoic equivalents of modern deposits from oceanic spreading centers: *Geol. Soc. Amer. Bull.*, v. 87, pp. 83-94.
- Bonatti, E., 1983, Hydrothermal metal deposits from the ocean rifts: a classification, in: *Hydrothermal Processes at Sea-floor Spreading Centers*, eds., P.A. Rona, K. Böstrom, L. Laubier and K.L. Smith, Jr.: *Plenum Press, New York & London*, 796 p.
- Bonnichsen, B., 1975, Geology of the Biwabik iron-formation, Dunka River area, Minnesota: *Econ. Geol.*, v. 70, pp. 319-340.
- Brikowski, T., and Norton, D., 1989, Influence of magma chamber geometry on hydrothermal activity at mid-ocean ridges: *Earth Plan. Sci. Lett.*, v. 93, pp.

241-255.

- Brookins, D.G., 1988, Eh-pH diagrams for geochemistry: Springer-Verlag, Berlin-Heidelberg-New York-London-Paris-Tokyo, 176 p.
- Brooks, C., 1977, Archaean variolites: Source of iron in the Precambrian environment?: *Can. J. Earth Sci.*, v. 14, pp. 511-513.
- Butler, P.Jr., 1969, Mineral compositions and equilibria in the metamorphosed iron-formation of the Cagnon region, Quebec, Canada: *J. Petrology*, v. 10, pp. 56-101.
- Button, A., 1976a, Iron-formation as an end-member in carbonate sedimentary cycles in the Transvaal Supergroup, South Africa: *Econ. Geol.*, v. 71, pp. 193-201.
- Button, A., 1976b, Transvaal and Hamersley basins-review of basin development and mineral deposits: *Min. Sci. Eng.*, v. 8, pp. 262-293.
- Button, A., 1986, The Transvaal sub-basin of the Transvaal Sequence, in: *Mineral Deposits of Southern Africa*, eds., C.R. Anhaeusser and S. Maske: *Geol. Soc. S. Afr.*, v. 1, pp. 811-817.
- Button, A., Brock, T.D., Cook, P.J., Eugster, H.P., Goodwin, A.M., James, H.L., Margulis, L., Neelson, K.H., Nriagu, J.O., Trendall, A.F., and Walter, M.R., 1982 (Dahlem Konferenzen), Sedimentary iron deposits, evaporites and phosphorites-state of the art report, in: *Mineral Deposits and the Evolution of the Biosphere*, eds., H.D. Holland and M. Schidlowski: Springer-Verlag, pp. 259-273.
- Cameron, E.M., 1983, Genesis of Proterozoic iron-formation: sulphur isotope evidence: *Geoch. Cosm. Acta*, v. 47, pp. 1069-1074.
- Carrigan, W.J., and Cameron, E.M., 1991, Petrological and stable isotope studies of carbonate and sulphide minerals from the Gunflint iron-formation, Ontario: evidence for the origin of Early Proterozoic iron-formation: *Prec. Res.*, v. 52, pp. 347-380.
- Chauvel, J.J., and Dimroth E., 1974, Facies types and depositional environment of the Sokoman iron-formation, Central Labrador Trough, Quebec, Canada: *Jour. of Sed. Petr.*, v. 44, No. 2, pp. 299-327.
- Clarke, W.B., Beg, M.A., and Craig, H., 1969, Excess ^3He in the sea: evidence

- for terrestrial primordial helium: *Earth Plan. Sci. Let.*, v. 6, pp. 213-220.
- Clemmey, H., and Badham, N., 1982, Oxygen in the Precambrian atmosphere: an evaluation of the geological evidence: *Geol.*, v. 10, pp. 141-146.
- Cloud, P., 1972, A working model of the primitive earth: *Am. J. Sci.*, v. 272, pp. 537-548.
- Cloud, P., 1973, Paleoecological significance of the banded iron-formation: *Econ. Geol.*, v. 68, pp. 1135-1143.
- Cloud, P., Curtis, C.D., Folinsbee, R.E., Holland, H.D., Jenkyns, H.C., Langridge, J., Lerman, A., Miller, S.L., Nissenbaum, A., and Veizer, J., (Awramik, S.M., Rapporteur), 1982, Biogeochemical evolution of the ocean-atmosphere system: state of the art report, in: *Mineral deposits and the Evolution of the Biosphere*, eds., H.D. Holland and M. Schidlowski: Springer-Verlag, pp. 309-320.
- Coleman, R.G., 1977, *Ophiolites*: Springer-Verlag, Berlin, 229 p.
- Crerar, D.A., Namson, J., Chyi, M.S., Williams, L., and Feigenson, M.D., 1982, Manganiferous cherts of the Franciscan Assemblage: I. General geology, ancient and modern analogues, and implications for hydrothermal convection at oceanic spreading centers: *Econ. Geol.*, v. 77, pp. 519-540.
- Danielson, A., Möller, P., and Dulski, P., 1992, The Europium anomalies in banded iron-formations and the thermal history of the oceanic crust: *Chem. Geol.*, v. 97, pp. 89-100.
- Davy, R., 1983, A contribution on the chemical composition of Precambrian iron-formations, in: *Iron-Formations: Facts and problems*, eds., A.F. Trendall and R.C. Morris: *Developments in Precambrian Geology* 6, *Els. Sci. Pbl.*, 535 p.
- Derry, L.A., and Jacobsen, S.B., 1990, The chemical evolution of Precambrian seawater: evidence from REE in banded iron-formations: *Geoch. Cosm. Acta*, v. 54, pp. 2965-2977.
- De Villiers, J., 1960, The manganese deposits of the Union of South Africa: *S. Afr. Geol. Sur., Handbook* 2, 280 p.
- De Villiers, P.R., 1970, The geology and mineralogy of the Kalahari Manganese Field north of Sishen, Cape Province: *S. Afr. Geol. Sur., Mem.* 59, 65 p.

- De Villiers, P.R., and Visser, J.N.J., 1977, The glacial beds of the Griqualand West Supergroup as revealed by four deep boreholes between Postmansburg and Sishen: *Trans. Geol. Soc. S. Afr.*, v. 80, pp. 1-8.
- De Villiers, J.E., 1983, The manganese deposits of Griqualand West, South Africa: Some mineralogical aspects: *Econ. Geol.*, v. 78, pp. 1108-1118.
- De Villiers, J.E., 1990, Note on the origin of the Griqualand West manganese and iron deposits: SAMANCOR, unpubl. rep., 6 p.
- Dimroth, E., 1975, Paleo-environment of iron-rich sedimentary rocks: *Geologische Rundschau*, v. 64, pp. 751-767.
- Dimroth, E., 1976, Aspects of the sedimentary petrology of cherty iron-formation, in: *Handbook of Strata-Bound and Stratiform Ore-Deposits*, ed., K.H. Wolf: *Els. Sci. Pbl.*, v. 7, 656 p.
- Dimroth, E., and Chauvel, J.J., 1973, Petrography of the Sokoman iron-formation in part of the Central Labrador Trough, Quebec, Canada: *Geol. Soc. Amer. Bull.*, v. 84, pp. 111-134.
- Dimroth, E., and Kimberley, M.M., 1976, Precambrian atmospheric oxygen: evidence in the sedimentary distributions of carbon, sulfur, uranium, and iron: *Can. Jour. of Earth Sci.*, v. 13, No. 9, pp. 1161-1185.
- Dirr, H.V.D., and Beukes, N.J., 1990, Sedimentology and geochemistry of the manganiferous marls, stromatolitic carbonates and banded iron-formation, Transvaal Supergroup, Griqualand West: *Abstracts, Geocongress '90*, *Geol. Soc. S. Afr.*, pp. 127-130.
- Dixon, R., 1985, Sugilite and associated minerals from Wessels mine, Kalahari Manganese Field: *Trans. Geol. Soc. S. Afr.*, v. 88, pp. 11-17.
- Dixon, R., 1986, Metamorphism in the Kalahari Manganese Field: *Ext. Abstr. Geocongress '86*, *Geol. Soc. S. Afr.*, pp. 505-508.
- Dixon, R., 1989, Sugilite and associated metamorphic silicate minerals from Wessels mine, Kalahari Manganese Field: *Dep. Min. En. Aff., Geol. Sur., Bull.* 93, 44 p.
- Doe, B.R., 1972, An introduction to John W. Gruner, in: *Studies in Mineralogy and Precambrian Geology*, eds., B.R. Doe and D.K. Smith: *Geol. Soc. Amer., Mem.* 135., pp. vii-ix.

- Dorr, J.V.N.II, 1973a, Iron-formation and associated manganese in Brazil, in: Genesis of Precambrian Iron and Manganese deposits: Proc. Kiev Symp. 1970, UNESCO Paris, 382 p.
- Dorr, J.V.N.II, 1973b, Iron-formation in South America: *Econ. Geol.*, v. 68, pp. 1005-1022.
- Drever, J.I., 1974, Geochemical model for the origin of Precambrian banded iron-formations: *Geol. Soc. Amer. Bull.*, v. 85, pp. 1099-1106.
- Dutton, C.E., and Zimmer, P.W., 1970, Iron-ore deposits of the Menominee District, Michigan, in: *Ore Deposits of the United States*, ed., J.D. Ridge: Amer. Inst. Min. Met. & Petr. Eng., Graton-Sales vol., v. I, pp. 538-550.
- Dymek, R.F., and Klein, C., 1988, Chemistry, petrology and origin of banded iron-formation lithologies from the 3800 ma Isua Supracrustal Belt, West Greenland: *Prec. Res.*, v. 39, pp. 247-302.
- Eichler, J., 1976, Origin of the Precambrian banded iron-formations, in: *Handbook of Strata-Bound and Stratiform Ore-Deposits*, ed., K.H. Wolf: Els. Sci. Pbl., v. 7, 656 p.
- Elderfield, H., 1977, The form of manganese and iron in marine sediments, in: *Marine Manganese Deposits*, ed., G.P. Glasby: Els. Sci. Pbl. Co, 523 p.
- Eugster, H.P., and Ming Chou, I., 1973, The depositional environments of Precambrian banded iron-formations: *Econ. Geol.*, v. 68, pp. 1144-1168.
- Evans, A.M., 1987, *An introduction to ore geology*: Blackwell Scientific Publications, 358 p.
- Evans, A.M., 1993, *Ore geology and industrial minerals: An introduction*: Blackwell Scientific Publications, 3rd edition, 390 p.
- Evensen, N.M., Hamilton, P.J., and O'Nions, R.K., 1978, Rare-earth abundances in chondritic meteorites: *Geoch. Cosm. Acta*, v. 42, pp. 1199-1212.
- Ewers, W.E., 1983, Chemical factors in the deposition and diagenesis of banded iron-formation, in: *Iron-Formations: Facts and problems*, eds., A.F. Trendall and R.C. Morris: *Developments in Precambrian Geology* 6, Els. Sci. Pbl., 558 p.
- Ewers, W.E., and Morris, R.C., 1981, Studies of the Dales Gorge Member of the Brockman iron-formation, Western Australia: *Econ. Geol.*, v. 76, pp.

1929-1953.

- Floran, R.J., and Papike, J.J., 1975, Petrology of the low-grade rocks of the Gunflint iron-formation, Ontario-Minnesota: *Geol. Soc. Amer. Bull.*, v. 86, pp. 1169-1190.
- Floran, R.J., and Papike, J.J., 1978, Mineralogy and petrology of the Gunflint iron-formation, Minnesota-Ontario: correlation of compositional and assemblage variations at low to moderate grade: *J. Petr.*, v. 19, part 2, pp. 215-288.
- Frankel, J.J., 1958, Manganese ores from the Kuruman district, Cape Province, South Africa: *Econ. Geol.*, v. 53, pp. 577-597.
- Frakes, L.A., 1979, *Climates throughout geologic time*: Elsevier Scientific Publ. Co., 310 p.
- Frakes, L.A., and Bolton, B.R., 1984, Origin of manganese giants: sea-level change and anoxic-oxic history: *Geology*, v. 12, pp. 83-86.
- Frakes, L.A., and Bolton, B.R., 1992, Effects of ocean chemistry, sea level, and climate on the formation of primary sedimentary manganese ore deposits: *Econ. Geol.*, v. 87, pp. 1207-1217.
- Francois, L.M., 1986, Extensive deposition of banded iron-formation was possible without photosynthesis: *Nature*, v. 320, pp. 352-354.
- French, B.M., 1968, Progressive contact metamorphism of the Biwabik iron-formation, Mesabi Range, Minnesota: *Minnes. Geol. Survey Bull.* v. 45, 103 p.
- French, B.M., 1973, Mineral assemblages in diagenetic and low-grade metamorphic iron-formation: *Econ. Geol.*, v. 68, pp. 1063-1074.
- Frick, C., 1986, The mineralogy and geochemistry of the banded ironstones in the Griqualand West and Olifantshoek Sequences: Extended abstracts, *Geocongress '86*, Johannesburg, pp. 513-517.
- Froelich, P.N., Klinkhammer, G.P., Bender, M.L., Luedtke, N.A., Heath, G.R., Cullen, D., Dauphin, P., Hammond, D., Hartman, P., and Maynard, V., 1979, Early oxidation of organic matter in pelagic sediments of the eastern equatorial Atlantic: suboxic diagenesis: *Geoch. Cosm. Acta*, v. 43, pp. 1075-1090.

- Fryer, B.J., 1977a, Trace element geochemistry of the Sokoman iron-formation: *Can. J. Earth Sci.*, v. 14, pp. 1598-1610.
- Fryer, B.J., 1977b, Rare earth evidence in iron-formations for changing Precambrian oxidation states: *Geoch. et Cosm. Acta*, V. 41, pp. 361-367.
- Fryer, B.J., 1983, Rare-earth elements in iron-formation, in: *Iron-Formations: Facts and problems*, eds., A.F. Trendall and R.C. Morris: *Developments in Precambrian Geology* 6, *Els. Sci. Pbl.*, 558 p.
- Fryer, B.J., Fyfe, W.S., and Kerrich, R., 1979, Archaean volcanogenic oceans: *Chem. Geol.*, v. 24, pp. 25-33.
- Fyfe, 1990, Tectonics and geochemical change, in: *Crustal Evolution and Orogeny*, ed., S.P.H. Sychanthavong: A.A. Balkema/Rotterdam, pp. 193-204.
- Garrels, R.M., 1987, A model for the deposition of the microbanded Precambrian iron-formations: *Amer. Jour. of Sci.*, v. 287, pp. 81-106.
- Garrels, R.M., Perry, E.A., and Mackenzie, F.T., 1973, Genesis of Precambrian iron-formations and the development of atmospheric oxygen: *Econ. Geol.*, v. 68, pp. 1173-1179.
- Glikson, A.Y., 1981, Uniformitarian assumptions, plate tectonics and the Precambrian earth, in: *Precambrian Plate tectonics*, ed., A. Kroner: *Developments in Precambrian Geology*, v. 4, pp. 91-102.
- Gole, M.J., 1980, Mineralogy and petrology of very low-metamorphic grade Archaean banded iron-formations, Weld Range, Western Australia: *Amer. Miner.*, v. 65, pp. 8-25.
- Gole, M.J., 1981, Archaean banded iron-formations, Yilgarn Block, Western Australia: *Econ. Geol.*, v. 76, pp. 1954-1974.
- Gole, M.J., and Klein, C., 1981, Banded iron-formations through much of Precambrian time: *J. Geol.*, v. 89, pp. 169-183.
- Goodwin, A.M., 1956, Facies relations in the Gunflint iron-formation: *Econ. Geol.*, v. 51, pp. 565-595.
- Gould, D., Rathbone, P.A., and Kimbell, G.S., 1987, The geology of the Molopo Farms Complex, Southern Botswana: *Geol. Sur. of the Rep. of Botswana*, Bulletin 23, v. 1, 177 p., (Text) & v. 2, 245 p., (Appendices).

- Govett G.J.S., 1966, Origin of banded iron-formations: *Geol. Soc. Amer. Bull.*, v. 77, pp. 1191-1212.
- Graf, J.L.Jr., 1978, Rare earth elements, iron-formations and sea-water: *Geochim. Cosmochim. Acta*, v. 42, pp. 1845-1850.
- Gregory, R.T., 1986, Oxygen isotope systematics of quartz-magnetite pairs from Precambrian iron-formations: evidence for fluid-rock interaction during diagenesis and metamorphism, in: *Fluid-Rock Interactions during Metamorphism*, eds., J.V. Walther and B.J. Wood: *Adv. in Phys. Geochem.*, v. 5, Springer-Verlag, pp. 132-153.
- Grobelaar, W.S., and Beukes, N.J., 1986, The Bishop and Glosam manganese mines and the Beeshoek iron-ore mine of the Postmasburg area, in: *Mineral Deposits of Southern Africa*, eds., C.R. Anhaeusser and S. Maske: *Geol. Soc. S. Afr.*, v. 1, pp. 957-961.
- Grobelaar, W.S., 1988, The Nchwaning manganese mine of the Kalahari Manganese Field: *Geobulletin*, v. 31, No. 2, pp. 34-35.
- Grobler, N.J., and Botha, B.J.V., 1976, Pillow-lavas and hyaloclastite in the Ongeluk andesite Formation in a road-cutting west of Griquatown, South Africa: *Trans. Geol. Soc. S. Afr.*, v. 79, pp. 53-57.
- Gross, G.A., 1965, *Geology of iron deposits in Canada: general geology and evaluation of iron deposits*, v. I: Dep. of Mines and Tech. Surveys, Econ. Geol. rep. No. 22, 173 p.
- Gross, G.A., 1972, Primary features in cherty iron-formations: *Sed. Geol.*, v. 7, pp. 241-261.
- Gross, G.A., 1973, The depositional environment of principal types of Precambrian iron-formations, in: *Genesis of Precambrian Iron and Manganese Deposits: Proc. Kiev Symp. 1970, UNESCO Paris*, 382 p.
- Gross, G.A., 1980, A classification of iron-formations based on depositional environments: *Can. Min.*, v. 18, pp. 215-222.
- Gross, G.A., 1983, Tectonic systems and the deposition of iron-formation: *Prec. Res.*, v. 20, pp. 171-187.
- Gross, G.A., 1990, Manganese and iron facies in hydrothermal systems, in: *Sediment-Hosted Mineral Deposits*, eds., Parnell, J., Lianjun Ye and

- Changming Chen: Intern. Assoc. Sedim., Spec. Publ. No. 11, Blackwell Scientific Publications, 227 p.
- Gross, G.A., 1991, Genetic concepts for iron-formation and associated metalliferous sediments, in: Historical Perspectives of Genetic Concepts and Case Histories of Famous Discoveries, eds., R.W. Hutchinson and R.I. Grauch: Econ. Geol., Monograph 8, pp. 51-81.
- Gross, G.A., and McLeod, C.R., 1980, A preliminary assessment of the chemical composition of iron-formations in Canada: Can. Miner., v. 18, pp. 223-229.
- Grout, F.F., 1919, The nature and origin of the Biwabik iron-bearing formation of the Mesabi range, Minnesota: Econ. Geol., v. 14, pp. 452-464.
- Grubb, P.L.C., 1971, Silicates and their paragenesis in the Brockman iron-formation of Wittenoom Gorge, Western Australia: Econ. Geol., v. 66, pp. 281-292.
- von Gruenewaldt, G., Behr, S.H., and Wilhelm, H.J., 1987, Some preliminary investigations of the Molopo Farms Complex, Botswana and its Ni-Cu sulphide mineralisation: Inst. Geol. Res. Bush. Comp., Univ. Pretoria, Res. rep. 64, 23 p.
- Gruner, J.W., 1922, The origin of sedimentary iron-formations-the Biwabik formation of the Mesabi range: Econ. Geol., v. 17, no. 6, pp. 407-460.
- Gruner, J.W., 1936, The structure and chemical composition of greenalite: Amer. Miner., v. 21, pp. 449-455.
- Gruner, J.W., 1937, Composition and structure of stilpnomelane: Amer. Miner., v. 22, pp. 912-925.
- Gruner, J.W., 1944a, The structure of stilpnomelane re-examined: Amer. Miner., v. 29, pp. 291-298.
- Gruner, J.W., 1944b, The composition and structure of minnesotaite, a common iron silicate in iron-formations: Amer. Miner., v. 29, pp. 363-372.
- Guilbert, J.M., and Park, C.F. Jr., 1986, The geology of ore deposits: W.H. Freeman and Co., New York, 985 p.
- Gutzmer, J., & Beukes, 1993, Fault-zone controlled hematitization and upgrading of manganese ores in the Kalahari Manganese Field, South Africa:

- Extended abstracts, 16th Colloquium of African Geology, Swaziland, vol. I, pp. 139-142.
- Horn, M.K., and Adams, J.A.S., 1966, Computer-derived geochemical balances and element abundances: *Geoch. Cosm. Acta*, v. 30, pp. 279-297.
- Haase, C.S., 1982, Metamorphic petrology of the Negaunee iron-formation, Marquette District, Northern Michigan: *Mineralogy, Metamorphic Reactions and Phase Equilibria: Econ. Geol.*, v. 77, pp. 60-81.
- Hälbich, I.W., and Altermann, W., 1992, The genesis of BIF in the Transvaal Supergroup, South Africa, in: *Source, Transport and Deposition of Metals*, eds., M. Pagel and J.L. Leroy: A.A. Balkema, Rotterdam, 841 p.
- Hälbich, I.W., Lamprecht, D., Altermann, W., and Horstmann, U.E., 1992, A carbonate-banded iron-formation transition in the Early Proterozoic of South Africa: *Journal of African Earth Sciences*, v. 15, No 2, pp. 217-236.
- Hälbich, I.W., Scheepers, R., Lamprecht, D., van Deventer, J.L., and De Kock, N.J., 1993, The Transvaal-Griqualand West banded iron-formation: geology, genesis, iron exploitation: *Jour. of Afr. Earth Sci.*, v. 16, No. 1/2, pp. 63-120.
- Han, Tsu-Ming, 1988, Origin of magnetite in Precambrian iron-formations of low metamorphic grade, in: *Proceedings Seventh IAGOD Symposium*, ed., E. Zachrisson: The International Association on the Genesis of Ore Deposits, pp. 641-656.
- Harmsworth, R.A., Kneeshaw, M., Morris, R.C., Robinson, C.J., and Shirastava, P.K., 1990, BIF-derived iron-ores of the Hamersley Province, in: *Geology of Mineral deposits of Australia and Papua New Guinea*, ed., F.E. Hughes: *Austr. Inst. Min. Metall.*, v. 2, Monogr. No. 14, pp. 617-643.
- Holland, H.D., 1973, The oceans: a possible source of iron in iron-formations: *Econ. Geol.*, v. 68, pp. 1169-1172.
- Holland, H.D., 1984, *The chemical evolution of the atmosphere and oceans: Princeton Series in Geochemistry*, Princ. Univ. Press, 582 p.
- Holland, H.D., and Beukes, N.J., 1990, A palaeoweathering profile from Griqualand West, South Africa: evidence for a dramatic rise in

- atmospheric oxygen between 2.2 and 1.9 BYBP: *Amer. J. Sci.*, v. 290-A, pp. 1-34.
- Hutchinson, R.W., 1981, Metallogenic evolution and Precambrian tectonics, in: *Precambrian Plate Tectonics*, ed., A. Kroner: *Developments in Precambrian Geology*, v. 4, pp. 733-759.
- Jacobsen, S.B., and Pimentel-Klose, M.R., 1988, A Nd isotopic study of the Hamersley and Michipicoten banded iron-formations: The source of REE and Fe in Archaean oceans: *Earth Plan. Sci. Let.*, v. 87, pp. 29-44.
- James, H.L., 1954, Sedimentary facies of iron-formation: *Econ. Geol.* v. 49, pp. 235-293.
- James, H.L., 1955, Zones of regional metamorphism in the Precambrian of Northern Michigan: *Geol. Soc. Amer. Bull.*, v. 66, pp. 1455-1487.
- James, H.L., 1969, Comparison between Red Sea deposits and older ironstone and iron-formation, in: *Hot Brines and recent Heavy Metal Deposits in the Red Sea*, eds., E.T. Degens and D.A. Ross: Springer-Verlag, Berlin, pp. 525-532.
- James, H.L., 1983, Distribution of banded iron-formation in space and time, in: *Iron-Formations: Facts and problems*, eds., A.F. Trendall and R.C. Morris: *Developments in Precambrian Geology* 6, *Els. Sci. Pbl.*, 558 p.
- James, H.L., and Trendall, A.F., 1982 (Dahlem Konferenzen), Banded-iron formation: distribution in time and palaeoenvironmental significance, in: *Mineral Deposits and the Evolution of the Biosphere*, eds., H.D. Holland and M. Schidlowski: Springer-Verlag, pp. 199-218.
- JCPDS-Joint Committee on Powder Diffraction Standards, First Edition, 1974, Selected powder diffraction data for minerals: Philadelphia, USA, 833 p.
- JCPDS-Joint Committee on Powder Diffraction Standards, 1980, Search Manual: International Centre for Diffraction Data, USA, 484 p.
- Jennings, M., 1986, The Middelplaats manganese ore deposit, Griqualand West, in: *Mineral Deposits of Southern Africa*, eds., C.R. Anhaeuser and S. Maske: *Geol. Soc. S. Afr.* v. 1, pp. 979-983.
- Kasting, J.F., 1987, Theoretical constraints on oxygen and carbon dioxide concentrations in the Precambrian atmosphere: *Prec. Res.*, v. 34, 205-

229.

- Kaufman, A.J., Hayes, J.M., and Klein, C., 1990, Primary and diagenetic controls of isotopic compositions of iron-formation carbonates: *Geoch. Cosm. Acta*, v. 54, pp. 3461-3473.
- Kimberley, M.M., 1978, Palaeoenvironmental classification of iron-formations: *Econ. Geol.*, v. 73, pp. 215-229.
- Kimberley, M.M., 1979, Geochemical distinctions among environmental types of iron-formations: *Chem. Geol.*, v. 25, pp. 185-212.
- Kimberley, M.M., 1989a, Nomenclature for iron-formations: *Ore Geology Reviews*, v. 5, pp. 1-12.
- Kimberley, M.M., 1989b, Exhalative origins of iron-formations: *Ore Geology Reviews*, v. 5, pp. 13-145.
- Klein, C., 1966, Mineralogy and petrology of the metamorphosed Wabush iron formation, southwestern Labrador: *J. Petrol.*, v. 7, pp. 246-305.
- Klein, C., 1973, Changes in mineral assemblages with metamorphism of some Precambrian banded iron-formations: *Econ. Geol.*, v.68, pp. 1075-1088.
- Klein, C., 1974, Greenalite, stilpnomelane, minnesotaite, crocidolite and carbonates in a very low-grade metamorphic Precambrian iron-formation: *Can. Miner.*, v. 12, pp. 475-498.
- Klein, C., 1978, Regional metamorphism of Proterozoic iron-formation, Labrador Trough, Canada: *Amer. Min.*, v. 63, pp. 898-912.
- Klein, C., 1983, Diagenesis and metamorphism of Precambrian banded iron-formations, in: *Iron-Formations: Facts and problems*, eds., A.F. Trendall and R.C. Morris: *Developments in Precambrian Geology 6*, *Els. Sci. Pbl.*, 558 p.
- Klein, C., and Fink R.P., 1976, Petrology of the Sokoman iron-formation in the Howells River Area, at the western edge of the Labrador Trough: *Econ. Geol.*, v. 71, pp. 453-487.
- Klein, C., and Bricker, O.P., 1977, Some aspects of the sedimentary and diagenetic environment of Proterozoic banded iron-formation: *Econ. Geol.*, v. 72, pp. 1457-1470.
- Klein, C., and Gole, M.J., 1981, Mineralogy and petrology of parts of the Mara

- Mamba iron-formation, Hamersley Basin, Western Australia: *Amer. Miner.*, v. 66, pp. 507-525.
- Klein, C., Beukes, N.J., and Schopf, J.W., 1987, Filamentous microfossils in the Early Proterozoic Transvaal Supergroup: their morphology, significance, and palaeoenvironmental setting: *Prec. Res.*, v. 36, pp. 81-94.
- Klein, C., and Beukes, N.J., 1989, Geochemistry and sedimentology of a facies transition from limestone to iron-formation deposition in the Early Proterozoic Transvaal Supergroup, South Africa: *Econ. Geol.*, v. 84, pp. 1733-1774.
- Klemm, D.D., 1979, A biogenetic model of the formation of the banded iron-formation in the Transvaal Supergroup, South Africa: *Miner. Depos.*, v. 14, pp. 381-385.
- Kleyenstuber, A.S.E., 1979, n' Mineralogiese ondersoek van hoetemperatuur-reduksieprodukte van mangaanerts vanuit die Mamatwanmyn, Kalaharimangaanveld. Unpubl. MSc thesis, Rand Africaans University, Johannesburg, 125 p.
- Kleyenstuber, A.S.E., 1984, The mineralogy of the manganese-bearing Hotazel Formation, of the Proterozoic Transvaal Sequence in Griqualand West, South Africa: *Trans. Geol. Soc. S. Afr.*, v. 87, pp. 257-272.
- Kleyenstuber, A.S.E., 1985, A regional mineralogical study of the manganese-bearing Voëlwater Subgroup in the Northern Cape Province: Unpubl. PhD thesis, Rand Africaans University, Johannesburg, 328 p.
- Kleyenstuber, A.S.E., 1991, ICAM '91 Excursion guide, Kalahari Manganese Field: *International Congress on Applied Mineralogy*, 23 p.
- Kranck, S.H., 1961, A study of phase equilibria in a metamorphic iron-formation: *J. Petrology*, v. 2, pp. 137-184.
- Krauskopf, K.B., 1967, *Introduction to geochemistry*: McGraw-Hill, New-York, 721 p.
- Kump, L.R., and Holland, H.D., 1992, Iron in Precambrian rocks: implications for the global oxygen budget of the ancient earth: *Geoch. Cosm. Acta*, v. 56, pp. 3217-3223.
- LaBerge, G.L., 1966, Altered pyroclastic rocks in South African iron-formation:

- Econ. Geol., v. 61, pp. 572-581.
- LaBerge, G.L., 1973, Possible biological origin of Precambrian iron-formations: Econ. Geol., v. 68, pp. 1098-1109.
- Lalou, C., 1983, Genesis of ferromanganese deposits: hydrothermal origin, in: Hydrothermal Processes at Seafloor Spreading Centers, eds., P.A Rona, K. Böstrom, L. Laubier and K.L. Smith, Jr.: Plenum Press, New York & London, 796 p.
- Lambert, I.B., and Groves, D.J., 1981, Early earth evolution and metallogeny, in: Handbook of Strata-bound and Stratiform Ore Deposits, ed., K.H. Wolf: Els. Sci. Pbl., v. 8, 592 p.
- Lamprecht, D.F., and Hälbich, I.W., 1988, A vertical transition from carbonates to banded iron-formation in the Griqualand West Sequence of the Transvaal Supergroup, at Finsch diamond mine, Northern Cape Province: Abstracts, Geocongress '88, Geol. Soc. S. Afr., pp. 783-786.
- Laznicka, P., 1992, Manganese deposits in the global lithogenetic system: quantitative approach: Ore Geology Reviews, v. 7, pp. 279-356.
- Lepp, H., and Goldich, S.S., 1964, Origin of the Precambrian iron-formations: Econ. Geol., v. 59, pp. 1025-1060.
- Leshner, C.M., 1978, Mineralogy and petrology of the Sokoman iron-formation near Ardua Lake, Quebec: Can. J. Earth. Sci., v. 15, pp. 480-500.
- Lougheed, M.S., 1983, Origin of Precambrian iron-formations in the Lake Superior region: Geol. Soc. Amer. Bull., v. 94, pp. 325-340.
- Lovley, D., Stolz, J., Nord, G., and Phillips, E., 1987, Anaerobic production of magnetite by a dissimilatory iron-reducing microorganism: Nature, v. 330, pp. 252-253.
- MacLeod, W.N., 1973, Iron-ores of the Hamersley Iron Province, Western Australia, in: Genesis of Precambrian Iron and Manganese deposits: Proc. Kiev Symp. 1970, UNESCO Paris, 382 p.
- Mancuso, J.J., Lougheed, M.S., and Wygant, T., 1971, Possible biogenic structures from the Precambrian Negaunee iron-formation, Marquette Range, Michigan: Amer. Jour. Sc., v. 271, pp. 181-186.
- Marchig, V., Gundlach, H., Möller, P. and Schley, F., 1982, Some geochemical

- indicators for discrimination between diagenetic and hydrothermal metalliferous sediments. *Marine Geology*, v. 50, pp. 241-256.
- Marsden, R.W., 1970, Geology of the iron-ores of the Lake Superior Region in the United States, in: *Ore deposits of the United States*, ed., J.D. Ridge: Amer. Inst. Min. Met. & Petr. Eng., Graton-Sales vol., v. I, pp. 489-507.
- Marsden, R.W., Emanuelson, J.W., Owens, J.S., Walker, N.E., and Werner, R.F., 1970, The Mesabi Iron Range, Minnesota, in: *Ore deposits of the United States*, ed., J.D. Ridge: Amer. Inst. Min. Met. & Petr. Eng., Graton-Sales vol., v. I, pp. 518-537.
- Marsh, J., 1985, Geochemical characterization of lavas of the Ongeluk Formation, Northern Cape: SAMANCOR, unpubl. rep., 5 p., 2 tbl., 2 fig.
- Maynard, B.J., 1983, *Geochemistry of sedimentary ore deposits*: Springer-Verlag, New York Inc., 305 p.
- Mel'nik, Y.P., 1982, Precambrian banded iron-formations: physicochemical conditions of formation: *Developments in Precambrian Geology* 5, Els. Sci. Pbl., 310 p.
- Miyano T., 1982, Stilpnomelane, iron-rich mica, K-feldspar and hornblende in banded iron-formation assemblages of the Dales Gorge Member, Hamersley Group, Western Australia: *Can. Min.*, v. 20, pp. 189-202.
- Miyano T., and Miyano, S., 1982, Ferri-annite from the Dales Gorge Member iron-formations, Wittenoom area, Western Australia: *Amer. Miner.*, v. 67, pp. 1179-1194.
- Miyano T., and Klein, C., 1983, Conditions of riebeckite formation in the iron-formations of the Dales Gorge Member, Hamersley Group, Western Australia: *Amer. Miner.*, v. 68, pp. 517-529.
- Miyano T., and Beukes N.J., 1984, Phase relations of stilpnomelane, ferri-annite and riebeckite in very low-grade metamorphosed iron-formations: *Trans. Geol. Soc. S. Afr.*, v. 87, pp. 111-124.
- Miyano T., and Beukes N.J., 1987, Physicochemical environments for the formation of quartz-free manganese oxide ores from the Early Proterozoic Hotazel Formation, Kalahari Manganese Field, South Africa: *Econ. Geol.*, v. 82, pp. 706-718.

- Miyano, T., Beukes, N.J., and van Reenen, D.D., 1987, Metamorphic evidence for early post-Bushveld sills in the Penge iron-formation, Transvaal Sequence, Eastern Transvaal: *S. Afr. J. Geol.*, v. 90(1), pp. 37-43.
- Miyano, T., and Klein, C., 1989, Phase equilibria in the system K_2O -FeO-MgO- Al_2O_3 - SiO_2 - H_2O - CO_2 and the stability limit of stilpnomelane in metamorphosed Precambrian iron-formations: *Contrib. Miner. Petrol.*, v. 102, pp. 478-491.
- Monster, J., Appel, P.W.U., Thode, H.G., Schidlowski, M., Carmichael, C.M., and Bridgwater, D., 1979, Sulfur isotope studies in Early Archaean sediments from Isua, West Greenland: implications for the antiquity of bacterial sulfate reduction: *Geoch. Cosm. Acta*, v. 43, pp. 405-413.
- Moore, J.M., 1989, A comparative study of metamorphosed supracrustal rocks from the Western Namaqualand Metamorphic Complex: Precambrian Research Unit, University of Cape Town, 370 p.
- Morey, G.B., Papike, J.J., Smith, R.W., and Weiblen, P.W., 1972, Observations on the contact metamorphism of the Biwabik iron-formation, East Mesabi District, Minnesota, in: *Studies in Mineralogy and Precambrian Geology*, eds., B.R. Doe and D.K. Smith: Geol. Soc. of America, Mem. 135, pp. 225-264.
- Morris, R.C., 1993, Genetic modelling for banded iron-formation of the Hamersley Group, Pilbara Craton, Western Australia: *Prec. Res.*, v. 60, pp. 243-286.
- Morris, R.C., and Horwitz, R.C., 1983, The origin of the iron-formation-rich Hamersley Group of Western Australia-deposition on a platform: *Prec. Res.*, v. 21, pp. 273-297.
- Morris, R.C., and Trendall, A.F., 1988, Discussion: a model for the deposition of the microbanded Precambrian iron-formations: *Am. J. Sci.*, v. 288, pp. 664-668.
- Mottl, M.J., and Holland, 1978, Chemical exchange during hydrothermal alteration of basalt by seawater: I. experimental results from major and minor elements in seawater: *Geoch. Cosm. Acta*, v. 42, pp. 1103-1117.
- Myers, C.R., and Neilson, K.H., 1988a, Bacterial manganese reduction and

- growth with manganese oxide as the sole electron acceptor: *Science*, v. 240, pp. 1319-1321.
- Myers, C.R., and Nealson, K.H., 1988b, Microbial reduction of manganese oxides: interactions with iron and sulfur: *Geoch. Cosm. Acta*, v. 52, pp. 2727-2732.
- Nealson, K.H., 1982 (Dahlem Konferenzen), Microbiological oxidation and reduction of iron, in: *Mineral Deposits and the Evolution of the Biosphere*, eds., H.D. Holland and M. Schidlowski: Springer-Verlag, pp. 51-66.
- Nealson, K.H., and Myers, C.R., 1990, Iron reduction by bacteria: a potential role in the genesis of banded iron-formations: *Amer. J. Sci.*, v. 290-A, pp. 35-45.
- Nehlig, P., 1993, Interactions between magma chambers and hydrothermal systems: oceanic and ophiolitic constraints: *Jour. Geoph. Res.*, v. 98, No. B11, pp. 19,621-19,633.
- Nel, C.J., 1984, Die mineralogie en geochemie van die Mamatwan-ertslikaam, Kalaharimangaanveld, Transvaal-Supergroep: Unpubl. MSc thesis, Rand Afrikaans University, Johannesburg, 119 p.
- Nel, C.J., Beukes, N.J., and De Villiers, J.P.R., 1986, The Mamatwan manganese mine of the Kalahari Manganese Field, in: *Mineral Deposits of Southern Africa*, eds., C.R. Anhaeuser and S. Maske: *Geol. Soc. S. Afr.*, v. 1, pp. 963-978.
- Norrish, K., and Hutton, J.T., 1969, An accurate x-ray spectrographic method for the analysis of a wide range of geological samples: *Geoch. Cosm. Acta*, v. 33, pp. 431-453.
- Park, C.F., 1946, The spilite and manganese problems of the Olympic Peninsula, Washington: *Amer. J. Sci.*, v. 244, pp. 305-323.
- Perry, E.C.Jr., 1983, Oxygen isotope geochemistry of iron-formation, in: *Iron-Formations: Facts and problems*, eds., A.F. Trendall and R.C. Morris: *Developments in Precambrian Geology 6*, *Els. Sci. Pbl.*, 558 p.
- Perry, E.C., and Ahmad, S.N., 1980, Oxygen isotope study of Transvaal System iron-formation from the vicinity of Kuruman, Cape Province, South Africa: *Geol. Soc. Amer., Abstr. Programs*, v. 12, 497 p.

- Perry, E.C., and Ahmad, S.N., 1981, Oxygen and carbon isotope geochemistry of the Krivoy Rog iron-formation, USSR: *Lithos*, v. 14, pp. 83-92.
- Perry, E.C.Jr, and Tan, F.C., 1973, Significance of carbon isotope variations in carbonates from the Biwabik iron-formation, Minnesota, in: *Genesis of Precambrian Iron and Manganese deposits: Proc. Kiev Symp. 1970, UNESCO Paris*, 382 p.
- Perry, E.C., Tan, F.C., and Morey, G.B., 1973, Geology and stable Isotope geochemistry of the Biwabik iron-formation, northern Minnesota: *Econ. Geol.*, v. 68, pp. 1110-1125.
- Phillips, W.R., and Griffen, D.T., 1981, *Optical mineralogy: the nonopaque minerals: W.H. Freeman and Co.*, 677 p.
- Pirajno, F., 1992, *Hydrothermal mineral deposits: principles and fundamental concepts for the exploration geologist: Springer-Verlag*, 709 p.
- Pride, D.E., and Hagner, A.F., 1972, Geochemistry and origin of the Precambrian iron-formation near Atlantic City, Fremont Count, Wyoming: *Econ. Geol.*, v. 67, pp. 329-338
- Rai, K.L., Sarkar, S.N., and Paul, P.R., 1980, Primary depositional and diagenetic features in the banded iron-formation and associated iron-ore deposits of Noamundi, Singhbum District, Bihar, India: *Mineral. Depos.*, v. 15, pp. 189-200.
- Redwood, S.D., 1993, Crocidolite and magnesite associated with Lake Superior-type banded iron-formation in the Chapare Group of Eastern Andes, Bolivia: *Trans. Inst. Min. Metall. (Sect. B: Applied Earth Science)*, v. 102, pp. B114-121.
- Reineck, H.E., and Singh, H.E., 1973, *Depositional sedimentary environments: Springer-Verlag*, 439 p.
- Riley, C.M., 1959, *Our mineral resources: John Wiley & Sons Inc.*, 338 p.
- Roy, S., 1976, Ancient manganese deposits, in: *Handbook of Strata-Bound and Stratiform Ore Deposits*, ed., K.H. Wolf: *Els. Sci. Pbl.*, v. 8, 656 p.
- Roy, S., 1981, *Manganese deposits: London Academic Press*, 458 p.
- Roy, S., 1992, Environments and processes of manganese deposition: *Econ. Geol.*, v. 87, pp. 1218-1236.

- Sakamoto, T., 1950, The origin of Precambrian banded iron-ores: *Amer. J. Sci.*, v. 248, pp. 449-474.
- van Schalkwyk, and Beukes, N.J., 1986, The Sishen iron-ore deposit, Griqualand West, in: *Mineral Deposits of Southern Africa*, eds., C.R. Anhaeusser and S. Maske: *Geol. Soc. S. Afr.*, v. I, pp. 931-956.
- Schissel, D., and Aro, P., 1992, The major Early Proterozoic sedimentary iron and manganese deposits and their tectonic setting: *Econ. Geol.*, v. 87, pp. 1367-1374.
- Schreiber, U.M., Eriksson, P.G., Meyer, P.C., and van der Neut, M., 1990, The sedimentology of the Boshhoek Formation, Transvaal Sequence. *S. Afr. J. Geol.*, v. 93, pp. 567-573.
- Schutte, S.S., and Cornell, D.H., 1990, Spilitization processes in the Proterozoic Ongeluk andesite Formation in Griqualand West, South Africa: Abstracts, *Geocongress '90*, *Geol. Soc. S. Afr.*, pp. 505-508.
- Schutte, S.S., 1992, Ongeluk volcanism in relation to the Kalahari manganese deposits: Unpubl. PhD thesis, University of Natal, Durban, 266 p.
- Scott, R.B., and Hajash, A.Jr., 1976, Initial submarine alteration of basaltic pillow lavas: A microprobe study: *Amer. J. Sci.*, v. 276, pp. 480-501.
- Seyfried, W.E.Jr., and Janecky, D.R., 1985, Heavy metal and sulfur transport during subcritical and supercritical hydrothermal alteration of basalt: Influence of fluid pressure and basalt composition and crystallinity: *Geoch. Cosm. Acta*, v. 49, pp. 2545-2560.
- Sharpe, M.R., Brits, R., and Engelbrecht, J.P., 1983, Rare earth and trace element evidence pertaining to the petrogenesis of 2,3 GA old continental andesites and other volcanic rocks from the Transvaal Sequence, South Africa: *Inst. Geol. Res. Bush. Comp., Univ. Pret., Res. Rep. 40*, 63 p.
- Shatskiy, N.S., 1954, On manganiferous formations and the metallogeny of manganese, paper I. Volcanogenic-sedimentary manganiferous formations: *Inter. Geol. Rev.*, V. 6, No. 6, pp. 1030-1055.
- Shaw, D.M., 1980, Development of the early continental crust, Part III. Depletion of incompatible elements in the mantle: *Prec. Res.*, v. 10, pp. 281-299.

- Shimizu, H., and Masuda, A., 1977, Cerium in chert as an indication of marine environment of its formation: *Nature*, v. 266, pp. 346-348.
- Shimizu, H., Unemoto, N., Masuda, A., and Appel, P.W.U., 1987, Sources of iron-formations in the Archaean Isua and Malene supracrustals, West Greenland: evidence from La-Ce and Sm-Nd isotopic data and REE abundances: *Geoch. Cosm. Acta*, v. 54, pp. 1147-1154.
- Sidder, G.B., 1991, Iron and manganese, in: *The Geology of North America*, eds. H.J. Gluskoter, D.D. Rice and R.B. Taylor: The Geol. Soc. of America, Economic Geology U.S., v. P-2, 622 p.
- Simonson, B.M., 1985, Sedimentological constraints on the origins of Precambrian iron-formations: *Geol. Soc. Amer. Bull.*, v. 96, pp. 244-252.
- Simonson, B.M., 1987, Early silica cementation and subsequent diagenesis in arenites from four Early Proterozoic iron-formations of North America: *J. Sed. Petr.*, v. 57, No. 3, pp. 494-511.
- Simpson, C., and Schmid, S.M., 1983, An evaluation of criteria to deduce the sense of movement in sheared rocks: *Geol. Soc. Amer. Bull.*, v. 94, pp. 1281-1288.
- Skinner, B.J., 1969, Earth resources: Foundations of Earth Sciences ser., Prentice-Hall, Inc., 150 p.
- Söhnge, P.G., 1977, Timing aspects of the manganese deposits of the Northern Cape Province (South Africa), in: *Time and Stratabound Ore Deposits*, eds., D.D. Klemm and H.J. Schneider: Springer-Verlag, pp. 115-122.
- Sokolov, G.A., and Grigor'ev V.M., 1977, Deposits of iron, in: *Ore deposits of the USSR*, ed., V.I. Smirnov: Pitman Publishing, v. I, 352 p.
- Taylor, J.H., 1974, Sedimentary ores of iron and manganese and their origin, in: *Sedimentary ores (Ancient & Modern rev.)*, ed., C.H. James: Special Publication No. 1, Dep. of Geology, Univ. of Leicester, pp. 171-186.
- Toth, J.R., 1980, Deposition of submarine crusts rich in manganese and iron: *Geol. Soc. Amer. Bull.*, v. 91, pp. 44-54.
- Towe, K.M., 1983, Precambrian atmospheric oxygen and banded iron-formations: a delayed ocean model: *Prec. Res.*, v. 20, pp. 161-170.
- Trendall, A.F., 1968, Three great basins of Precambrian banded iron-formation

- deposition: a systematic comparison: *Geol. Soc. Amer. Bull.*, v. 79, pp. 1527-1544.
- Trendall, A.F., 1973a, Time-distribution and type-distribution of Precambrian iron-formations in Australia, in: *Genesis of Precambrian Iron and Manganese deposits: Proc. Kiev Symp. 1970, UNESCO Paris*, 382 p.
- Trendall, A.F., 1973b, Iron-formations of the Hamersley Group of Western Australia: type examples of varved Precambrian evaporites, in: *Genesis of Precambrian Iron and Manganese deposits: Proc. Kiev Symp. 1970, UNESCO Paris*, 382 p.
- Trendall, A.F., 1973c, Precambrian iron-formation of Australia: *Econ. Geol.*, v. 68, pp. 1023-1034.
- Trendall, A.F., 1973d, Varve cycles in the Weeli Wolli Formation of the Precambrian Hamersley Group, Western Australia: *Econ. Geol.*, V. 68, pp. 1089-1097.
- Trendall, A.F., 1975, Geology of Western Australian iron-ore, in: *Economic Geology of Australia and Papua New Guinea*, ed., C.L. Knight: The Austr. Inst. Min. Metal., Monogr. Ser. No. 5, pp. 883-892.
- Trendall, A.F., 1979, Iron, in: *Mining in Western Australia*, ed., R.T. Prider: Univ. of West. Austr. press, 304 p.
- Trendall, A.F., 1983a, Introduction, in: *Iron-Formations: Facts and problems*, eds., A.F. Trendall and R.C. Morris: *Developments in Precambrian Geology* 6, *Els. Sci. Pbl.*, 558 p.
- Trendall, A.F., 1983b, The Hamersley Basin, in: *Iron-Formations: Facts and problems*, eds., A.F. Trendall and R.C. Morris: *Developments in Precambrian Geology* 6, *Els. Sci. Pbl.*, 558 p.
- Trendall, A.F., and Blockley, J.G., 1970, The iron-formations of the Precambrian Hamersley Group, Western Australia, with special reference to the associated Crocidolite: *West. Aust. Geol. Sur. Bull.* 119, 366 p.
- Truswell, J.F., 1990a, Early Proterozoic red beds on the Kapvaal Craton: *Econ. Geol. Res. Unit, University of the Witwatersrand, Johannesburg, Inf. Circ.* No. 223, 96 p.
- Truswell, J.F., 1990b, The Transvaal and Griqualand West Sequences: some

- current issues: Econ. Geol. Res. Unit, Univ. of the Witwatersrand, Johannesburg, Information Circular No. 232, 69 p.
- Tsikos, H., 1991, A metallogenetic study of the manganese-ore occurrences at Othrys region, Greece: Unpubl. Diploma thesis, University of Athens, Greece, 152 p.
- Van Hise, C.R., and Leith, C.K., 1911, Geology of the Lake Superior Region: U. S. Geol. Survey, Mon. 52, 641 p.
- Visser, J.N.J., 1971, The deposition of the Griquatown glacial member in the Transvaal Supergroup: Trans. Geol. Soc. S. Afr., v. 74, pp. 187-199.
- Vokes, F.M., 1976, The abundance and availability of mineral resources, in: World mineral supplies: Assessment and perspective, eds., G.J.S. Govett and M.H. Govett: Developm. in Econ. Geol., v. 3, Els. Sci. Pbl., 472 p.
- Walker, J.C.G., 1977, Evolution of the atmosphere: MacMillan, New York, 318 p.
- Walker, J.C.G., 1984, Suboxic diagenesis in banded iron-formations: Nature, v. 309, pp. 340-342.
- Walker, J.S.G., Klein, C., Schidlowski, M., Stevenson, D.J., and Walter, M.R., 1983, in: The Earth's Earliest Biosphere: Its Origin and Evolution, ed., J.W. Schopf: Princeton University Press, Princeton, NJ, pp. 260-290.
- Wiggering, H., and Beukes, N.J., 1990, Petrography and geochemistry of a 2000-2200-ma-old hematitic palaeo-alteration profile on Ongeluk basalt of the Transvaal Supergroup, Griqualand West, South Africa: Prec. Res., v. 46, pp. 241-258.
- Wilhelm, H.J., von Gruenewaldt, G., and Behr, S.H., 1990, Investigations on the Molopo Farms Complex, Botswana: stratigraphy and petrology: Abstracts, Geocongress '90, Geol. Soc. S. Afr., pp. 733-736.
- Young, T.P., 1989, Phanerozoic ironstones: an introduction and review, in: Phanerozoic Ironstones, eds., T.P. Young and W.E.G. Taylor: Geol. Soc. London, Sp. Pbl. No. 46, 251 p.
- Zajac, I.S., 1974, The stratigraphy and mineralogy of the Sokoman iron-formation in the Knob Lake area, Quebec and Newfoundland: Geol. Surv. Can. Bull., v. 220, 159 p.

APPENDICES

Fig. A1. The Early Proterozoic Kalahari Manganese Field comprises five known structurally preserved basins, which represent erosion relics of the Hotazel Formation of the Voëlwater Subgroup, consisting of banded iron-formations interbedded with manganese ore units. Of these five structural basins, the Kalahari basin is the largest and most important, extending in a north-westerly direction from the Mamatwan mine in the south, for a distance of 34 km to the Black Rock and Wessels mine in the north. The total area is underlain by manganese ore which occurs in three distinct layers (Kleyenstuber, 1991).

The area of study is situated at the southern tip of the Kalahari Basin where the low-grade, Mamatwan manganese mine is located. Both the manganese lithologies and the BIFs in that area have been affected by diagenetic to low-grade metamorphic processes, and are suitable for detailed mineralogical and geochemical studies. Instead, the northern parts of the basin have been affected by later hydrothermal processes that have resulted in significant enrichment of the Mn-horizons which, nevertheless, attain limited thicknesses (up to 5m).

A notable feature in the study rocks is the major change in thickness of the lower Mn-horizon and overlying BIF unit, from the vicinity of the Mamatwan mine northwards. The Mn-horizon has an approximate thickness of 40m just north of the Mamatwan mine (borehole R-65) and it decreases dramatically down to 18m in borehole R-59, within a distance of approximately 1000m. The Mn-body then retains a thickness of ± 20 m in the remaining boreholes. The overlying BIF unit shows the opposite trend: it is thin in borehole R-65 (20m), it increases up to 45m in borehole R-59 and it has an approximate thickness of 40m in the remaining boreholes. This lateral thickness variation can be roughly depicted in Fig. A1, although the vertical scale of the boreholes is approximate (1:4000). According to the writers observations, the mineralogical and geochemical composition of the lower Mn-body remains essentially constant in all the boreholes of this study. On the other hand, variations in the overlying BIF unit are related to the presence or absence of well-developed, granular, silicate-rich lithologies (see also text, ¶5.2.3).

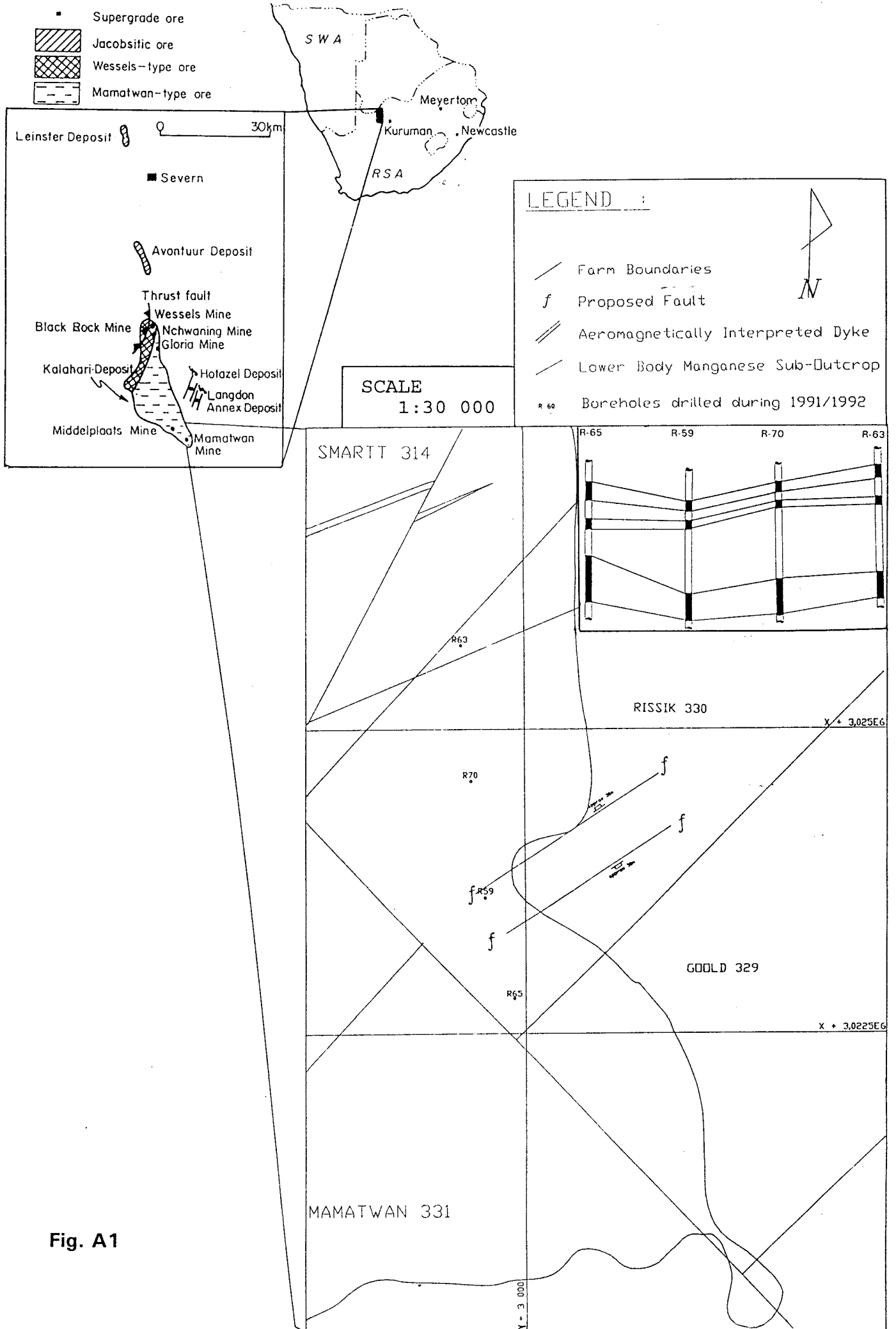


Fig. A1

Table A1. Major element and trace element compositions for rocks of this study (total Fe as Fe₂O₃; all volatiles as LOI).

	R59-1	R59-2	R59-3	R59-13	R59-14	R59-15	R59-16
SiO ₂	36.00	39.35	30.38	41.83	40.89	41.87	45.38
TiO ₂	0.04	0.04	0.05	0.04	0.05	0.04	0.07
Al ₂ O ₃	0.18	0.18	0.46	0.30	0.36	0.36	0.86
Fe ₂ O ₃	39.56	44.33	32.81	45.76	46.39	45.67	36.70
MnO	0.13	0.32	2.21	0.29	0.24	0.20	0.04
MgO	2.45	2.75	2.18	2.48	2.42	2.19	2.77
CaO	11.12	6.23	15.77	4.21	3.55	2.06	7.67
Na ₂ O	0.02	0.02	0.05	0.02	0.01	0.02	0.02
K ₂ O	0.04	0.02	0.07	0.05	0.04	0.02	0.02
P ₂ O ₅	0.05	0.10	0.05	0.14	0.15	0.13	0.11
LOI	11.11	7.31	15.65	5.54	6.29	7.34	6.29
H ₂ O-	0.28	0.24	0.37	0.22	0.42	0.40	0.42
TOTAL	100.98	100.89	100.05	100.88	100.81	100.30	100.35
Zn	23	15	17	17	13	17	16
Cu	20	25	20	21	22	23	18
Ni	41	40	42	43	42	43	42
Co	<4	<4	6	nd	nd	nd	<4
Cr	26	28	33	31	36	37	41
V	<4	<4	5	5	7	9	17
Ba	36	20	147	15	3	8	4
Sc	2	2	<1	3	4	4	6
Rb	4	<3	9	4	2	2	5
Nb	<3	<3	<3	4	<3	4	4
Zr	4	4	5	5	9	9	11
Y	7	9	7	10	16	15	12
Sr	145	82	305	68	58	45	140
La	<5	<5	9	8	15	12	10
Ce	20	23	19	20	25	31	27
Nd	<5	<5	<5	6	6	9	9

Table A1 (cont.):

	R59-17	R59-18	R63-5	R63-8	R63-9	R63-10	R63-11
SiO2	40.31	38.67	33.50	30.30	39.15	36.10	36.60
TiO2	0.05	0.05	0.04	0.03	0.04	0.04	0.04
Al2O3	0.45	0.28	0.16	0.15	1.33	0.02	0.13
Fe2O3	42.70	52.43	39.60	35.32	39.96	51.24	52.22
MnO	0.64	0.60	1.38	0.55	0.13	0.14	0.09
MgO	2.72	2.09	3.04	2.40	3.12	1.98	1.95
CaO	3.85	2.37	10.74	15.62	8.27	5.05	3.80
Na2O	0.01	0.01	0.02	0.01	0.11	0.01	0.01
K2O	0.02	0.01	0.01	0.01	0.48	0.01	0.02
P2O5	0.19	0.28	0.08	0.07	0.13	0.18	0.13
LOI	9.21	3.43	10.45	14.49	7.56	5.96	5.64
H2O-	0.68	0.36	0.38	0.35	0.70	0.23	0.27
TOTAL	100.83	100.58	99.40	99.30	100.98	100.96	100.90
Zn	19	14	31	13	17	14	24
Cu	19	24	24	22	21	25	24
Ni	42	53	43	41	38	51	46
Co	<4	nd	6	<4	<4	<4	<4
Cr	40	43	27	23	29	35	35
V	11	8	<4	<4	<4	<4	<4
Ba	3	7	38	40	111	7	14
Sc	4	3	2	nd	2	3	2
Rb	3	<3	nd	<3	47	<3	<3
Nb	<3	5	4	<3	3	<3	5
Zr	9	8	6	<3	11	<3	4
Y	17	21	10	5	11	10	10
Sr	54	52	169	299	214	95	140
La	10	9	30	14	13	6	<5
Ce	27	21	15	21	27	23	15
Nd	8	7	<5	5	6	<5	<5

Table A1 (cont.):

	R63-12	R63-13	R63-14	R63-20	R65-2	R65-3	R65-12
SiO ₂	39.82	45.77	46.24	23.07	37.66	35.97	30.16
TiO ₂	0.04	0.06	0.05	0.06	0.03	0.04	0.04
Al ₂ O ₃	0.16	0.62	0.28	0.40	0.19	0.18	0.20
Fe ₂ O ₃	51.01	39.77	50.00	47.59	34.79	43.97	42.28
MnO	0.09	0.33	0.35	10.51	0.15	0.37	1.12
MgO	2.01	3.24	1.01	2.96	2.22	2.49	3.04
CaO	3.12	2.42	1.35	3.61	12.95	7.58	12.29
Na ₂ O	0.01	0.02	0.02	0.02	0.01	0.01	0.02
K ₂ O	0.01	0.05	0.01	0.01	0.01	0.01	0.03
P ₂ O ₅	0.17	0.09	0.00	0.08	0.05	0.11	0.11
LOI	4.21	7.86	1.44	10.25	12.40	8.92	11.20
H ₂ O-	0.34	0.72	0.16	0.52	0.23	0.30	0.46
TOTAL	100.99	100.95	100.91	99.08	100.69	99.95	100.95
Zn	18	19	<5	15	11	17	16
Cu	26	21	26	30	19	25	26
Ni	50	40	54	59	39	43	48
Co	<4	<4	<4	70	<4	nd	5
Cr	33	37	53	48	24	31	30
V	<4	10	9	<4	<4	<4	<4
Ba	13	18	21	2003	6	<2	73
Sc	2	4	3	3	<1	3	2
Rb	<3	5	<3	nd	<3	<3	3
Nb	<3	3	4	nd	3	<3	<3
Zr	3	12	9	nd	3	4	6
Y	10	10	5	<3	7	9	11
Sr	117	55	22	39	231	93	156
La	9	7	10	9	7	9	10
Ce	21	27	19	<13	22	24	22
Nd	6	8	<5	nd	6	<5	<5

Table A1 (cont.):

	R-65-19	R65-20	R65-21	R65-30	R65-31	R70-11	R70-12
SiO ₂	42.89	39.60	26.27	28.63	17.08	24.51	52.64
TiO ₂	0.04	0.05	0.05	0.05	0.06	0.05	0.05
Al ₂ O ₃	0.18	0.04	0.44	0.32	0.23	0.28	3.85
Fe ₂ O ₃	45.90	49.18	51.12	48.14	45.90	36.40	31.46
MnO	0.39	0.52	1.96	5.24	17.65	0.75	0.07
MgO	2.66	2.64	2.51	2.81	5.32	0.90	5.64
CaO	4.07	2.58	8.55	4.44	0.96	20.63	0.22
Na ₂ O	0.01	0.01	0.01	0.02	0.02	0.03	0.26
K ₂ O	0.04	0.02	0.05	0.04	0.00	0.06	1.76
P ₂ O ₅	0.18	0.18	0.19	0.07	0.07	0.07	0.01
LOI	4.40	5.02	9.16	9.60	11.39	16.92	3.28
H ₂ O-	0.22	0.29	0.46	0.37	0.32	0.27	1.17
TOTAL	100.98	100.13	100.77	99.73	99.00	100.87	100.41
Zn	15	16	11	37	40	12	15
Cu	26	27	28	25	30	26	15
Ni	44	54	59	52	58	49	26
Co	<4	<4	<4	35	31	<4	<4
Cr	31	54	49	42	47	29	25
V	<4	9	6	6	nd	<4	<4
Ba	<2	<2	17	72	3537	117	535
Sc	3	3	4	3	2	nd	2
Rb	5	<3	<3	4	nd	8	189
Nb	<3	4	5	<3	nd	<3	nd
Zr	5	6	8	7	nd	<3	26
Y	14	17	18	10	nd	7	3
Sr	79	24	125	14	14	602	30
La	8	14	16	7	10	6	20
Ce	27	30	34	14	<13	21	38
Nd	5	8	9	nd	nd	<5	8

Table A1 (cont.):

	R70-13	R70-14	R70-15	R70-16	R70-17	R70-18	R70-19
SiO ₂	43.15	40.49	38.06	37.84	40.15	43.86	42.99
TiO ₂	0.04	0.03	0.04	0.04	0.04	0.05	0.04
Al ₂ O ₃	0.15	0.16	0.12	0.12	0.16	0.49	0.32
Fe ₂ O ₃	45.58	46.09	50.02	52.96	50.70	41.39	44.00
MnO	0.12	0.14	0.14	0.16	0.16	0.40	0.48
MgO	1.90	1.86	2.24	2.24	2.13	2.83	0.94
CaO	4.60	5.60	4.69	2.75	2.33	2.54	6.27
Na ₂ O	0.01	0.01	0.01	0.01	0.01	0.01	0.02
K ₂ O	0.04	0.04	0.03	0.02	0.03	0.02	0.02
P ₂ O ₅	0.10	0.14	0.20	0.14	0.22	0.09	0.14
LOI	4.85	6.00	5.10	4.20	4.24	8.42	5.25
H ₂ O-	0.20	0.30	0.25	0.20	0.32	0.53	0.40
TOTAL	100.73	100.86	100.90	100.68	100.49	100.63	100.87
Zn	12	16	13	20	15	15	13
Cu	23	23	25	26	21	21	25
Ni	45	46	47	53	44	38	46
Co	<4	nd	<4	nd	nd	<4	<4
Cr	32	31	32	34	33	35	38
V	<4	<4	<4	<4	<4	9	9
Ba	12	6	13	14	6	7	56
Sc	3	2	2	2	2	4	4
Rb	4	3	5	<3	4	4	4
Nb	<3	nd	nd	nd	nd	nd	nd
Zr	3	<3	<3	<3	<3	6	4
Y	7	7	9	11	13	8	11
Sr	95	112	119	79	64	53	252
La	8	9	<5	9	12	11	14
Ce	25	18	19	27	21	25	34
Nd	nd	<5	nd	<5	<5	6	9

Table A2a. Averages of bulk analyses of Precambrian banded iron-formations recalculated to 100% on a H₂O and CO₂-free basis. Total Fe as Fe₂O₃. 1. Voëlwater BIF (this study); 2. Brockman BIF, Australia (Klein & Gole, 1981); 3. Marra Mamba BIF, Australia (Klein & Gole, 1981); Asbesheuwels BIF (Klein & Beukes, 1989; Beukes & Klein, 1990a); 5. Sokoman BIF, Canada (Klein & Gole, 1981); and, 6. Biwabik BIF, U.S.A (Klein & Gole, 1981).

	1	2	3	4	5	6
SiO ₂	41.24	43.73	48.16	50.93	46.69	49.58
TiO ₂	0.04	0.06	0.18	0.01	0.04	0.06
Al ₂ O ₃	0.29	1.34	1.61	0.08	0.61	1.11
TFe	48.20	44.04	40.42	40.13	43.04	43.19
MgO	2.46	3.92	4.93	3.48	3.91	3.10
MnO	0.52	0.27	0.13	0.25	1.12	0.71
CaO	7.06	4.98	3.71	4.79	4.20	1.94
Na ₂ O	0.02	0.44	0.37	0.20	0.17	0.06
K ₂ O	0.03	0.95	0.42	0.04	0.20	0.17
P ₂ O ₅	0.14	0.27	0.08	0.09	0.04	0.09

Table A2b. Average transition metal data from several banded iron-formations of the world. 1. Voëlwater BIF (this study); 2. Brockman BIF, Australia (Trendall & Pepper, 1977; in Davy, 1983); 3. Griquatown BIF (Zn, Ni, Co and Sc: Klein & Beukes, 1989 and Beukes & Klein, 1990a; Cu, Cr and V: Hälbich et al., 1993); 4. Kuruman BIF (Zn, Ni, Co and Sc: Klein & Beukes, 1989 and Beukes & Klein, 1990a; Cu, Cr and V: Hälbich et al., 1993); 5. Superior-type BIF averages, Canada (Gross & McLeod, 1980); and, 6. Algoma-type BIF averages, Canada (Gross & McLeod, 1980).

	1	2	3	4	5	6
Zn	17	47	13	19	40	330
Cu	23	101	13	12	14	149
Ni	46	12	15	21	37	103
Co	2	2	0	0	28	41
Cr	35	14	24	24	112	118
V	2	14	6	9	42	109
Sc	3	0	0	0	18	8

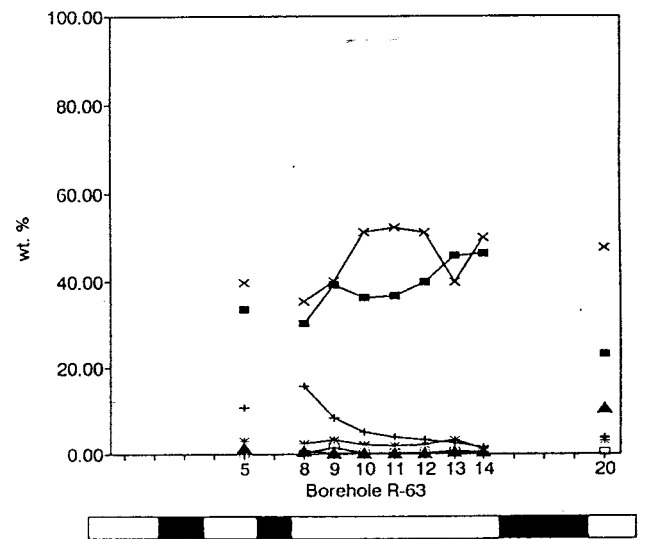
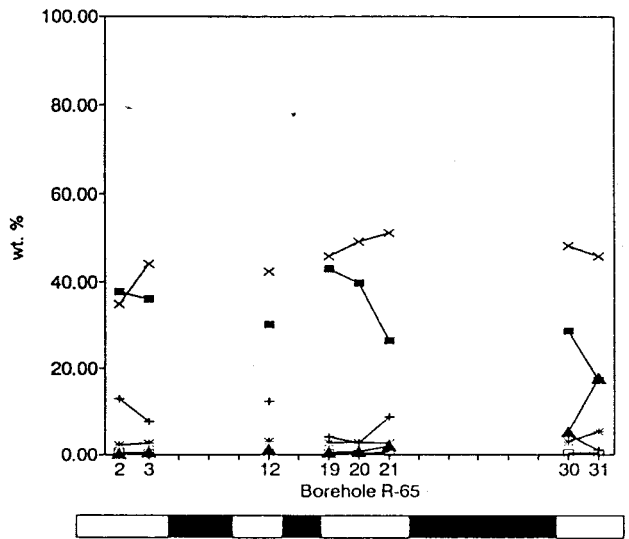
Table A3. Average LREE analyses of several Superior-type banded iron-formation occurrences of the world. 1. Voëlwater BIF (this study); 2. Gunflint BIF, U.S.A (Danielson et al., 1992); 3. Asbesheuwels BIF (Beukes & Klein, 1990a); 4. BIF, Mesabi Range, Minnesota (Fryer, 1977b); 5. BIF, Mesabi Range, Minnesota (Danielson et al., 1992); 6. Sokoman BIF, Canada (Fryer, 1977b); 7. Sokoman BIF, Canada (Danielson et al., 1992); 8. Brockman BIF, Australia (Fryer, 1977b); 9. Brockman BIF, Australia (Danielson et al., 1992); 10. Marra Mamba BIF, Australia (Danielson et al., 1992); and, 11. Weeli Wolli BIF, Australia (Danielson et al., 1992).

	1	2	3	4	5	6	7	8	9	10	11
La	10.03	8.28	1.28	12.60	4.14	2.15	3.19	5.71	14.62	1.00	8.85
Ce	22.71	17.23	1.77	20.60	9.10	3.51	5.75	8.14	28.67	1.67	16.83
Nd	5.10	0.99	nd	11.00	4.59	1.87	2.67	3.39	19.07	0.80	4.10

Table A4. Representative microprobe analyses for members of the dolomite-ankerite series, for rocks of this study.

FeO	16.24	14.61	15.60	15.16	15.52	14.71	14.89	15.04	15.67	13.40	13.29	15.14
MnO	0.94	1.03	0.85	0.94	0.92	1.00	0.94	0.89	0.89	1.32	2.03	1.33
MgO	7.18	7.79	7.00	6.95	6.55	7.54	6.84	6.36	6.78	8.64	9.16	7.19
CaO	26.89	30.12	27.65	30.47	29.59	30.52	31.35	30.78	29.69	29.71	32.63	31.47
CO ₂	48.75	46.45	48.90	46.48	47.42	46.23	45.98	46.93	46.97	46.93	42.89	44.87
TOTAL	51.25	53.55	51.10	53.52	52.58	53.77	54.02	53.07	53.03	53.07	57.11	55.13

Fig. A2. Geochemical profiles of the six most abundant major elements as well as of the 12 most abundant trace elements for the rocks of this study.



- * MgO
- x Fe₂O₃
- + CaO
- ▲ MnO
- Al₂O₃
- SiO₂

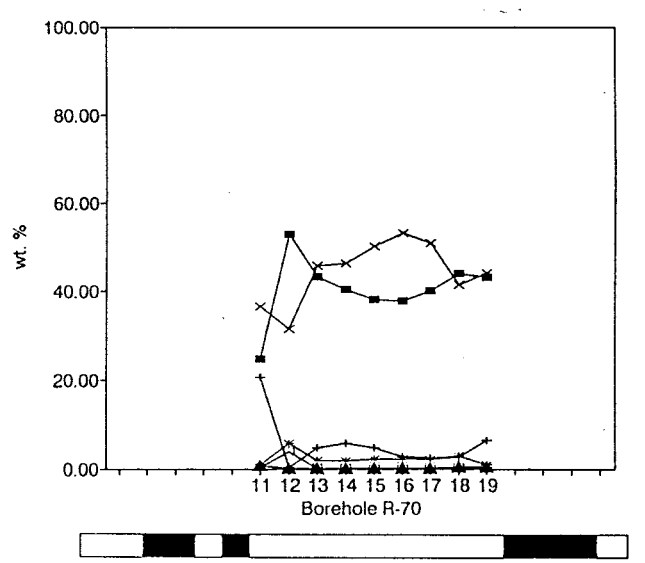
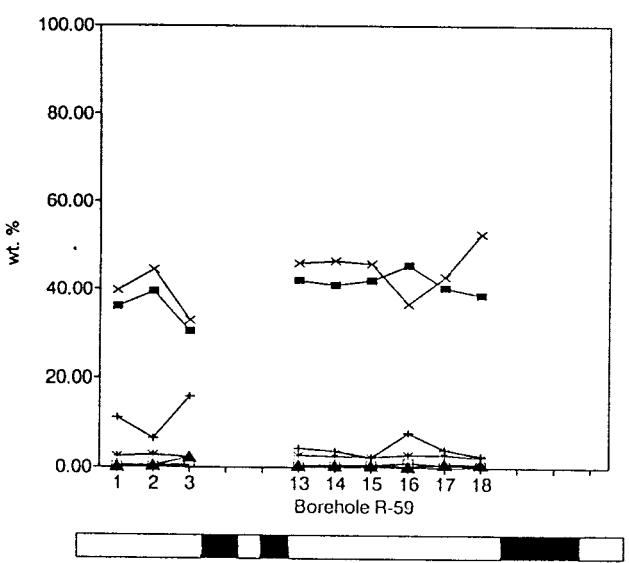
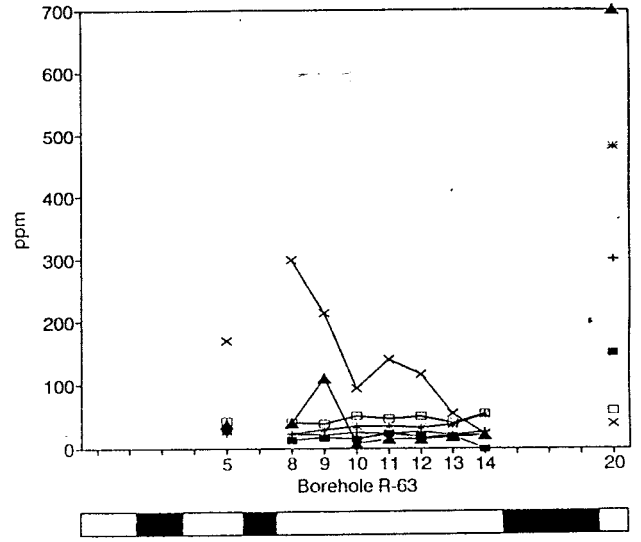
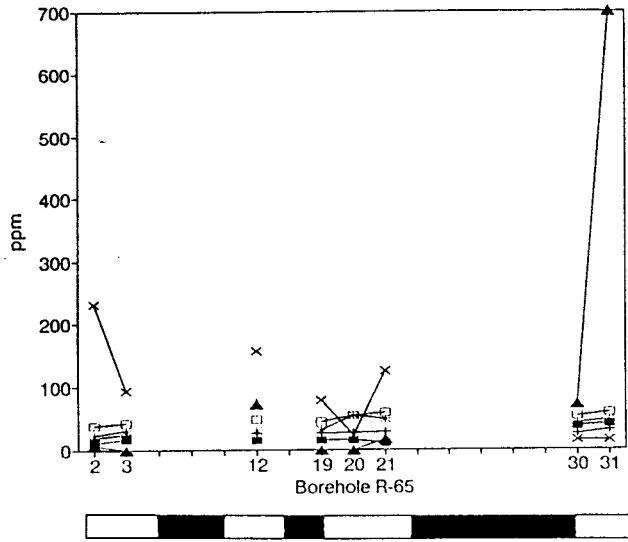


Fig. A2 (cont.):



* Cr
x Sr
+ Cu

▲ Ba
□ Ni
■ Zn

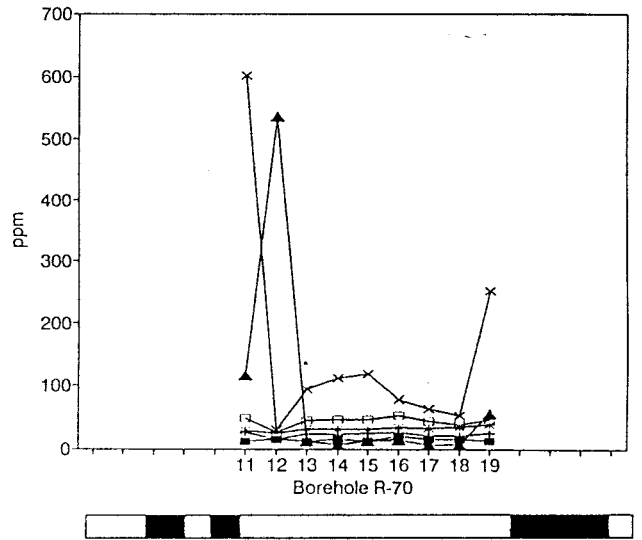
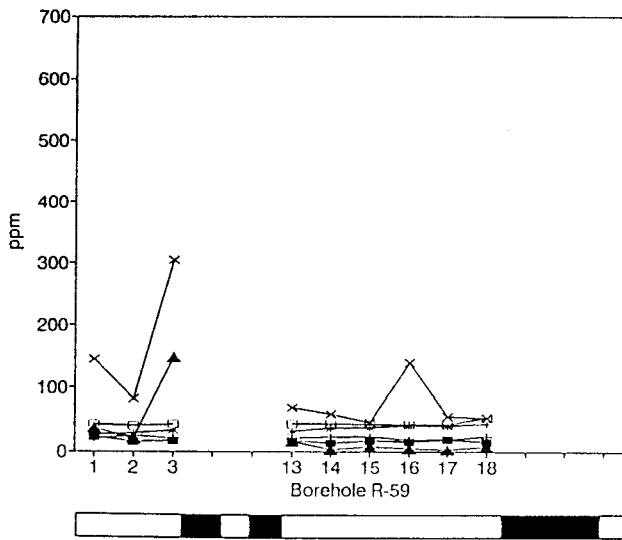
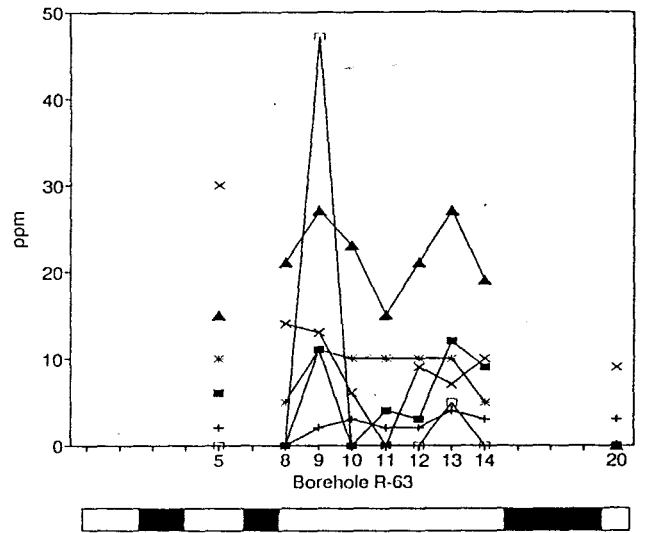
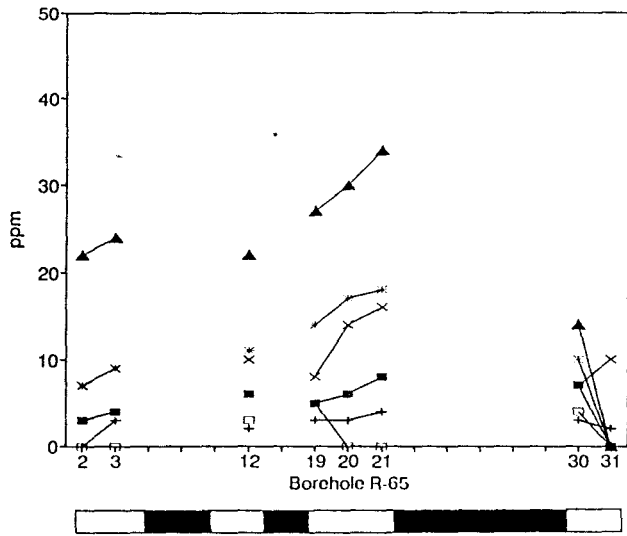


Fig. A2 (cont.):



* Y
x La
+ Sc

▲ Ce
□ Rb
■ Zr

